FIRE AND CLIMATE IN A LODGEPOLE FOREST OF CENTRAL IDAHO:

ANNUAL, DECADAL, CENTENNIAL, AND MILLENNIAL PERSPECTIVES

Lar Osvard Svenson

A thesis

submitted in partial fulfillment

of the requirements for the degree of

Master of Science in Geology

Boise State University

May 2010

BOISE STATE UNIVERSITY GRADUATE COLLEGE

DEFENSE COMMITTEE AND FINAL READING APPROVALS

of the thesis submitted by

Lar Osvard Svenson

Thesis Title: Fire and Climate in a Lodgepole Forest of Central Idaho: Annual, Decadal, Centennial, and Millennial Perspectives

Date of Final Oral Examination: 30 November 2009

The following individuals read and discussed the thesis submitted by student Lar Osvard Svenson, and they evaluated his presentation and response to questions during the final oral examination. They found that the student passed the final oral examination.

Jennifer Pierce, Ph.D.	Chair, Supervisory Committee
David Wilkins, Ph.D.	Member, Supervisory Committee
Dana Perkins, Ph.D.	Member, Supervisory Committee

The final reading approval of the thesis was granted by Jennifer Pierce, Ph.D., Chair of the Supervisory Committee. The thesis was approved for the Graduate College by John R. Pelton, Ph.D., Dean of the Graduate College.

ABSTRACT

Fire history of the high-elevation forest of the Sawtooth Valley in central Idaho was reconstructed using tree rings (providing annual to decadal resolution over the past ~400 years) and radiocarbon dating of charcoal (providing centennial to millennial resolution over the past ~8000 years). Fourteen annually resolved fires were reconstructed between 1632 and 1933 AD from fire-scarred Douglas-fir (*Pseudotsuga menziesii*) and lodgepole pine (*Pinus contorta* var *latifolia*). Stand ages of lodgepole pine indicate that at least five annually resolved fires in the ~28,000 ha study area were stand-replacing (SR). Multi-watershed SR fires burned in 1632 and 1842, and single-watershed SR fires burned in 1739, 1783, and 1933. Comparison of fire dates with independent reconstructions of drought (PDSI) and July temperature indicates that most fires burned during summers that were significantly warm and dry. Drought-induced fires (PDSI < -1, n = 11) burned at the tail end of a positive surge of spring Pacific Decadal Oscillation (PDO), which included a significantly positive (> 95% CL) anomaly the year before the fire. Eight of 11 drought-induced fires burned during combined positive phases of spring PDO and the Atlantic Multidecadal Oscillation (AMO) Index, a centered 10-year moving average of AMO anomalies. This subset of fires coincided with significantly positive spring PDO the year of the fire and the year before (> 95% and 99% CL, respectively). The multi-watershed SR fires of 1632, the most extensive (at least 4 watersheds) reconstructed in this study, were preceded by the longest protracted La Niña event (11 years) reconstructed for the past 484 years. Multidecadal periods of low frequency for all fires (n = 20) coincided with combined cool phases of the AMO and July temperature in central Idaho. Charcoal samples from nine soil sites and two incised alluvial sites provide millennial-scale records of fire. Summed probabilities from 16 calibrated radiocarbon dates show relatively high (compared with the early and middle Holocene) fire probabilities during the past ~1500 years, with peaks in ~720 AD and ~1630 AD. The ~1630 peak in the charcoal record likely corresponds with multi-watershed fires in 1632 from the fire-scar record, indicating good correspondence between these two proxy records of fire. A cool period between ~1280 and 1350 AD coincided with a deep trough in radiocarbon probabilities of fire in the Sawtooth Valley and the nearby montane forests of the South Fork Payette drainage.

TABLE OF CONTENTS

ABSTRACT ii

LIST OF TABLES vii

LIST OF FIGURES viii

INTRODUCTION 1

Study Area 2

Fire and Climate in High-Elevation Forests of the Rocky Mountains 4

Past ~400 Years 4

Centennial to Millennial Timescales 5

Predicting Drought-Induced Fire 7

Climate vs. Fuels 10

METHODS 11

Dating Fire Scars 11

Stand Ages 11

Statistical Analyses: Relationships between Fire and Climate 13

Charcoal Collection, Processing, and Analysis 14

RESULTS: TIMING AND EXTENT OF FIRES IN THE SAWTOOTH VALLEY 16

Fire-Scar Locations 17

Categorization of Fire Years 19

Locations of Annually Resolved Fires 20

Stand-Replacing Fires 20
Fires That Were Not Stand-Replacing 25
Lodgepole Pine Regeneration 27
Fire by Decade 30
Statistical Analyses of Annually Resolved Fires 31
Drought 31
Temperature 33
Sea Surface Temperature (SST) Oscillations 35
DISCUSSION OF FIRE DATES AND ANALYSES 46
Drought and Temperature 46
Sea Surface Temperature (SST) Oscillations 54
Spring PDO 54
Combined Phases of Spring PDO and Decadal AMO 54
Constructive Synergy between Seven-Year PDO and Winter Niño-3 57
Periods of Low Fire Frequency 58
Stand-Replacing vs. Low-Intensity Fires 61
Stand-Replacing Fires: Climatic Nuts and Bolts 62
CHARCOAL: RESULTS AND DISCUSSION 72
Incised Alluvial Environments 73
Soil Charcoal 74
^{14}C Ages and Calibrated Dates 78
Graphical Analyses of Summed Probabilities 79

Probability of Fire and Reconstructed July Temperature in Central Idaho 81

Drought, Fire Probabilities, and Erosion over the Past ~1500 Years 86

Contemporary Analogues 93

CONCLUSIONS 95

WORKS CITED 97

APPENDIX A: DENDROCHRONOLOGY 104

Dating Fire Scars 105

Lodgepole Cores 105

APPENDIX B: CHARCOAL 108

Potential Inaccuracies from Inbuilt Age 109

Reporting of Radiocarbon Ages 110

Charcoal Sites: Supplementary Information 110

LIST OF TABLES

Table 1. Locations of fire-scarred Douglas-fir (PSME) and lodgepole pine (PICO) 18

Table 2. Fire years by category 20

Table 3. Anomalies of climatic reconstructions during fire years 48

Table 4. Radiocarbon ages and calibrated dates from 16 charcoal samples (11 sites) in the Sawtooth Valley 77

Table 5. Locations and elevations of the 15 lodgepole plots 107

Table 6. Supplementary information on charcoal samples from the Sawtooth Valley 111

LIST OF FIGURES

Figure 1. Located in the Sawtooth Valley of central Idaho, the study area (outlined in black on the digital elevation model) covers ~28,000 ha 3

Figure 2. The Valley Road Fire of 2005 (solid red polygon) burned ~17,000 hectares on the east side of the Sawtooth Valley 4

Figure 3. Areas homogeneous in color and texture were outlined by polygons as potential plots for coring lodgepole pine 13

Figure 4. Locations of fire-scarred Douglas-fir (pink) and lodgepole pine (yellow) in the Sawtooth Valley 17

Figure 5. Multi-watershed fires burned in 1632 (pink) and 1842 (yellow) 21

Figure 6. A fire-scarred Douglas-fir (DFCF09, pink dot) records a fire in 1842 west of Redfish Lake 22

Figure 7. Single-watershed fires burned in 1739 (yellow), 1783 (green), and 1933 (red) 23

Figure 8. Fire history in the Decker watershed 24

Figure 9. A fire-scarred Douglas-fir (DFCF10) southwest of the Ranger Station records a fire in 1783 25

Figure 10. Low-intensity fires burned in 1799 (red), 1844 (yellow), and 1889 (green) 26

Figure 11. Point fires burned in 1686 (red), 1712 (yellow), 1734 (green), 1756 (orange), 1782 (pink), and 1930 (blue) 27

Figure 12. Across all plots, regeneration in lodgepole pine (number of trees per decade) followed stand-replacing fires in 1632, 1739, 1783, and 1842 29

Figure 13. Number of watersheds burned by decade 30

Figure 14. Reconstructed PDSI (Cook *et al.* 2004) was significantly dry (> 99.9% CL) the year of the fire (year 0) between 1600 and 1950 (n = 14) 32

Figure 15. Reconstructed annual temperature (point 14, Briffa *et al.* 1992) was significantly warm (> 95% CL) the year of the fire (year 0) between 1600 and 1950 (n = 14) 34

Figure 16. Reconstructed July temperature for central Idaho (Biondi *et al.* 1999/2006) was significantly warm (> 99.9% CL) the year of the fire (year 0) between 1600 and 1950 (n = 14) 34

Figure 17. Drought-induced fires were preceded six years before (year -6) by significantly negative (> 95% CL) annual PDO reconstructed from western Pacific records (Shen *et al.* 2006) on the interval between 1600 and 1950 (n = 11) 37

Figure 18. Drought-induced fires did not coincide significantly with annual PDO reconstructed from eastern Pacific records (D'Arrigo *et al.* 2001) in any year of the nine-year window on the interval between 1700 and 1950 (n= 9) 38

Figure 19. Reconstructed spring PDO (D'Arrigo and Wilson 2006) was significantly positive (>95% CL) the year before the fire (year -1) between 1600 and 1950 (n = 11) 39

Figure 20. Reconstructed spring PDO (D'Arrigo and Wilson 2006) was more positive than expected in the years leading up to the fire 39

Figure 21. Reconstructed spring PDO was significantly positive the year of the fire (year 0, >95% CL) and the year before (year -1, > 99% CL) when year 0 coincided with combined positive phases of the AMO Index (Gray *et al.* 2004) and spring PDO (D'Arrigo and Wilson 2006) between 1600 and 1950 (n = 8) 41

Figure 22. Drought-induced fires were preceded the year before (year -1) by significantly negative (> 95% CL) reconstructed winter Niño-3 (D'Arrigo *et al.* 2005) between 1600 and 1950 (n = 11) 42

Figure 23. Reconstructed winter Niño-3 (D'Arrigo *et al.* 2005) was significantly negative (> 95% CL) the year of the fire (year 0) and six years before the fire (year -6) when year 0 coincided with combined negative phases of seven-year PDO and winter Niño-3 between 1600 and 1950 (n = 4) 45

Figure 24. Multi-watershed fires in 1632 coincided with significantly warm (>99.9 % CL) July temperature (Biondi *et al.* 1999/2006, dashed line) and significantly dry (>99.9% CL) summer PDSI (Cook *et al.* 2004, solid line) 49

Figure 25. The single-watershed fire of 1739 coincided with significantly warm (>99.9% CL) July temperature (Biondi *et al.* 1999/2006, dashed line) and significantly dry (>99% CL) summer PDSI (Cook *et al.* 2004, solid line) 50

Figure 26. The single-watershed fire of 1783 coincided with significantly warm (>99.9% CL) July temperature (Biondi *et al.* 1999/2006, dashed line) and significantly dry (>99.9% CL) summer PDSI (Cook *et al.* 2004, solid line) 51

Figure 27. Multi-watershed fires in 1842 coincided with anomalously (but not significantly) warm July temperature (Biondi *et al.* 1999/2006, dashed line) and significantly dry (>99.9% CL) summer PDSI (Cook *et al.* 2004, solid line) 52

Figure 28 The single-watershed fire of 1933 coincided with significantly warm (>99.9% CL) July temperature (Biondi *et al.* 1999/2006, dashed line) and significantly dry (>99.9% CL) summer PDSI (Cook *et al.* 2004, solid line) 53

Figure 29. Spring PDO (dashed line, D'Arrigo and Wilson 2006) and AMO anomalies (solid line, Gray *et al.* 2004) on center-weighted, 20-year moving averages 56

Figure 30. Gray bars represent the number of watersheds burned by decade for the set of all fires (n = 20) 60

Figure 31. Reconstructed PDSI for the United States in 1632 62

Figure 32. Reconstructed PDSI for the United States in 1739 65

Figure 33. Reconstructed PDSI for the United States in 1783 66

Figure 34. Reconstructed PDSI for the United States in 1842 67

Figure 35. Reconstructed PDSI for the United States in 1933 68

Figure 36. PDSI for the United States at the end of August 2004 70

Figure 37. PDSI for the United States at the end of August 2005 71

Figure 38. Charcoal sites: blue = incised fan, green = incised floodplain, pink = soil in-situ, yellow = soil depositional 72

Figure 39. Both incised alluvial charcoal sites and one depositional soil-charcoal site (SC12) are on the east side of the Sawtooth Valley 73

Figure 40. Soil-charcoal sites in the southwestern corner of the study area 75

Figure 41. Soil-charcoal sites in the northwestern corner of the study area 76

Figure 42. Summed probabilities of fire from radiocarbon dating of charcoal on a 100-year, centered moving average (n = 16) 80

Figure 43. Fire probabilities between 450 AD and the present on a 50-year, center-weighted moving average (n = 12) 81

Figure 44. Probability of fire in the Sawtooth Valley (bold line) and reconstructed July temperature for central Idaho (Biondi *et al.* 1999/2006, thin line) on 50-year, center-weighted moving averages in years AD 83

Figure 45. Probability of fire in the Sawtooth Valley (red line) and reconstructed summer PDSI for central Idaho (point 69, Cook *et al.* 2004, blue line) on 50-year, center-weighted moving averages 85

Figure 46. Probability of fire for the Sawtooth Valley (bold line, n = 16) and South Fork of the Payette (SFP, Pierce *et al.* 2004, thin line, n = 91) on 50-year, centered moving averages 86

Figure 47. Probability of fire in the Sawtooth Valley (red line), reconstructed summer PDSI for central Idaho (point 69, Cook *et al.* 2004, blue line), and reconstructed Northern Hemisphere temperature (Esper *et al.* 2002, black line, in degrees Celsius) on 50-year, center-weighted moving averages in years AD 90

Figure 48. Fire probabilities for the Sawtooth Valley by charcoal category on centered, 100-year moving averages 92

Figure 49. The 2005 Valley Road Fire in the Sawtooth Valley decreased the capacity of the soil to absorb water 94

Figure 50. Fifteen lodgepole plots were sampled in the Sawtooth Valley 106

INTRODUCTION

Large, stand-replacing fires in high-elevation forests of the western United States burn infrequently, but account for most of the area burned (Schoennagel *et al.* 2004). Because climate in high-elevation forests is cool and effectively wet, large fires tend to burn during summers that are significantly dry (Kipfmueller and Swetnam 2000; Schoennagel *et al.* 2005; Sibold and Veblen 2006). Oscillations in sea surface temperatures (SSTs) have shown promise as predictors of drought-induced fire in high-elevation forests of the southern Rocky Mountains (Sibold and Veblen 2006, Schoennagel *et al.* 2007), but SST-based fire prediction in the central and northern Rockies appears more tenuous (Schoennagel *et al.* 2005).

This study uses fire-scarred trees and stand ages from a lodgepole-pine-dominated forest in the Sawtooth Valley of central Idaho (central Rocky Mountains) to determine when fires burned during the past ~400 years. The resulting fire record is then compared with climatic indices reconstructed independently from tree rings and other proxies to examine past relationships between fire and climate. Charcoal from soils and incised alluvial sites was radiocarbon dated to examine fire frequencies on centennial to millennial timescales over the past ~8000 years. Summed probabilities from charcoal dates were compared with reconstructed drought and temperature over the past ~1500 years. An understanding of natural variation in the relationship between fire and climate prior to the 20th century will help elucidate the distinction in present times between natural and anthropogenically modified fire regimes.

Study Area

The Sawtooth Range was glacially sculpted during the Pleistocene. Lateral and terminal moraines, deposited by three glacial advances between ~12,000 and 17,000 years ago, extend into the axial valley (Thackray 2008). Well-drained glacial outwash and stream terraces in the valley are dominated by sagebrush (*Artemisia tridentata*), while less-permeable till on moraines is dominated by forest. This study focuses on the forested moraines (Figure 1). Douglas-fir (*Pseudotsuga menziesii*) dominates the tops of moraines and warmer south-facing slopes, while lodgepole pine (*Pinus contorta* var *latifolia*) dominates north-facing slopes and valley frost-pockets (Cochran and Berntsen 1973). Mountain pine beetle (*Dendroctonus ponderosae*), a native bark beetle, has been at epidemic levels in lodgepole stands in the Sawtooth Valley since ~2000 (Page and Jenkins 2007b). At higher elevations, Engelmann spruce (*Picea engelmannii*) grow in wetlands, and subalpine fir (*Abies lasiocarpa*) are scattered among lodgepole pine, but neither tree constitutes a large proportion of the morainal forests.

High base-elevation in the Sawtooth Valley results in a cool, effectively wet climate. Stanley, Idaho, at the lower (northern) end of the valley, is at 1908 m, and elevations in the study area range from ~2000 to 2400 m. At the Stanley weather station (108676) the warmest month is July, with an average maximum temperature of 25.9 C; the coldest month is December, with an average minimum temperature of -18.2 C. Summers are dry, with average precipitation of 15 mm each in July and August (Western Regional Climate Center 2009, http://www.wrcc.dri.edu/cgi-bin/cliMAIN.pl?id8676).

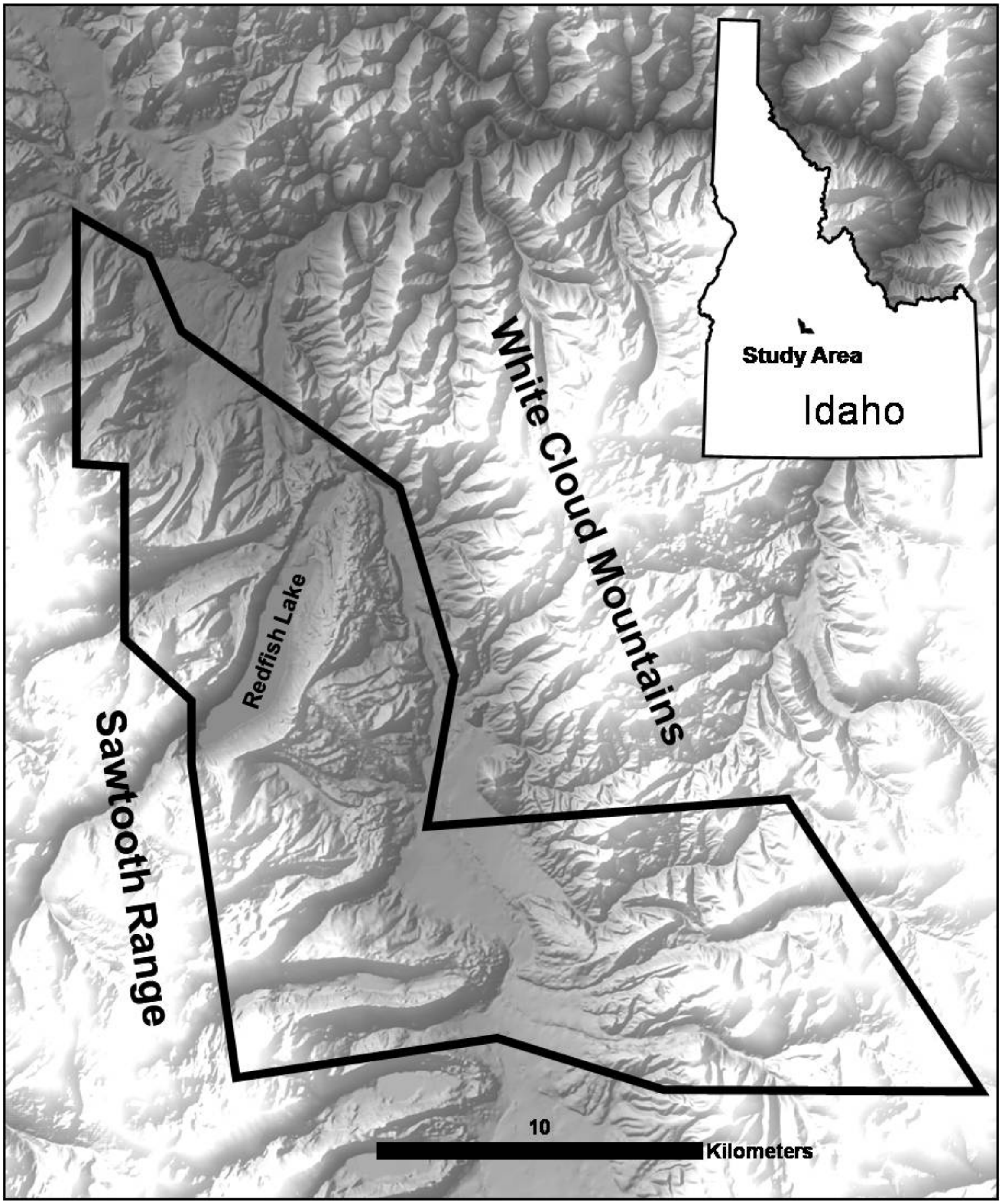

Figure 1. Located in the Sawtooth Valley of central Idaho, the study area (outlined in black on the digital elevation model) covers ~28,000 ha.

Fire records for the Sawtooth National Forest extend back to 1926. Between 1926 and 2005, only small point-fires were recorded in the Sawtooth Valley. The anthropogenically ignited 2005 Valley Road Fire, which burned ~17,000 ha on the east side of the valley, was the first fire in the historical record large enough to be a polygon (Figure 2).

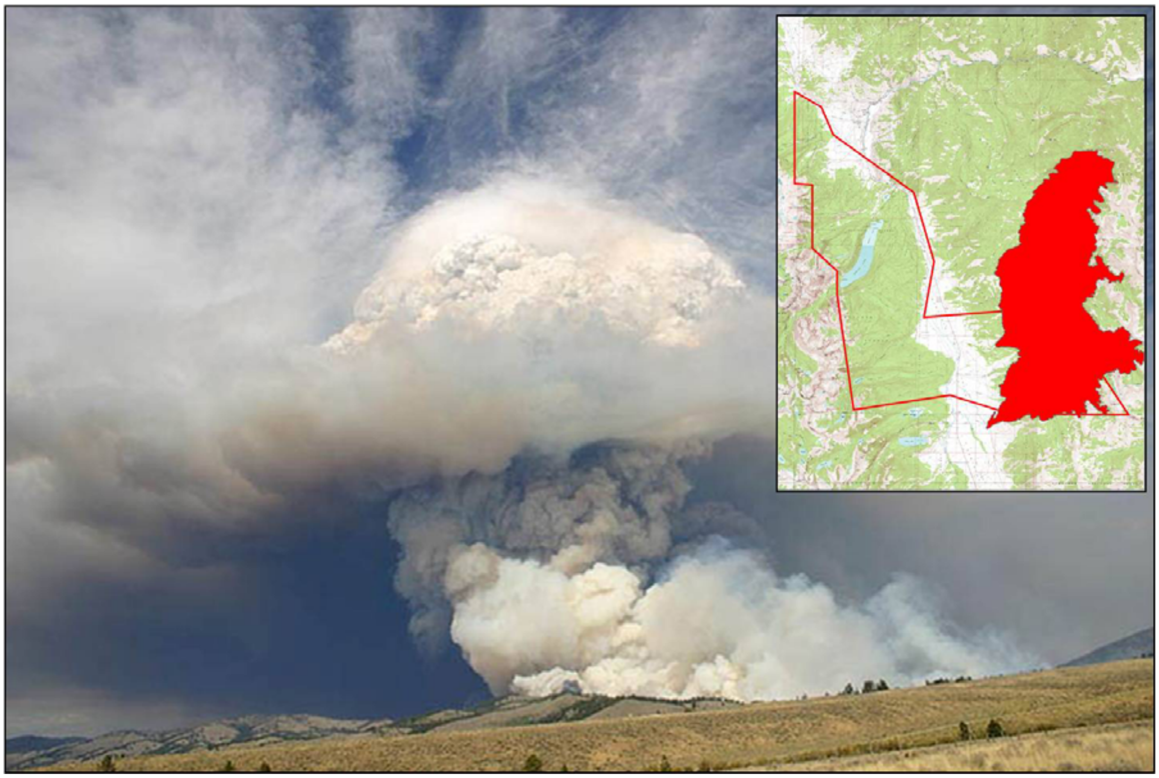

Figure 2. The Valley Road Fire of 2005 (solid red polygon) burned ~17,000 hectares on the east side of the Sawtooth Valley. (Photo by Lynne Stone, Boulder-White Clouds Council.)

Fire and Climate in High-Elevation Forests of the Rocky Mountains

<u>Past ~400 Years</u>

Annually resolved relationships between fire and climate in high-elevation forests have been deciphered by comparing fire-scar records with dendroclimatic reconstructions. Approximately 40 days (1000 hours) without precipitation are required to dry large, dead fuels and smaller live fuels to the point where they can carry a stand-replacing fire (Schoennagel *et al.* 2004). It should be no surprise, therefore, that severe to extreme summer drought coincided with years of large, stand-replacing fires in Rocky Mountain National Park (southern Rockies), Yellowstone National Park (central Rockies), and Jasper National Park (northern Rockies, Schoennagel *et al.* 2005). Stand-replacing fires in a subalpine forest in southeastern Wyoming burned synchronously with other large fires in the western United States during significantly dry years, indicating that regional drought drives regional fire (Kipfmueller and Baker 2000).

<u>Centennial to Millennial Timescales</u>

Sediment cores from subalpine lakes in the Rocky Mountains indicate periods of lower-than-present water levels during the middle Holocene (~7000 to 4500 cal yr BP), implying periods of long-term aridity (Shuman *et al.* 2009). Lake records from north-central Idaho indicate a cooler or wetter climate during the past ~3000 years, accompanied by lower fire frequency (Brunelle *et al.* 2005).

<u>Fire-Climate Inferences from the Geomorphic Response to Fire</u>

Fire-induced water repellency, surface-sealing effects of ash, reduced ground cover, and reduction in soil strength due to root decay all act to increase erosion following forest fires (DeBano 2000; Meyer *et al.* 2001). Fire-induced debris flows, hyperconcentrated flows, or stream flows (flash floods or sheet floods) deposit sediments ranging in size from silt to large boulders and charred wood on small-tributary alluvial fans. Contemporary analogues indicate that large convective storms in the summer or rain-on-snow in the winter provide sediment transport from burned basins to fans (Meyer *et al.* 1995, 2001). Alluvial fans can be incised by large storms or a drop in mainstem base-level, revealing older fire-related deposits and burned surfaces (Meyer and Wells

1997). Radiocarbon dating of charcoal from alluvial fans has elucidated the relationship between fire and climate during the past ~8000 years (Meyer *et al.* 1995; Pierce *et al.* 2004).

During the Medieval Climatic Anomaly (MCA, ~900 to 1250 AD) lodgepole pine forests in YNP (presently cool and effectively wet) and ponderosa pine (*Pinus ponderosa*) and mixed-conifer forests in the South Fork of the Payette (SFP) drainage in central Idaho (presently warmer and drier) were both characterized by stand-replacing fires, inferred from radiocarbon dates of charcoal in relatively thick, fire-related debris-flow deposits (Meyer *et al.* 1995; Pierce *et al.* 2004). These fires likely burned during multidecadal droughts, with peaks in drought area across the western United States centered around 936, 1034, 1150, and 1253 AD (Cook *et al.* 2004). Reduced drought area across the west between ~1050 and 1125 AD (Cook *et al.* 2004) and high lake levels in the Carson Sink (Nevada) at some point between ~1035 and 1300 AD (Adams 2003) suggest that multidecadal drought was punctuated by a multidecadal period (or periods) of wetness, which would have facilitated regeneration of forests.

During the Little Ice Age (LIA, ~1550 to 1850 AD) fire-induced erosion in the ponderosa pine and mixed-conifer forests of the SFP was dominated by thin sheet-flood deposits, suggesting frequent, low-intensity fires; the lodgepole pine forest of YNP was characterized by few fire-induced deposits, suggesting long intervals between fires (Meyer *et al.* 1995; Pierce *et al.* 2004). Both fire regimes indicate that the LIA was cooler and effectively wetter than during the MCA mega-droughts, a conclusion supported by reconstructed drought area for the western United States (Cook *et al.* 2004) and by other records indicating cooler conditions in the Northern Hemisphere (Grove

1988). The difference in fire regimes during the LIA between the SFP and YNP likely reflects differences in base elevation and forest type. But the similarity of fire regimes during the MCA suggests that climatic extremes can drive large, high-intensity fires and fire-induced erosion across forest types (Pierce *et al.* 2004).

Predicting Drought-Induced Fire

On annual to millennial timescales, large fires in high-elevation forests of the Rocky Mountains have coincided with drought. Is drought in the western United States a random and unfathomable occurrence, or are there underlying causes of drought with observable and measurable cycles that can be used to predict drought? Oscillations in sea surface temperatures (SSTs) potentially could provide long-range (>10 years) prediction of drought-induced fire. Large fires in the southern Rocky Mountains (Colorado) burned during combined negative phases of annual Pacific Decadal Oscillation (PDO) and El Niño-Southern Oscillation (ENSO, specifically winter Niño-3) in the context of a positive Atlantic Multidecadal Oscillation (AMO) Index (Sibold and Veblen 2006; Schoennagel *et al.* 2007).

Large fires in Yellowstone National Park (YNP, central Rocky Mountains) and Jasper National Park (JNP, northern Rocky Mountains) did not coincide significantly with annual PDO or winter Niño-3 (Schoennagel *et al.* 2005). Fires in both YNP and JNP burned most frequently (but non-significantly) during combined positive phases between 1700 and 1978. Fires that burned during combined positive phases coincided significantly with positive anomalies of annual PDO and winter Niño-3, suggesting a constructive synergy between the two oscillations during fire years. This finding did not explain a connection with Pacific SSTs for the majority of large fires in YNP or JNP, but did delineate one pathway through which SSTs can affect drought and fire.

Sea Surface Temperatures, Summer Drought, and Fire in Central Idaho

The Palmer Drought Severity Index (PDSI) is an indicator of soil moisture (Palmer 1965). Summer (June, July, August) PDSI for central Idaho has been reconstructed from tree rings for centuries prior to instrumental record keeping (Cook *et al.* 2004). Summer PDSI is autocorrelated with previous seasons, meaning winter or spring conditions could affect summer drought (Palmer 1965).

Winter Precipitation. The positive phase of the PDO tends to be associated with increased winter precipitation in coastal Alaska and northern Mexico, but with decreased winter precipitation in much of the interior United States (Mantua *et al.* 1997). Between 1941 and 1990 the PDO and Niño-3 were negatively correlated with April 1 snowpack in central Idaho, though correlations were stronger for the PDO than for Niño-3 (McCabe and Dettinger 2002).

Spring Temperature. Regional-fire years across a range of forest types in Idaho and western Montana during the 20th century did not coincide significantly with winter precipitation, but did coincide significantly with warm spring (March, April, May) temperatures (Morgan *et al.* 2008). Warm springs are correlated with early snowmelt in the central Rocky Mountains and across much of the western United States (Stewart *et al.* 2005). In Idaho during the past two decades large fires tended to burn during years of early snowmelt (Kunkel and Pierce 2010). Thus it appears that the amount of snowpack has less effect on the severity of the summer fire season than the timing of snowmelt (Morgan *et al.* 2008). Annual fire frequency and extent across the west since 1970 has correlated positively with warm spring temperatures and early snowmelt, particularly at higher elevations (Westerling *et al.* 2006). Warm springs in western North America (Minobe 1997, 2000) and in Idaho and western Montana (Morgan *et al.* 2008) are associated with the positive phase of spring PDO.

Summer Precipitation and Temperature. Because summers in central Idaho are relatively dry, climatic variables affecting winter snowfall (which accounts for 62% of annual precipitation, Serreze *et al.* 1999) or spring melting might appear to be more strongly connected to fire occurrence than those affecting summer precipitation. Timing and magnitude of summer storms, however, might make a critical difference in the moisture content of fuels. Regional-fire years across a range of forest types in Idaho and western Montana during the 20th century coincided with significantly low summer precipitation (Morgan *et al.* 2008). The positive phase of the AMO tends to decrease summer precipitation across most of the United States (Enfield *et al.* 2001). El Niño conditions in central Idaho are associated with increased August precipitation, though this could be offset by the tendency of positive PDO to intensify summer drought (Barlow *et al.* 2001). Anomalously warm summer temperatures can offset increases in precipitation, and exacerbate decreases in precipitation, through increased evapotranspiration. Summer drought, therefore, contains signals of both precipitation and temperature (Palmer 1965). In Idaho and western Montana regional-fire years in ponderosa pine (*Pinus ponderosa*) forests prior to the 20th century and across a range of forest types during the 20th century burned during summers that were significantly warm (Heyerdahl *et al.* 2008; Morgan *et al.* 2008).

Climate vs. Fuels

Despain (1990) delineated a life history of a lodgepole stand in spruce-fir habitat from germination of an even-aged cohort following a stand-replacing fire to a closed canopy with little understory that is “nearly unburnable” under normal drought conditions to the dying off of the original cohort and succession to spruce and fir. As the stand ages, large, dead fuels accumulate and ladder fuels germinate, making the forest more susceptible to crown fire. According to this model, 200 to 400 years could pass before fuel accumulation would be sufficient to support a large, stand-replacing fire. When fire weather is extreme, however, stand-replacing fires can burn over large areas, regardless of fuel accumulation (Bessie and Johnson 1995). Fuels or age structure can affect fire intensity and extent when fire weather is not extreme (Turner and Romme 1994).

METHODS

Dating Fire Scars

If a tree is scarred by fire, a "catface" forms that can record subsequent fires (e.g., Barrett and Arno 1988). Small sections were cut from fire scars and cross-dated using the list method (Yamaguchi 1991) to determine fire dates. Cross-dating was verified with program Cofecha (Holmes 1983, Grissino-Mayer 2001). Care was taken in the field in the interpretation of scarred lodgepole to distinguish between scars from fire and scars from attack by mountain pine beetle (Mitchell *et al.* 1983). If there were no beetle galleries on the scar, it was assumed the scar was the result of fire. (For details on dating fire scars, see Appendix A.)

Stand Ages

Cores from 160 lodgepole pine were extracted and processed according to standard procedures (Stokes and Smiley 1968). The purpose of dating the lodgepole cores was to ascertain whether stands were even in age, indicating germination following a stand-replacing disturbance (e.g., Kipfmueller and Baker 2000; Sibold *et al.* 2006). A stand was assumed to have been replaced by fire if it was even in age (Barrett and Arno 1988) and if most cores showed wide rings near the pith (Sibold *et al.* 2006). In even-aged stands dating to the 1800s the presence (or absence) of surface charcoal helped determine if fire was the agent of disturbance. Stands uneven in age were useful as well because survivor trees of similar age (in a single plot or scattered among plots) supplied evidence of older (earlier than the 1800s) stand-replacing disturbance.

Areas on an aerial photo (Figure 3) that were homogeneous in color and texture were outlined with polygons as potential areas for plots (e.g., Kipfmueller and Baker 2000). The 11 plots were chosen to sample evenly across the study area, with larger polygons preferred over smaller. I cored the five largest lodgepole surrounding fire-scarred trees if a 15-tree plot was not proximate, for a total of 15 plots.

Lodgepole seeds can germinate the year after the fire (Wright and Bailey 1982). The even-aged cohort, however, usually will take 15 to 25 years to regenerate completely (Barrett and Arno 1988), meaning only the oldest trees in an “even-aged” stand will approximately date the fire. To find the oldest trees in an old-growth stand, the 15 largest trees in a plot should be cored (Kipfmueller and Baker 1998). Accordingly, I cored the ~15 largest trees in circular plots 40 m in diameter. (For details on determining lodgepole stand ages, see Appendix A.)

Figure 3. Areas homogeneous in color and texture were outlined by polygons as potential plots for coring lodgepole pine.

Statistical Analyses: Relationships between Fire and Climate

I compared dates of annually resolved fires with paleoclimatic reconstructions from tree rings and other proxy records. Reconstructions included drought, temperature, and sea surface temperature (SST) oscillations. The dependent variable in these analyses was fire/no fire (categorical data); the independent variables were the reconstructed climatic indices (continuous data). On a climatic index zero is “normal” (usually the average from the instrumental period), and positive or negative values are anomalies (departures from normal). Because statistical tests assume independence among experimental units (years), reconstructions were used only if temporal autocorrelation in the first, second, and third orders was less than 0.6 (written communication with Henry Grissino-Mayer). Reconstructions with greater autocorrelation were analyzed graphically or as members of combined phases. Because of small sample size (n = 14 or fewer), parametric statistical tests would be inappropriate. A non-parametric test, superposed epoch analysis (SEA), part of the FHX2 software (Grissino-Mayer 2001), was used instead. SEA creates a window of years, with the fire at year zero. I chose a nine-year window, including six years before the fire and two years after, to identify multi-year climatic patterns that might be associated with fire. To test the null hypothesis that fires coincided with climatic anomalies by chance, SEA simulates 1000 windows (the 9 years in each simulated window chosen randomly) and creates an average for each year (the null distribution); for each average, SEA constructs a confidence interval. SEA then determines averages in nine-year windows with fire at year zero (the observed). The observed averages for each year in the window are compared to the confidence intervals from the 1000 random simulations (the expected). A departure is significant (the null hypothesis is rejected) if it exceeds at least the 95% confidence level.

Charcoal Collection, Processing, and Analysis

Charcoal was collected from two incised alluvial deposits (an alluvial fan and a floodplain) and nine holes dug in soils. Fire-induced alluvial deposits were identified by an abundance of charcoal in the deposit or by a soil surface that had been burned and then buried by the deposit (Meyer *et al.* 1995; Pierce *et al.* 2004). Charcoal from soils was considered to represent a burned surface if fragments were found in more than one location at roughly the same depth around the perimeter of the hole. This liberal definition means that some “burned surfaces” likely consisted of re-worked charcoal, which might not have been stratigraphically correct (older charcoal might have been deposited above younger). Most soil-charcoal samples that were dated appeared to have been associated with burned surfaces.

Charcoal samples were processed with acid-base washes according to standard procedures (http://www.physics.arizona.edu/ams/education/pretreat.htm) and were radiocarbon dated at the University of Arizona AMS facility. Radiocarbon ages were calibrated to calendar years before 1950 with the CALIB 5.0.1 program (Stuiver and Reimer 1993) to obtain date ranges (generally greater than 100 years) and fire probabilities for each year in the range. The probabilities were then summed for graphical analyses. (See Appendix B for details.)

RESULTS: TIMING AND EXTENT OF FIRES IN THE SAWTOOTH VALLEY

Fourteen fires were dated to a year. Stand-replacing fires that were annually resolved burned in multiple watersheds roughly every 100 to 200 years between 1632 and 1933. An additional six fires were dated to the decade. The set of all fires (n = 20), including all sizes and intensities, burned in at least one watershed every 10 to 20 years, with the exception of fire-free periods from 1800 to 1841 and 1890 to 1929. Fire-free periods coincided with combined cool phases of the Atlantic Multidecadal Oscillation (AMO) and July temperature in central Idaho.

Annually resolved fires burned during summers that were significantly warm and dry. Drought-induced fires (PDSI < -1) burned at the tail end of a positive surge of spring Pacific Decadal Oscillation (PDO), including a significantly positive anomaly (> 95% CL) the year before the fire. Most drought-induced fires burned during combined positive phases of spring PDO and decadal AMO. This subset of fires coincided with significantly positive spring PDO the year of the fire and the year before (> 95% and 99% CL, respectively).

Fire-Scar Locations

Fire-scarred sections were cut from 10 Douglas-fir and five lodgepole pine (Figure 4, Table 1). Fire-scarred Douglas-fir generally were found on tops of moraines or in rocky areas, where they were sheltered from stand-replacing fires. Fire-scarred lodgepole were found along a 1933 burn perimeter (Figure 6) and in areas at lower elevations that apparently had burned at low intensity. Most fires were dated to a single year (annual resolution, e.g., 1844). If a fire scar could not be annually resolved (if, for example, injury, rot, or indeterminate ring boundaries precluded exact dating), the scar was considered to be interannually resolved (e.g., ~1844).

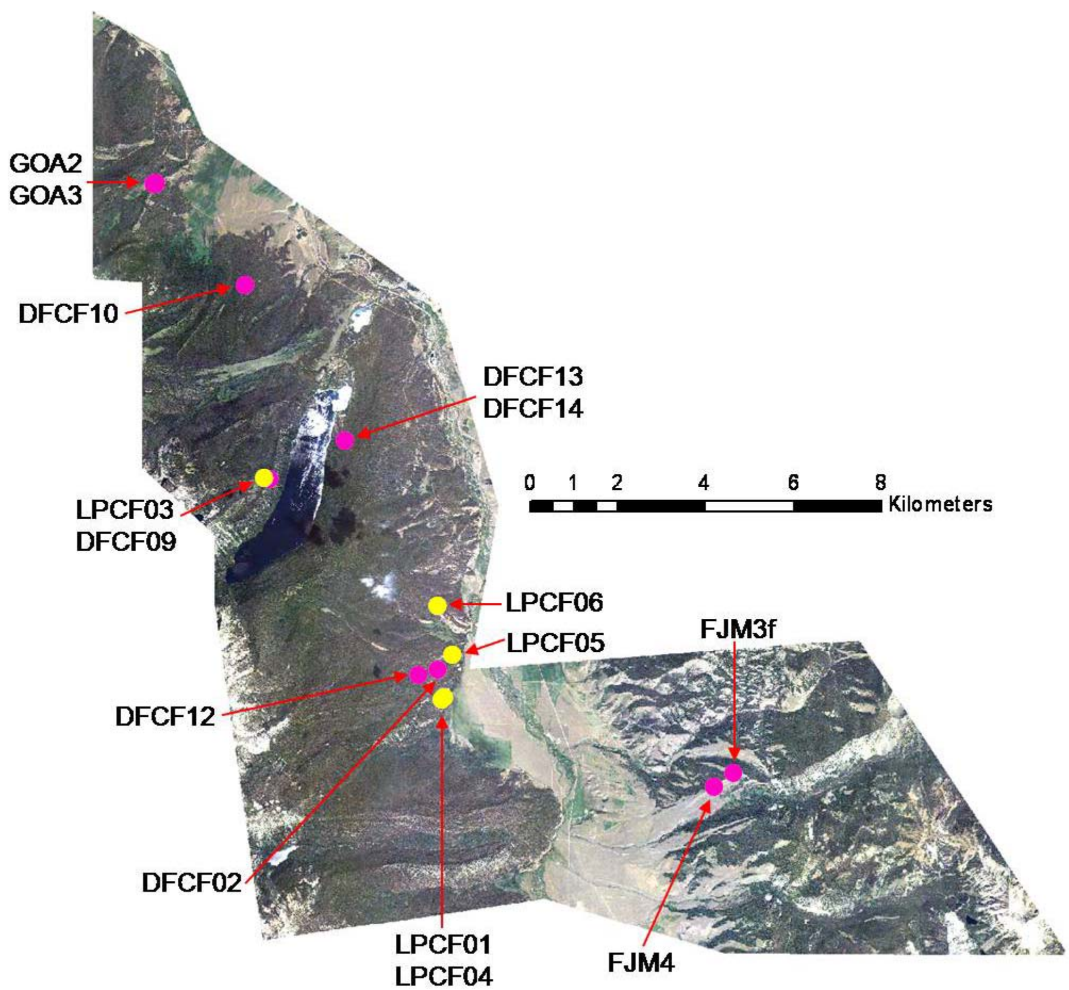

Figure 4. Locations of fire-scarred Douglas-fir (pink) and lodgepole pine (yellow) in the Sawtooth Valley.

Table 1. Locations of fire-scarred Douglas-fir (PSME) and lodgepole pine (PICO). A bracket ([ ) before the First Ring date indicates a pith date; a parenthesis ({) indicates the pith was not included in the section. Trees in the Sawtooth Valley begin putting on latewood in late July or early August.

Tree	Species	Location	lat/lon	Fires	Latewood	First Ring
GOA2	PSME	Goat Creek moraine	44° 11'43"	1842	yes	[1682
			114° 58' 57"	1782	yes	
GOA3	PSME	Goat Creek moraine	44° 11' 42"	1842	?	{1802
			114° 58' 57"			
DFCF10	PSME	Ranger Station	44° 10' 10"	~1799	?	{1587
			114° 57' 00"	1783	?	
				1712	?	
				1686	yes	
				1632	?	
DFCF09	PSME	West Redfish Lake	44° 07' 12"	1842	yes	[1376
			114° 56' 26"	1632	?	
LPCF03	PICO	West Redfish Lake	44° 07' 13"	1933	?	[1846
			114° 56' 32"			
DFCF14	PSME	East Redfish Lake	44° 07' 50"	1734	yes	[1591
			114° 54' 49"	1632	?	
DFCF13	PSME	East Redfish Lake	44° 07' 49"	~1756	?	[1545
			114° 54' 50"	~1632	?	
LPCF06	PICO	Bull Moose Trail	44° 05' 18"	1844	yes	[1790
			114° 52' 52"			
DFCF12	PSME	Near Decker Lake	44° 04' 14"	1739	?	{1257
			114° 53' 12"	1632	?	
				~1500	yes	
				~1428	yes	
LPCF04	PICO	Lower Huckleberry	44° 03' 54"	1799	yes	[1739
			114° 52' 42"	1930	yes	
LPCF01	PICO	Lower Huckleberry	44° 03' 52"	1889	yes	[1743
			114° 52' 43"	1799	yes	
LPCF05	PICO	Lower Decker	44° 04' 31"	1889	yes	[1764
			114° 52' 31"	1844	yes	
DFCF02	PSME	Lower Decker	44° 04' 19"	~1844	?	{1730
			114° 52' 49"			
FJM3f	PSME	4th of July moraine	44° 02' 48"	~1873	?	{1873
			114° 46' 36"			
FJM4	PSME	4th of July moraine	44° 02' 36"	1756	yes	{1611
			114° 47' 1"	1734	yes	
				~1654	yes	

Categorization of Fire Years

Fires were assigned to one of two categories and one of five sub-categories (Table 2). The two categories are **stand-replacing** and **not stand-replacing**. The distinction is somewhat artificial in that evidence of older stand-replacing fires might no longer exist or might not have been found if it did exist. The two sub-categories of stand-replacing fire are **single-watershed** and **multi-watershed**. Most watersheds in the study area are ~1000 ha, ranging between 200 and 1700 ha. Some single-watershed fires appear to have burned large portions of the watershed (e.g., 1739, ~ 700 ha), whereas others apparently burned only small portions (e.g., 1933, <100 ha), meaning this sub-category contains considerable variation in area burned. Multi-watershed fires were the paleoanalogues of the 2005 Valley Road Fire. At least one fire-scarred tree needed to be associated with an even-aged lodgepole stand (or, in the case of the 1632 fires, with survivor trees of similar age) for a multi-watershed fire to be categorized as stand-replacing. Multi-watershed fires were not necessarily one large fire, but might have been separate fires ignited by multiple lightning strikes (or ignitions by humans) during a year in which climate was conducive to fire. As with single-watershed fires, multi-watershed fires vary considerably in area burned. Fire-scarred trees in four watersheds and lodgepole germination dates in a fifth watershed suggest the fires of 1632 were at least as intense and extensive as the Valley Road Fire of 2005 (~17,000 ha), whereas two lodgepole stands dating to the 1880s indicate burn patches of high severity but small extent (likely <100 ha together).

The sub-categories of fires that were not stand-replacing are **low-intensity**, **point (single watershed)**, and **point (multi-watershed)**. Low-intensity fires burn surface fuels and scar trees, but do not produce pulses of regeneration in lodgepole forests and therefore do not affect age structure (Sibold *et al.* 2007). If two or more fire-scarred lodgepole did not appear to be part of a paleofire perimeter and were not associated with a younger, even-aged cohort, the fire was categorized as low-intensity. Point fires refer to fire-scarred Douglas-fir not associated with an even-aged lodgepole cohort.

Table 2. Fire years by category. A simple date (e.g., 1632) means the fire was dated to a single year (annually resolved). An approximate date (e.g., ~1844) means the fire was interannually resolved. Two lodgepole stands that were replaced by fire but not associated with fire-scarred trees dated to the 1880s.

Stand-Replacing		Not Stand-Replacing		
Multi-Watershed	Single-Watershed	Point		Low-Intensity
1632	1739	Single-Watershed	Multi-Watershed	
1842	1783	~1654	1734	1799
1880s	~1873	1686		1844
	1933	1712		1889
		~1756		
		1756		
		1782		
		~1799		
		1930		

Locations of Annually Resolved Fires

<u>Stand-Replacing Fires</u>

Multi-watershed fires burned in 1632 and 1842 (Figure 5). Fire scars dating to 1632 were found in four watersheds, making 1632 the year with the largest number of watersheds burned. A lodgepole pine in the Huckleberry watershed has an estimated germination date (EGD) of 1635, the oldest lodgepole cored in the study area. Two other lodgepole in the same plot (Plot 5) have EGDs of 1657 and 1666. If these lodgepole were part of the cohort that germinated after the fires of 1632, the area burned would be extended to five watersheds.

The fires of 1842 burned in at least two watersheds and coincided with a pulse of regeneration across the lodgepole plots (Figure 12). Lodgepole Plot 12 and a fire-scarred Douglas-fir (DFCF09) west of Redfish Lake (Figure 6) confirm that the fire was stand-replacing in that watershed. Two fire-scarred Douglas-fir (GOA2, 3) on a moraine over Goat Creek also record fires in 1842 (Figure 4). The five largest lodgepole surrounding GOA2 are uneven in age, though the oldest EGD, 1847, likely was associated with the fires of 1842.

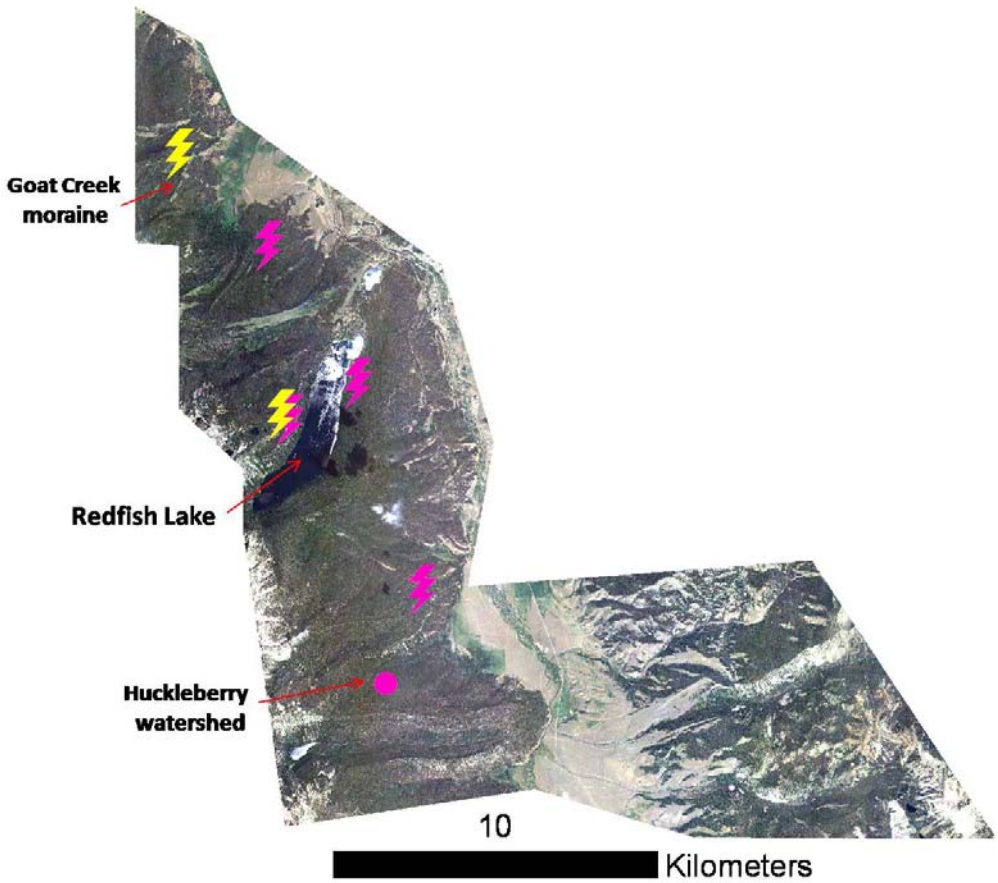

Figure 5. Multi-watershed fires burned in 1632 (pink) and 1842 (yellow). The pink circle (Huckleberry Watershed) represents a lodgepole pine, the oldest in the study area, with an estimated germination date of 1635; if this tree germinated after the fires of 1632, the area burned would be extended into a fifth watershed.

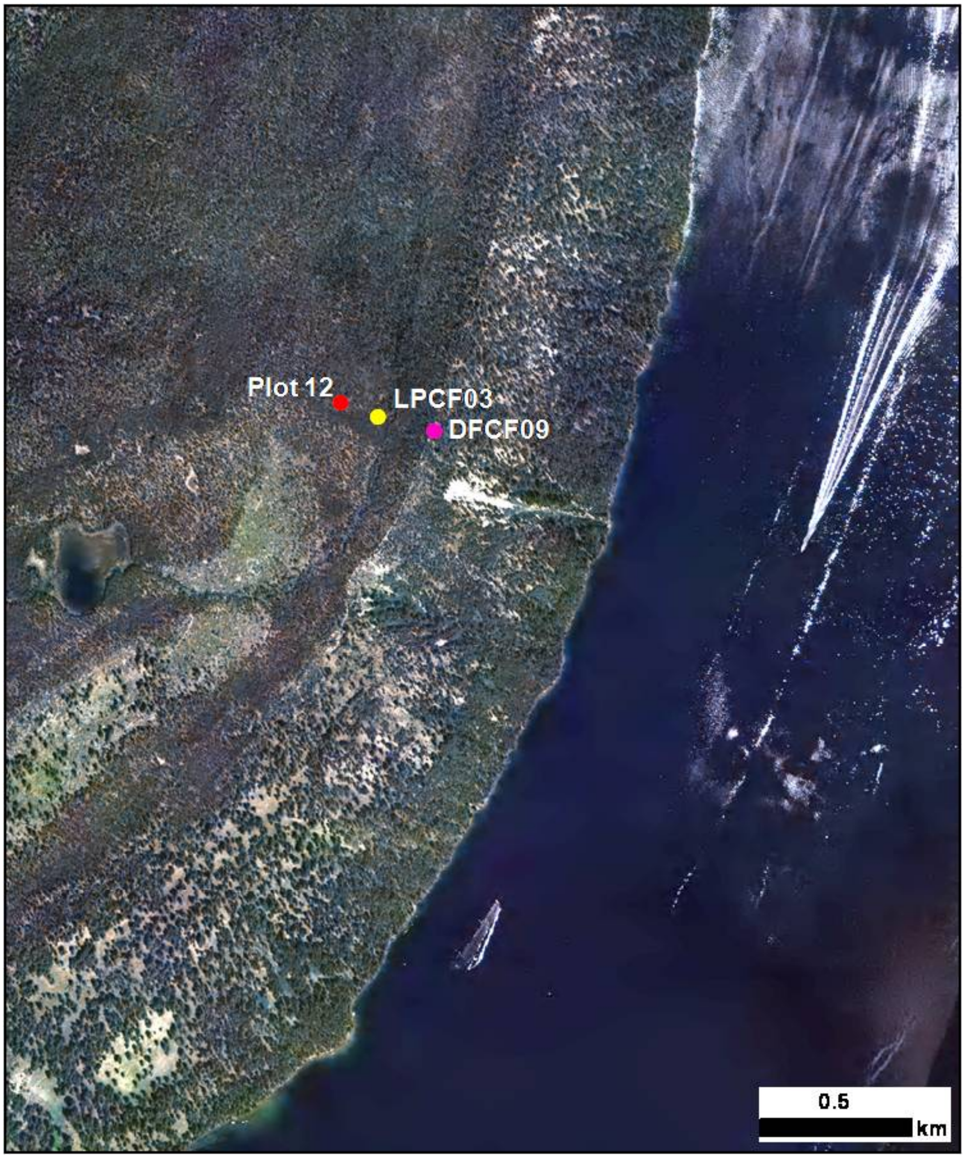

Figure 6. A fire-scarred Douglas-fir (DFCF09, pink dot) records a fire in 1842 west of Redfish Lake. Lodgepole Plot 12 (red dot) represents a stand that is even in age, with oldest estimated germination date (EGD) 1844. A fire-scarred lodgepole pine (LPCF03, yellow dot) records a fire in 1933 and was part of the even-aged cohort that germinated after the fires of 1842 (EGD 1846). LPCF03 is part of a burn perimeter separating the 1840s and 1850s trees of Plot 12 from a younger cohort to the south that germinated after the fire of 1933.

Single-watershed fires burned in 1739, 1783, and 1933 (Figure 7). A fire-scarred Douglas-fir (DFCF12) in the Decker watershed records the 1739 fire, which appears to have burned much of the watershed (Figure 8), as evidenced by even-aged Plot 3 (oldest EGD 1739) and by survivor trees in Plot 1 (oldest EGD 1738), Plot 2 (oldest EGD 1742), Plot 8 (oldest EGD 1739), and Plot 22 (oldest EGD 1739).

A fire-scarred Douglas-fir (DFCF10) near the Ranger Station (Figure 9) records the 1783 fire, which coincided with a small pulse of regeneration across the lodgepole plots (Figure 12) and was confirmed to have been stand-replacing by the even-aged cohort in Plot 15 (oldest EGD 1789).

The fire of 1933 was confirmed as stand-replacing because the fire-scarred lodgepole (LPCF03) was part of a perimeter of fire-scarred lodgepole separating the older trees in Plot 12 (which germinated after the 1842 fire) from a younger cohort to the south, which were not cored because they appeared (based on smaller size and higher density) to have germinated after the fire of 1933 (Figure 6).

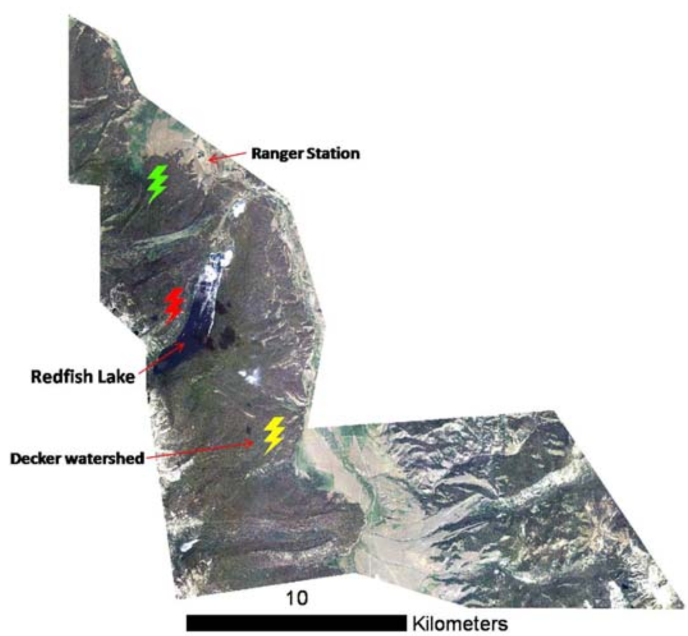

Figure 7. Single-watershed fires burned in 1739 (yellow), 1783 (green), and 1933 (red).

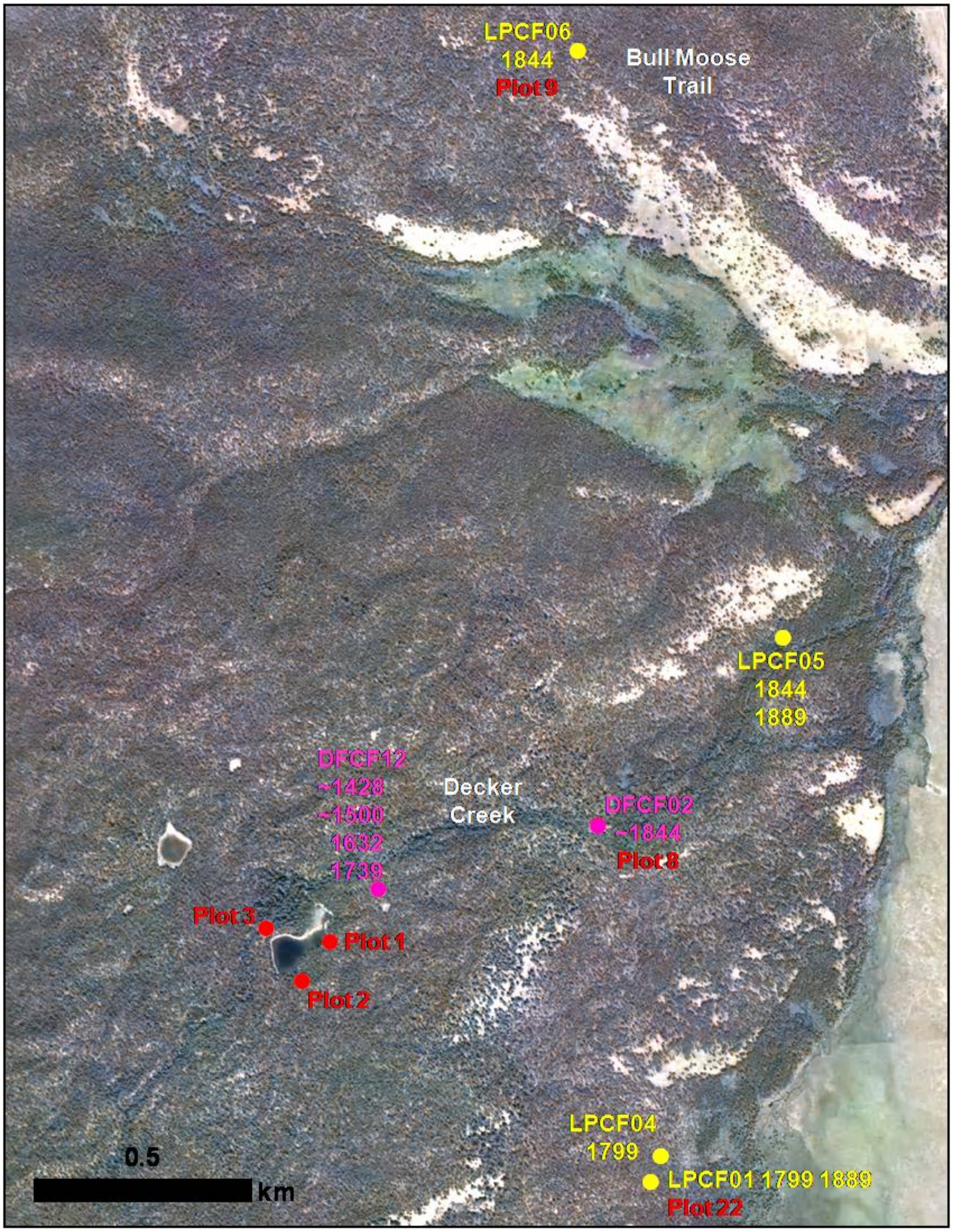

Figure 8. Fire history in the Decker watershed. Fire-scarred Douglas-fir (pink) and lodgepole pine (yellow) record fires of both high and low intensity. Fire intensity was inferred from lodgepole plots (red).

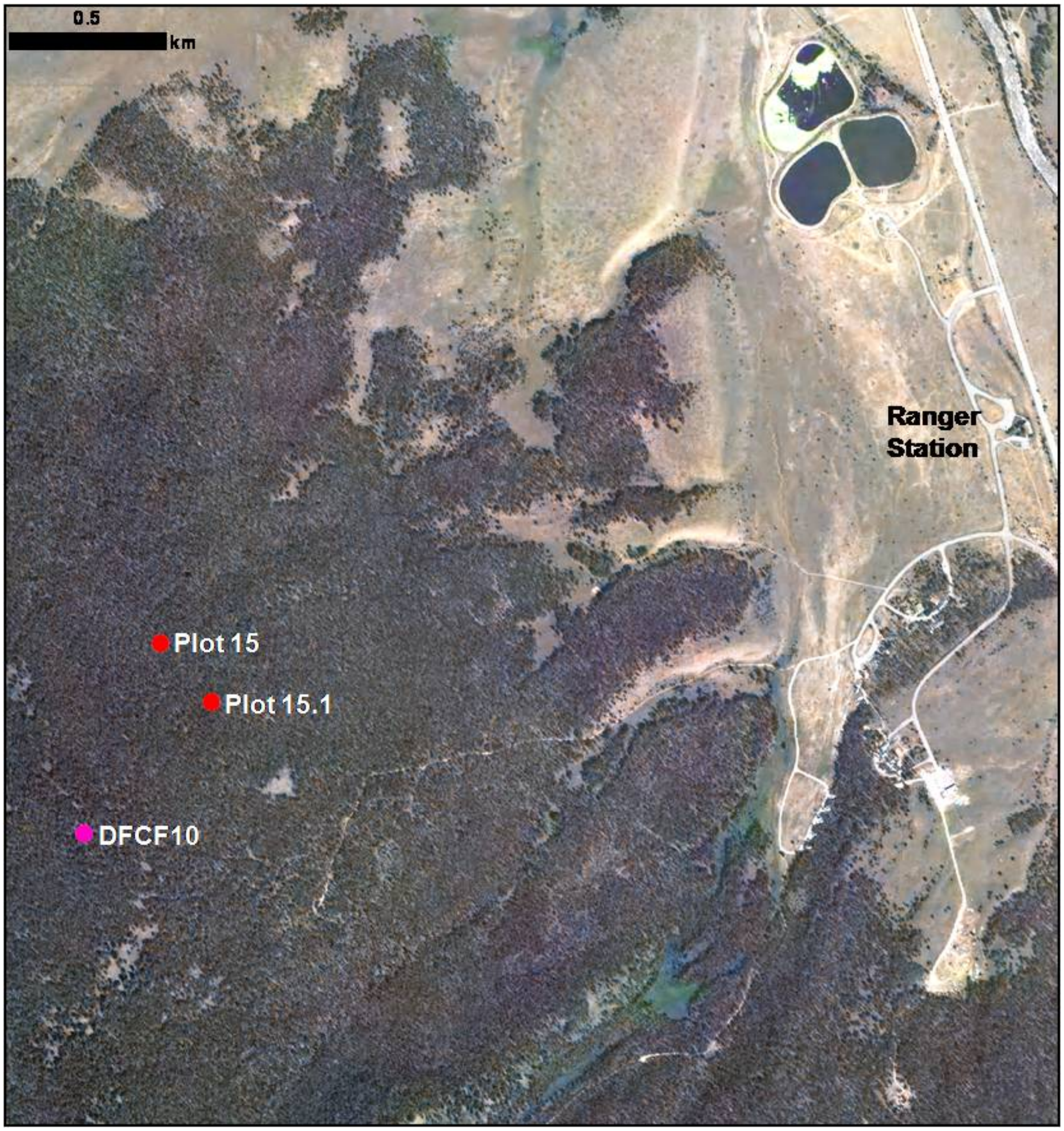

Figure 9. A fire-scarred Douglas-fir (DFCF10) southwest of the Ranger Station records a fire in 1783. Plot 15 contains an even-aged cohort with oldest estimated germination date 1789. Plot 15.1 is an even-aged stand dating to the 1880s, but does not appear to have been replaced by fire.

Fires That Were Not Stand-Replacing

Fires in 1799 and 1844 (figures 8 and 10) were not associated with a pulse of regeneration in nearby lodgepole and were therefore categorized as low-intensity. A scarred lodgepole dating the 1889 fire (figures 8 and 10) was at the center of a plot showing a pulse of regeneration in the 1910s. Because the pulse of regeneration occurred 10 to 20 years after the 1889 fire, the fire was categorized as low-intensity.

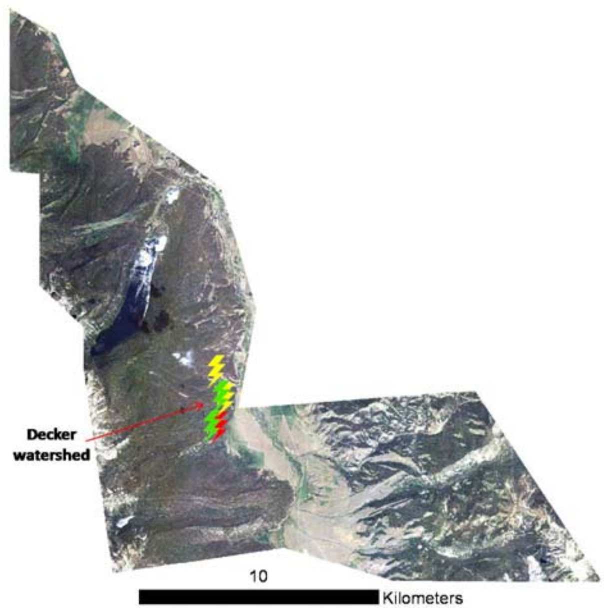

Figure 10. Low-intensity fires burned in 1799 (red), 1844 (yellow), and 1889 (green).

Point fires burned in 1686, 1712, 1734, 1756, 1782, and 1930 (Figure 11). Because five of six of these fires burned before 1800, some likely were stand-replacing, but no evidence has survived or was found. The possibility cannot be excluded, therefore, that the fires of 1734, which burned in two different watersheds on opposite sides of the valley, were stand-replacing, multi-watershed fires. If so, then stand-replacing, multi-watershed fires would have burned in 1632, 1734, and 1842, meaning these fires would have burned roughly every 100 to 200 years (depending on whether 1734 is included).

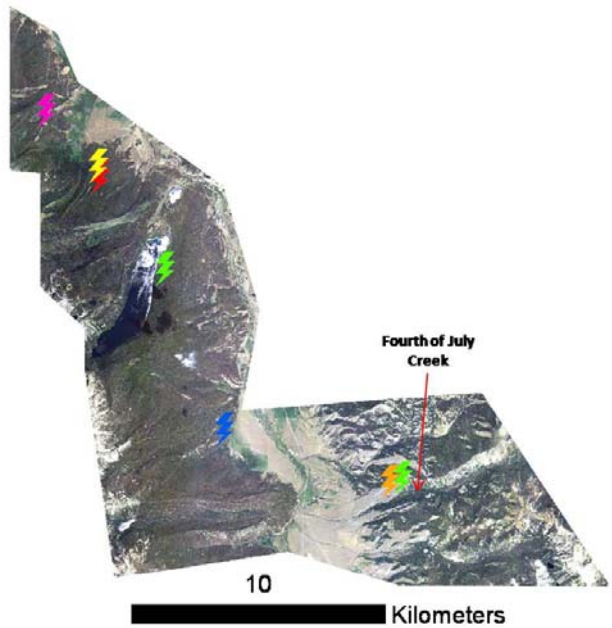

Figure 11. Point fires burned in 1686 (red), 1712 (yellow), 1734 (green), 1756 (orange), 1782 (pink), and 1930 (blue).

Lodgepole Pine Regeneration

Pulses of regeneration across lodgepole plots coincided with fires in 1632, 1739, 1783, and 1842 (Figure 12). The large pulse of regeneration in the 1880s was due in part to small burn patches that were not associated with fire-scarred trees (indicating the fires were not large in area). Plot 15.1 (Figure 9) also dates to the 1880s, but the absence of fire-scarred trees or surface charcoal and the presence of narrow rings near most of the piths suggest the stand was not replaced by fire. The death date (1887) of a whitebark pine (*Pinus albicaulus*) in a nearby Sawtooth/Salmon River study area was categorized as a “probable” beetle kill based on the presence of blue-stain fungi associated with mountain pine beetle (Perkins and Swetnam 1996). The coincidence of the death of this tree with the pulse of regeneration in the Sawtooth Valley in the 1880s supports the hypothesis of a pine-beetle epidemic during that decade.

Perkins and Swetnam (1996) attributed the 1819 death of a whitebark pine to mountain pine beetle based on the presence of beetle galleries on the stem, suggesting that the pulse of regeneration across lodgepole plots (Figure 12) in the Sawtooth Valley in the 1810s and 1820s (which was not associated with a known fire-scar date) was the result of an earlier pine-beetle epidemic. Lodgepole plots in the Sawtooth Valley were targeted to find even-aged stands that had been replaced by fire. For future research, a random selection of plots across the study area might prove more efficacious at identifying pulses of regeneration resulting from pine-beetle epidemics, which will not necessarily appear as even-aged stands on an aerial photo. Such sampling would help answer the question of whether lodgepole regeneration in the Sawtooth Valley has been driven more by fire or by mountain pine beetle.

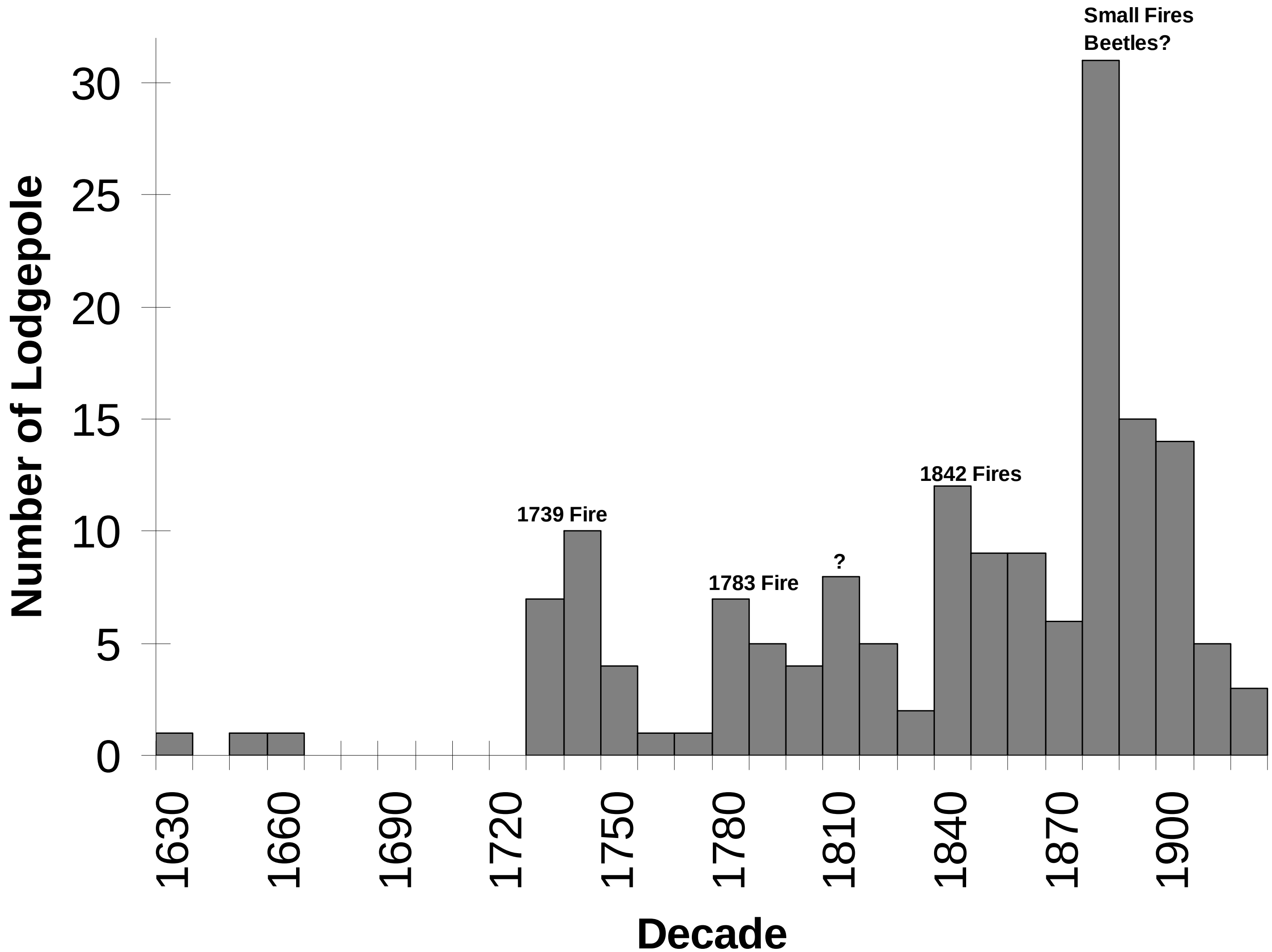

Figure 12. Across all plots, regeneration in lodgepole pine (number of trees per decade) followed stand-replacing fires in 1632, 1739, 1783, and 1842.

Fire by Decade

Fires that were dated to a year, approximately to a year, or to a decade were combined to quantify the number of watersheds burned by decade (Figure 13). This categorization includes all known fires, regardless of size or intensity (n = 20). Between the fires of 1632 and the 1930s, no more than two consecutive decades passed without fire in at least one watershed, with the exception of apparently fire-free intervals from 1800 to 1841 and 1890 to 1929.

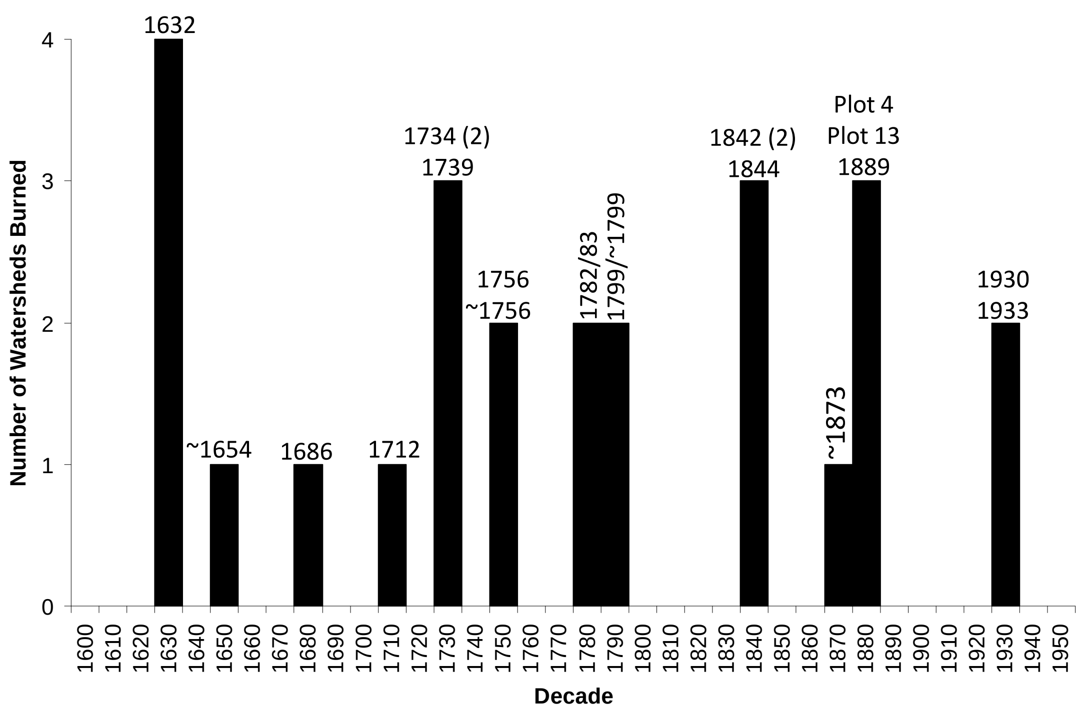

Figure 13. Number of watersheds burned by decade. Dates above bars are annually or interannually resolved dates from fire scars. Numbers in parentheses clarify the number of watersheds burned in particular years. Plots above bars indicate stands that were replaced by fire, but not associated with fire-scarred trees.

Statistical Analyses of Annually Resolved Fires

Reconstructed drought and temperature were compared in superposed epoch analysis (SEA) with the 14 annually resolved fire years, but reconstructed sea surface temperature (SST) oscillations were compared only with the 11 fires that burned during years of significant drought (referred to henceforth as drought-induced fires). Significant drought was defined as a negative anomaly of the Palmer Drought Severity Index (PDSI, Cook *et al.* 2004) the year of the fire that exceeded the 95% confidence level (PDSI < -1), as determined by SEA (n = 14). Drought-induced fires burned in 1632, 1686, 1712, 1739, 1756, 1782, 1783, 1842, 1889, 1930, and 1933. Fires that did not burn during significant drought (1734, 1799, 1844) were excluded from comparisons with SSTs because non-drought variables such as age structure, fuel accumulation, or ignitions (natural or human) might have been more influential than drought. Inclusion of these fires would have muddied the climatic signal, potentially masking significant relationships between SSTs and drought-induced fire. The 11 drought-induced fires include all five fires known to have been stand-replacing; none of the three fires that were excluded appear to have been stand-replacing.

Drought

Reconstructed summer PDSI (point 69, central Idaho, Cook *et al.* 2004) was compared with the 14 annually resolved fires in SEA to determine if fires burned during significantly dry years. On the PDSI index anomalously wet years are assigned positive values and anomalously dry years are assigned negative values. Values generally range between +6 and -6. Values between -1 and -1.9 are categorized as mild drought, between -2 and -2.9 as moderate drought, between -3 and -3.9 as severe drought, and values of -4 or less are categorized as extreme drought (Palmer 1965). These classifications are arbitrary and have no connection with a finding of significance in SEA.

Fire years (year 0) were significantly dry (> 99.9% CL) between 1600 and 1950 (Figure 14, Cook *et al.* 2004). The year after the fire (year +1) also was significantly dry (> 99% CL).

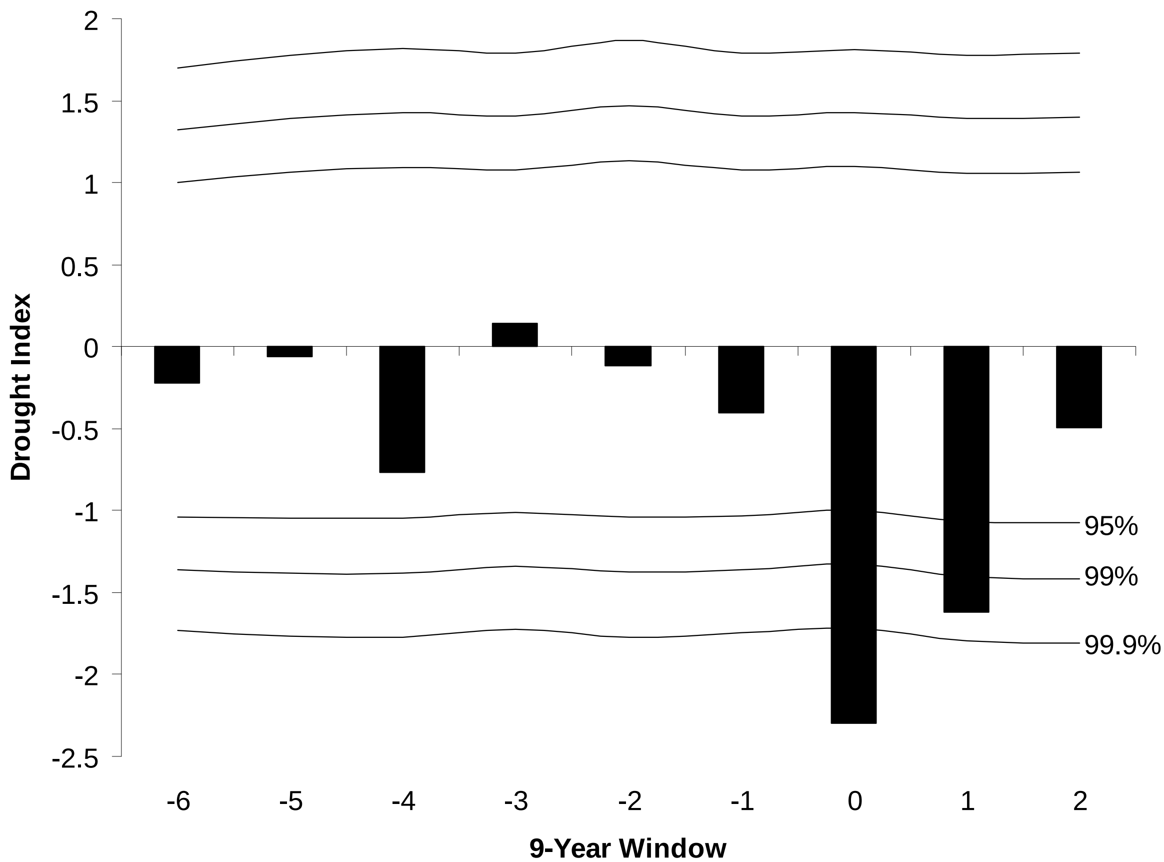

Figure 14. Reconstructed PDSI (Cook *et al.* 2004) was significantly dry (> 99.9% CL) the year of the fire (year 0) between 1600 and 1950 (n = 14). Autocorrelation: first order = 0.20, second order = 0.00, third order = -0.09.

Temperature

To determine if the 14 annually resolved fires burned during significantly warm years, I tested two different tree-ring temperature reconstructions in SEA. Briffa *et al.* (1992) reconstructed annual temperature from latewood densities as a set of grid points across the western United States. The index reports anomalies in degrees Celsius from the instrumental mean, with positive and negative values representing anomalously warm and cool years, respectively. I tested the two grid points that are closest (both ~400 km) to the Sawtooth Valley. Point 13 is centered on the west side of the Washington Cascades (Pacific Northwest); point 14 is centered near Yellowstone National Park (central Rocky Mountains). Only point-14 temperatures coincided significantly with fire in the Sawtooth Valley. Biondi *et al.* (1999/2006) reconstructed July temperature at sites in the Salmon River/Sawtooth area of central Idaho using whitebark pine and Douglas-fir. The index is based on standard deviations from the mean temperature of the instrumental period.

Annual temperature (Briffa *et al.* 1992) and July temperature (Biondi *et al.* 1999/2006) were significantly warm (> 95% and 99.9% CL, respectively) the year of the fire (figures 15 and 16). July temperature also was significantly warm the year after the fire (> 95% CL).

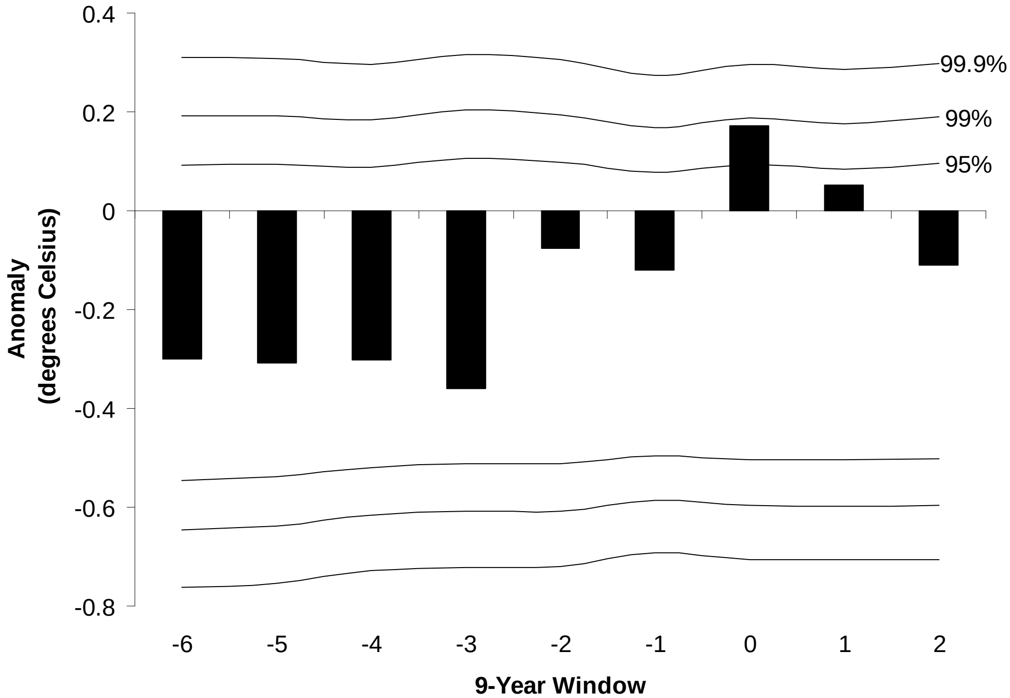

Figure 15. Reconstructed annual temperature (point 14, Briffa *et al.* 1992) was significantly warm (> 95% CL) the year of the fire (year 0) between 1600 and 1950 (n = 14). Autocorrelation: first order = 0.12, second order = 0.12, third order = 0.09.

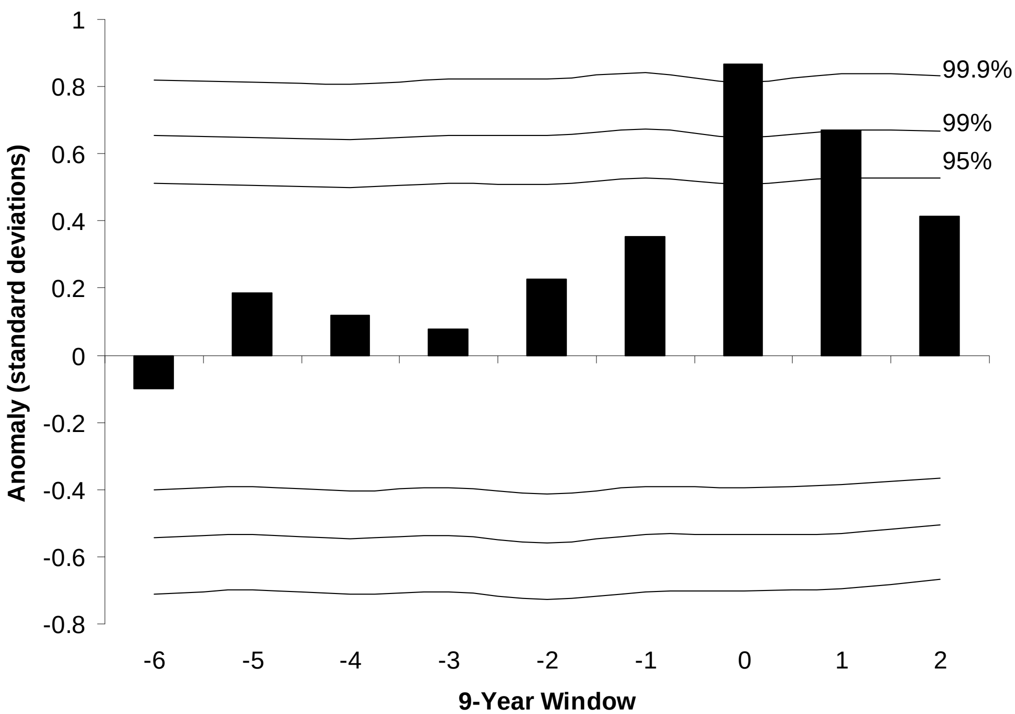

Figure 16. Reconstructed July temperature for central Idaho (Biondi *et al.* 1999/2006) was significantly warm (> 99.9% CL) the year of the fire (year 0) between 1600 and 1950 (n = 14). Autocorrelation: first order = 0.53, second order = 0.14, third order = 0.18.

Sea Surface Temperature (SST) Oscillations

Pacific Decadal Oscillation (PDO)

PDO wavelengths range from interannual to multidecadal to centennial (e.g., Mantua *et al.* 1997; Minobe 2000; D'Arrigo and Wilson 2006; Shen *et al.* 2006). To test if drought-induced fires coincided with significant anomalies of spring PDO, I used the Asian spring (March, April, May) PDO reconstruction of D'Arrigo and Wilson (2006), the only spring PDO reconstruction available. Because no available reconstruction focuses only on the summer, winter, or fall season, the next best choice was a reconstruction of annual PDO. Two reconstructions of annual PDO extend far enough back to cover all fire years. Shen *et al.* (2006) reconstructed PDO from historical records of summer rainfall in eastern China. MacDonald and Case (2005) reconstructed PDO from trees in California and Alberta, Canada. Because Shen *et al.* (2006) is much less autocorrelated than MacDonald and Case (2005), which possesses first-order autocorrelation greater than 0.7, I used Shen *et al.* (2006) in SEA. On a seven-year moving average, Shen *et al.* (2006) and MacDonald and Case (2005) agree on the sign of nine of 11 drought-induced fires (82%). Year by year, the two reconstructions agree on the sign of seven of 11 fires (64%), implying that locations on opposite sides of the Pacific bias annual responses to PDO (though this disagreement at the annual level might also result from the large differences in autocorrelation). The moderately autocorrelated annual PDO reconstruction of D'Arrigo *et al.* (2001) extends back only to 1700, but I tested it in SEA to provide an eastern Pacific (mostly trees from coastal Alaska) alternative to the western Pacific perspective of Shen *et al.* (2006). Year by year, the eastern Pacific reconstructions of D'Arrigo *et al.* (2001) and MacDonald and Case (2005) show 56% agreement on the sign of drought-induced fires; agreement between D'Arrigo *et al.* (2001) and Shen *et al.* (2006), reconstructed from opposite sides of the Pacific, also is 56%.

Annual PDO Reconstructed from Western Pacific Records. Shen *et al.* (2006) shows a strongly negative (but non-significant) surge in the three years leading up to drought-induced fires and a significantly negative anomaly (> 95% CL) six years before (Figure 17). A second SEA (not shown) in a 15-year window (12 years leading up to the fire) calculated years -7 through -12 as near normal, indicating that the negative surge in the 9-year window was a unique event associated with fire and not a persistent autocorrelation in the PDO cycle. Shen *et al.* (2006) was also compared with the subset of fires known to have been stand-replacing (1632, 1739, 1783, 1842, 1933). Year -1 was strongly negative, but no year in the nine-year window departed significantly (results not shown).

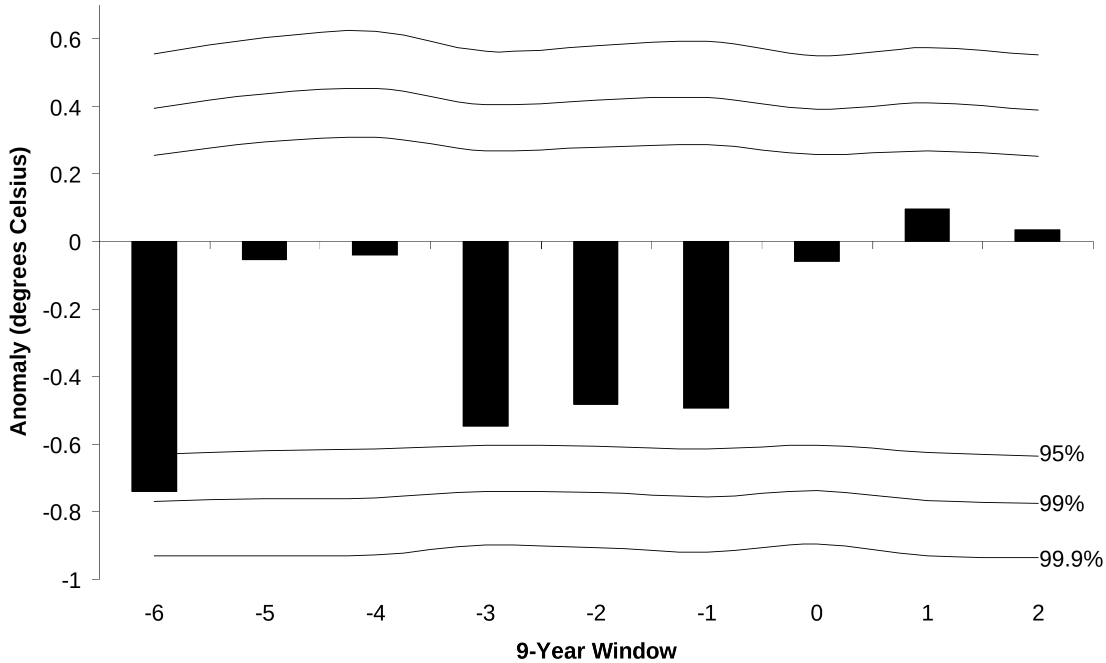

Figure 17. Drought-induced fires were preceded six years before (year -6) by significantly negative (> 95% CL) annual PDO reconstructed from western Pacific records (Shen *et al.* 2006) on the interval between 1600 and 1950 (n = 11). Autocorrelation: first order = 0.09, second order = 0.01, third order = 0.06.

Annual PDO Reconstructed from Eastern Pacific Records. D'Arrigo *et al.* (2001) did not depart significantly in any year of the nine-year window when compared with drought-induced fires (Figure 18) or with fires known to have been stand-replacing (results not shown).

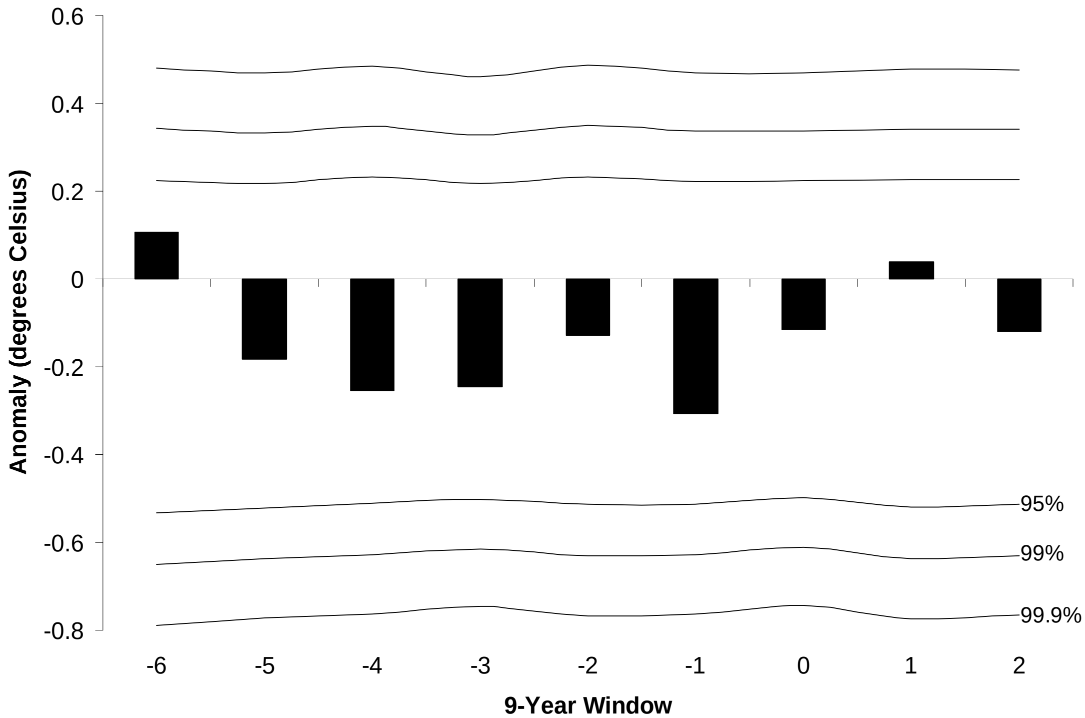

Figure 18. Drought-induced fires did not coincide significantly with annual PDO reconstructed from eastern Pacific records (D'Arrigo *et al.* 2001) in any year of the nine-year window on the interval between 1700 and 1950 (n= 9). Autocorrelation: first order = 0.37, second order = 0.27, third order = 0.04.

Spring PDO. D'Arrigo and Wilson (2006) was significantly positive (exceeding the 95% confidence level) the year before the fire (year -1, Figure 19). When spring PDO was compared with the subset of drought-induced fires known to have been stand-replacing, the results (not shown) were similar to Figure 19. Observed spring PDO (average values in the nine-year window when fire was at year 0, black bars in figures 19 and 20) was more positive than expected compared with values generated from 1000 random simulations in SEA (Figure 20, gray bars), indicating that fires coincided with a positive surge in spring PDO in the nine-year window.

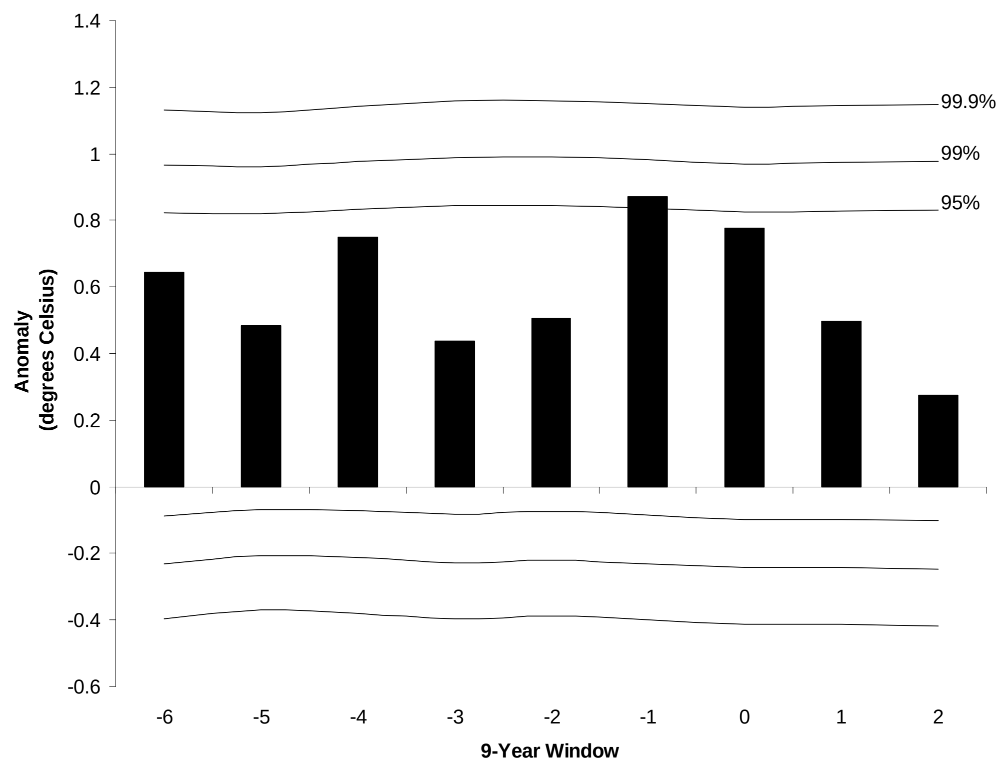

Figure 19. Reconstructed spring PDO (D'Arrigo and Wilson 2006) was significantly positive (>95% CL) the year before the fire (year -1) between 1600 and 1950 (n = 11). Autocorrelation: first order = 0.60, second order = 0.02, third order = 0.09.

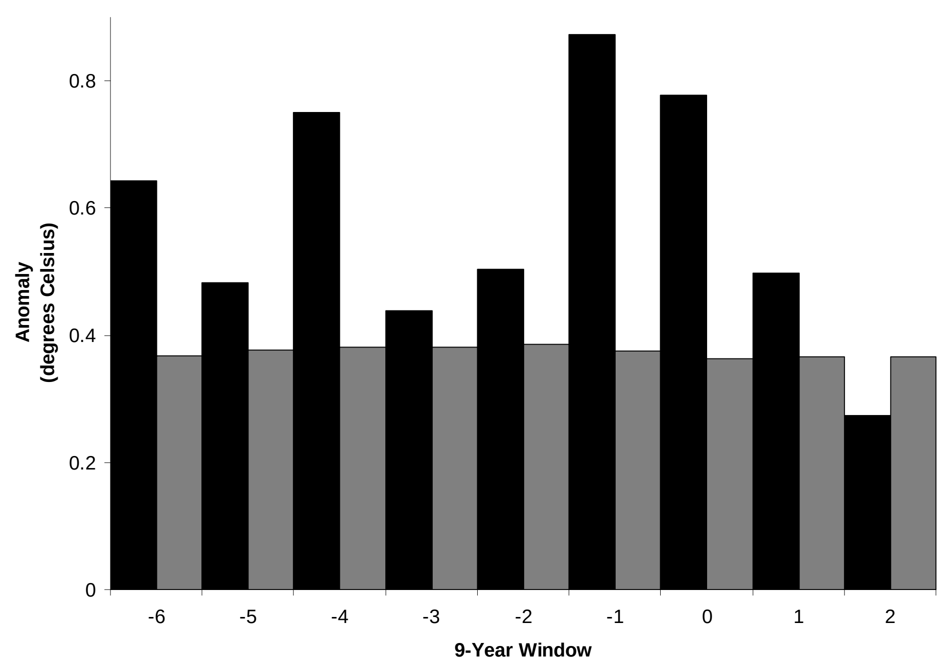

Figure 20. Reconstructed spring PDO (D'Arrigo and Wilson 2006) was more positive than expected in the years leading up to the fire. Black bars are average spring PDO for 9-year windows with fire in year 0. Gray bars are the expected values generated from 1000 random simulations in SEA.

Combined Phases of PDO and Atlantic Multidecadal Oscillation (AMO)

During the 20th century the two leading principal components of multidecadal drought frequency (explaining 52% of total variation) in the United States were correlated, respectively, with the PDO and AMO; drought frequency in the northwest was most strongly correlated with combined positive phases (McCabe *et al.* 2004). In the Sawtooth Valley most drought-induced fires burned during combined positive phases of spring PDO (D'Arrigo and Wilson 2006) and decadal AMO (AMO Index, reconstructed from the rings of AMO-sensitive trees on both sides of the Atlantic, Gray *et al.* 2004). This suggests that the strongest climatic connection for most drought-induced fires was a significantly positive anomaly of spring PDO the year of the fire in the context of a positive phase of decadal AMO, while fires that burned during mixed phases are better explained by some other climatic connection (e.g., ENSO). I compared in SEA the subset of drought-induced fires that burned during the plus-plus phase combination of spring PDO and the AMO Index with spring PDO. (Climatic anomalies during fire years are reported in Table 3.) To create this subset, I excluded 1712 (spring PDO positive, AMO Index neutral), 1842 (spring PDO positive, AMO Index negative), and 1889 (spring PDO negative, AMO Index positive).

Eight of 11 drought-induced fires (including 4 of 5 fires known to have been stand-replacing) burned during years when spring PDO and the AMO index were both positive (Table 3). Spring PDO during this subset of years—1632, 1686, 1739, 1756, 1782, 1783, 1930, and 1933—was significantly positive the year of the fire and the year before (> 95% and 99% CL, respectively, Figure 21).

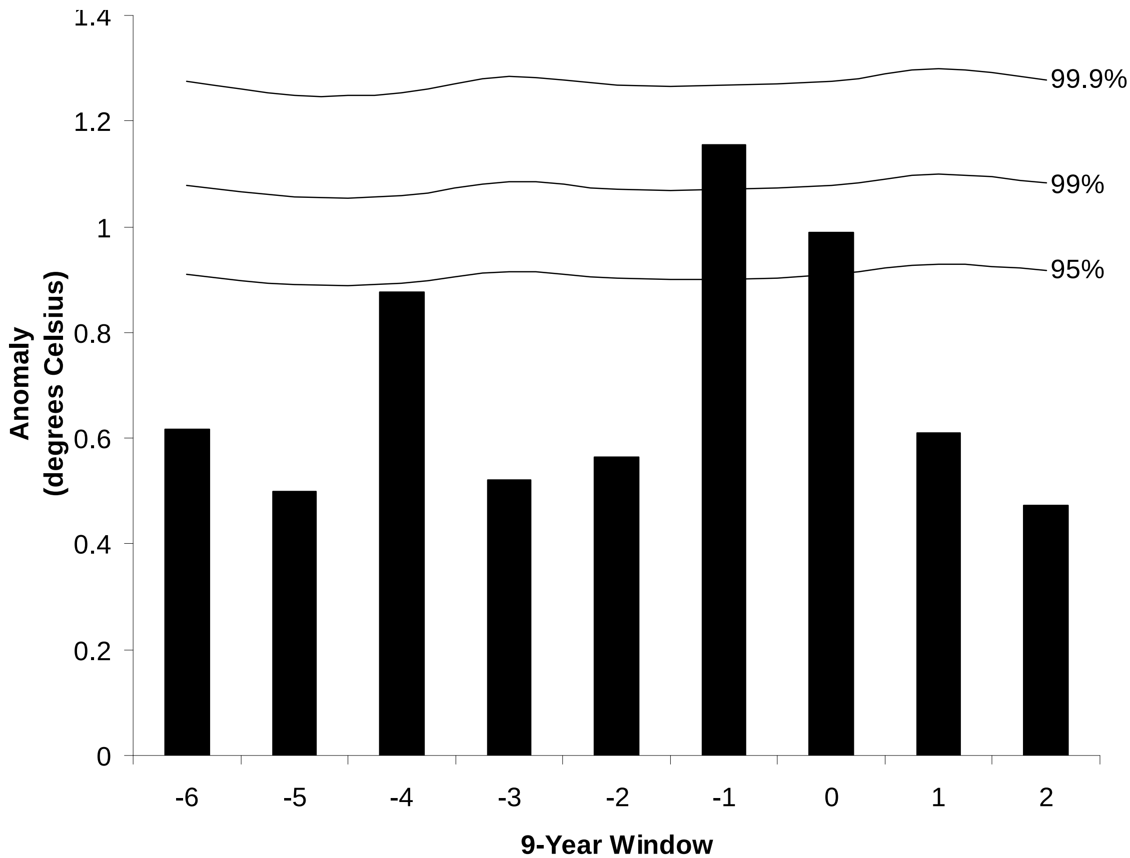

Figure 21. Reconstructed spring PDO was significantly positive the year of the fire (year 0, >95% CL) and the year before (year -1, > 99% CL) when year 0 coincided with combined positive phases of the AMO Index (Gray *et al.* 2004) and spring PDO (D'Arrigo and Wilson 2006) between 1600 and 1950 (n = 8). Autocorrelation: first order = 0.60, second order = 0.02, third order = 0.09.

El Niño-Southern Oscillation (ENSO)

The "classic" ENSO wavelength is between two and eight years (D'Arrigo *et al.* 2005), meaning ENSO oscillates at higher frequencies than the PDO. To test whether fires coincided with significant anomalies of ENSO, I used the D'Arrigo *et al.* (2005) reconstruction of the Niño-3 zone of the eastern Pacific for the winter season (December, January, February), based on tree rings from the southwestern United States and northern Mexico. I used the Gergis and Fowler (2009) reconstruction of El Niño/La Niña events as a second proxy in the interpretation of individual fire years. Gergis and Fowler (2009) is a multi-proxy reconstruction, based on tree rings from both sides of the Pacific, corals, an ice core from Peru, and documentary records from various locations. This multi-proxy record is calibrated to the Coupled ENSO Index, a combination of the Southern Oscillation Index (which measures atmospheric pressure) and Niño 3.4 (which measures sea-surface temperature).

Winter Niño-3. D'Arrigo *et al.* (2005) was significantly negative (exceeding the 95% confidence level) the year before the fire (year -1) between 1600 and 1950 (Figure 22). When winter Niño-3 was compared with the subset of fires known to have been stand-replacing, the results (not shown) were similar to Figure 22, except that the significantly negative anomaly shifted from year -1 to year -6.

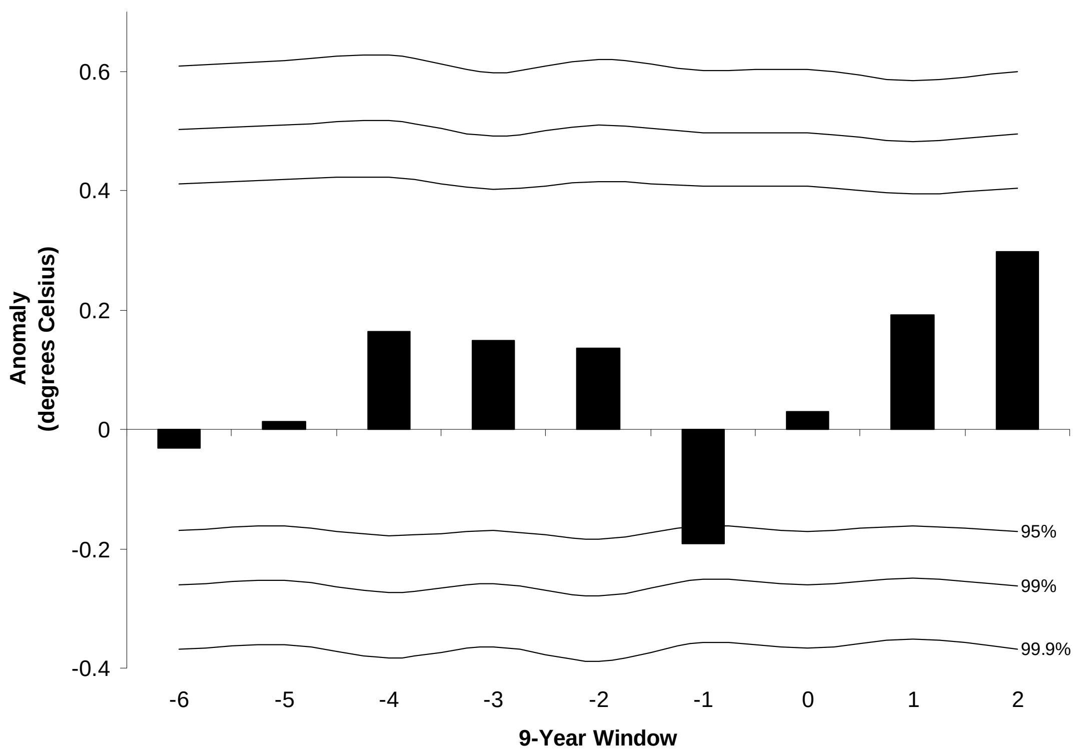

Figure 22. Drought-induced fires were preceded the year before (year -1) by significantly negative (> 95% CL) reconstructed winter Niño-3 (D'Arrigo *et al.* 2005) between 1600 and 1950 (n = 11). Autocorrelation: first order = 0.14, second order = -0.32, third order = -0.05.

Combined Phases of Seven-Year PDO and Winter Niño-3

McCabe and Dettinger (2002) identified two principal components (PCs) of interannual variation in April 1 snowpack in the western United States; the two PCs explain 61% of snowpack variability. The first PC (explaining 45%) correlates with interannual variations in the PDO; the second PC (explaining 16%) correlates with a combination of decadal PDO and interannual ENSO. Gershunov and Barnett (1998) found that combined same-sign phases of PDO and ENSO synergize to increase the strength and consistency of the signal, but that mixed-sign combinations are weaker and less consistent. To test the hypothesis that combined same-sign phases of the PDO and ENSO coincided with drought-induced fires, I isolated four subsets of fires that burned during combined phases of seven-year-averaged PDO (referred to henceforth as 7-year PDO) and annually resolved winter Nino-3 (D'Arrigo *et al.* 2005). I then compared the fire subsets with winter Niño-3 in SEA. The finding of McCabe and Dettinger (2002) was that the second PC of snowpack involved decadal PDO, but I tested seven-year PDO because Figure 17 shows that a surge of negative PDO in years -6 through -1 was associated with fire in year 0. To determine the sign of seven-year PDO (Table 3), I calculated seven-year moving averages for three annual PDO reconstructions: D'Arrigo *et al.* (2001), MacDonald and Case (2005), and Shen *et al.* (2006). Sign was assigned based on agreement of at least two of three reconstructions. Because D'Arrigo *et al.* (2001) extends back only to 1700, fires in the 1600s required agreement between both MacDonald and Case (2005) and Shen *et al.* (2006).

Of the 11 drought-induced fires, four burned during years when seven-year PDO (D'Arrigo *et al.* 2001; MacDonald and Case 2005; Shen *et al.* 2006) and winter Niño-3

(D'Arrigo *et al.* 2005) were both negative (1632, 1739, 1782, 1842); four burned when seven-year PDO was negative and winter Niño-3 was positive (1712, 1756, 1783, 1889); two burned when both signs were positive (1686 and 1930); and one burned when seven-year PDO was positive and winter Niño-3 was negative (1933). Because SEA requires at least three fire dates, testing the combined phases of PDO (+) / Niño-3 (+) and PDO (+) / Niño-3 (-) was not an option, but the combined phases of PDO (-) / Niño-3 (-) and PDO (-) / Niño-3 (+) were tested.

Winter Niño-3 (D'Arrigo *et al.* 2005) was significantly negative (> 95% CL) the year of the fire (year 0) and six years before (year -6) when fire in year 0 coincided with combined negative phases of seven-year PDO and winter Niño-3 (Figure 23), confirming that combined same-sign phases synergize to increase strength and consistency of signal (Gershunov and Barnett 1998). The positive anomaly of winter Niño-3 two years after the fire nearly equaled the upper limit of the 95% confidence level, indicating a strong variability in Niño-3 amplitudes in the nine-year window.

Gergis and Fowler (2009) reconstructed 1632 as an "extreme" La Niña event (though the winter Niño-3 of D'Arrigo *et al.* 2005 was near neutral at -0.08), 1739 as a "very strong" La Niña event, and 1782 as a "weak" La Niña event (though the winter Niño-3 value of D'Arrigo *et al.* 2005 was -0.77, > 99.9% CL). Gergis and Fowler (2009) did not reconstruct 1842 as a La Niña event, but Winter Niño-3 (D'Arrigo *et al.* 2005) was -0.59 (> 99% CL).

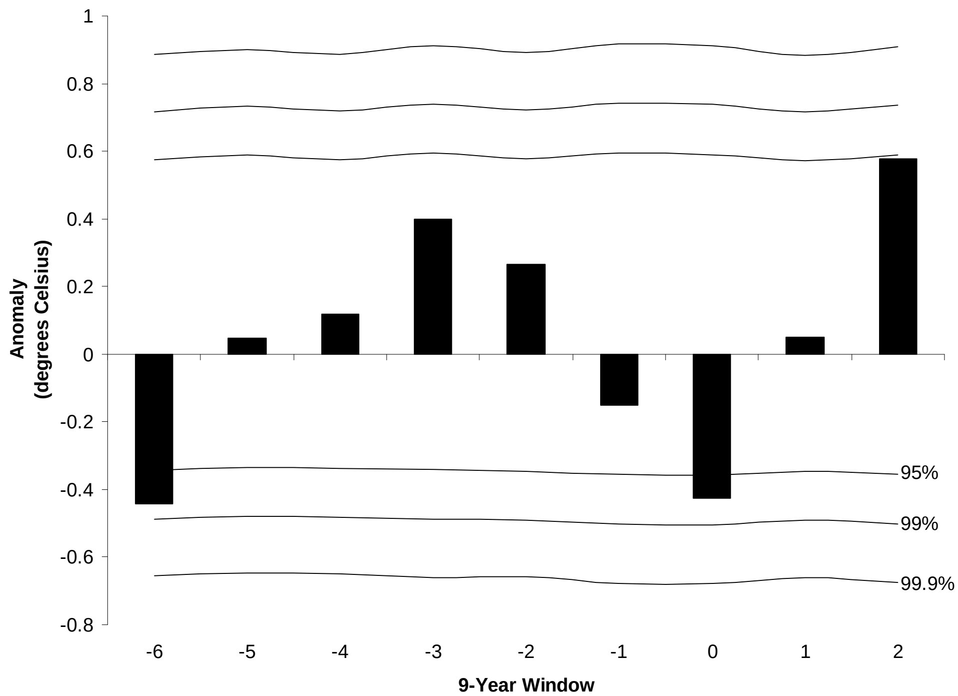

Figure 23. Reconstructed winter Niño-3 (D'Arrigo *et al.* 2005) was significantly negative (> 95% CL) the year of the fire (year 0) and six years before the fire (year -6) when year 0 coincided with combined negative phases of seven-year PDO and winter Niño-3 (D'Arrigo et al. 2005) between 1600 and 1950 (n = 4). Autocorrelation: first order = 0.14, second order = -0.32, third order = -0.05.

When drought-induced fires coincided with combined phases of negative seven-year PDO and positive winter Niño-3, winter Niño-3 did not depart significantly in any year of the nine-year window (results not shown), confirming that mixed-sign combinations are weaker and less predictable in signal than same-sign synergy (Gershunov and Barnett 1998) and indicating that these fires would be better explained by other climatic variables.

DISCUSSION OF FIRE DATES AND ANALYSES

Drought and Temperature

Fires in the Sawtooth Valley between 1632 and 1933 burned during years that were significantly dry (Figure 14). The year after the fire was also significantly dry, due in part to the low-intensity fire of 1799, which burned during a significantly wet year and was followed by a significantly dry year (Cook *et al.* 2004). The significant anomaly the year after the fire likely also resulted from temporal autocorrelation in the set of all fires, which tended to be clumped (e.g., 1782/83, 1930/33).

Annual temperature in the central Rocky Mountains (Briffa *et al.* 1992) was significantly warm the year of the fire (Figure 15). Annual temperature correlates most strongly with the instrumental spring season (April and May) and the month of August (Briffa *et al.* 1992), suggesting the importance of both early snowmelt and summer drought in setting the stage for fires. July temperature (Biondi *et al.* 1999/2006) in central Idaho was significantly warm the year of the fire (Figure 16). Of the 11 drought-induced fires (PDSI < -1), 10 burned during years when July temperature was at least anomalously warm, and eight burned during years when July temperature was significantly warm (> 0.51 standard deviations from the instrumental mean, as determined by SEA, Table 3). Two of three drought-induced fires excluded from analysis of combined positive phases of spring PDO and decadal AMO (1712 and 1842) burned during years when July temperature was not significantly warm, whereas seven of eight fires that were included burned during years when July temperature was significantly warm.

The five fires known to have been stand-replacing burned in climatic windows of opportunity, in which July temperature was significantly warm (with the exception of 1842, which was only anomalously warm) and summer PDSI was significantly dry (figures 24 through 28). Fire scars for which season could be determined all were latewood (Table 1), indicating that significantly warm summer temperatures were required to dry the cool, effectively wet forest to the point where crown fires could spread.

Table 3. Anomalies of climatic reconstructions during fire years. PDSI: summer reconstruction of Cook *et al.* (2004). PDSI YB: PDSI the year before the fire. July Temperature (standard deviations): Biondi *et al.* (1999/2006). Spring PDO: D'Arrigo and Wilson (2006). Spring PDO YB: spring PDO the year before the fire. Seven-year (averaged) PDO: At least 2/3 agreement among Shen *et al.* (2006), MacDonald and Case (2005), and D'Arrigo *et al.* (2001). El Niño/La Niña event (W=weak, M=moderate, S=strong, VS=very strong, E=extreme): Gergis and Fowler (2009). Niño-3 (winter): D'Arrigo *et al.* (2005). Niño-3 YB: winter Niño-3 the year before the fire. AMO Index: Gray *et al.* (2004). Values referred to in the text as "significant" are based on comparison with confidence levels generated in SEA for that subset of fires.

Fire	1632	1686	1712	1734	1739	1756	1782	1783	1799	1842	1844	1889	1930	1933
PDSI	-4	-2.3	-1.2	-0.72	-1.4	-4.9	-2.9	-4.9	2.6	-2.6	-0.71	-4.7	-1.5	-2.9
PDSI YB	-1.1	2.9	-0.77	1.6	1.3	0.21	0.28	-2.9	-3.1	-0.76	-2.9	0.47	-0.98	0
July Temperature	1.4	0.25	-0.03	1.4	1.4	1.8	0.94	1.8	0.25	0.11	-1.1	0.66	2.2	1.4
Spring PDO	1	0.51	0.4	-0.17	0.16	0.94	2.1	1.2	0.46	0.71	0.15	-0.47	1.5	0.44
Spring PDO YB	1.5	0.57	-0.26	-0.26	0.3	0.17	1.6	2.1	-0.2	0.54	0.01	0.07	1.5	1.4
Seven-Year PDO	- (2/2)	+ (2/2)	- (2/3)	- (3/3)	- (2/3)	- (3/3)	- (3/3)	- (3/3)	+ (2/3)	- (2/3)	- (2/3)	- (3/3)	+ (2/3)	+ (3/3)
El Niño event			W	W			W	M	S		M	W	M	W
La Niña event	E	M			VS	M	W							
Niño-3	-0.08	0.2	0.38	-0.38	-0.27	0.27	-0.77	0.22	0.45	-0.59	0.33	1.1	0.22	-0.39
Niño-3 YB	-0.31	-1	0.07	-0.86	0.39	0.08	-0.27	-0.77	-0.25	-0.41	-0.16	0.4	-0.54	0.28
AMO Index	0.16	0.8	0	0.09	0.07	0.07	0.48	0.44	-0.38	-1.1	-0.85	0.28	1.1	1.2

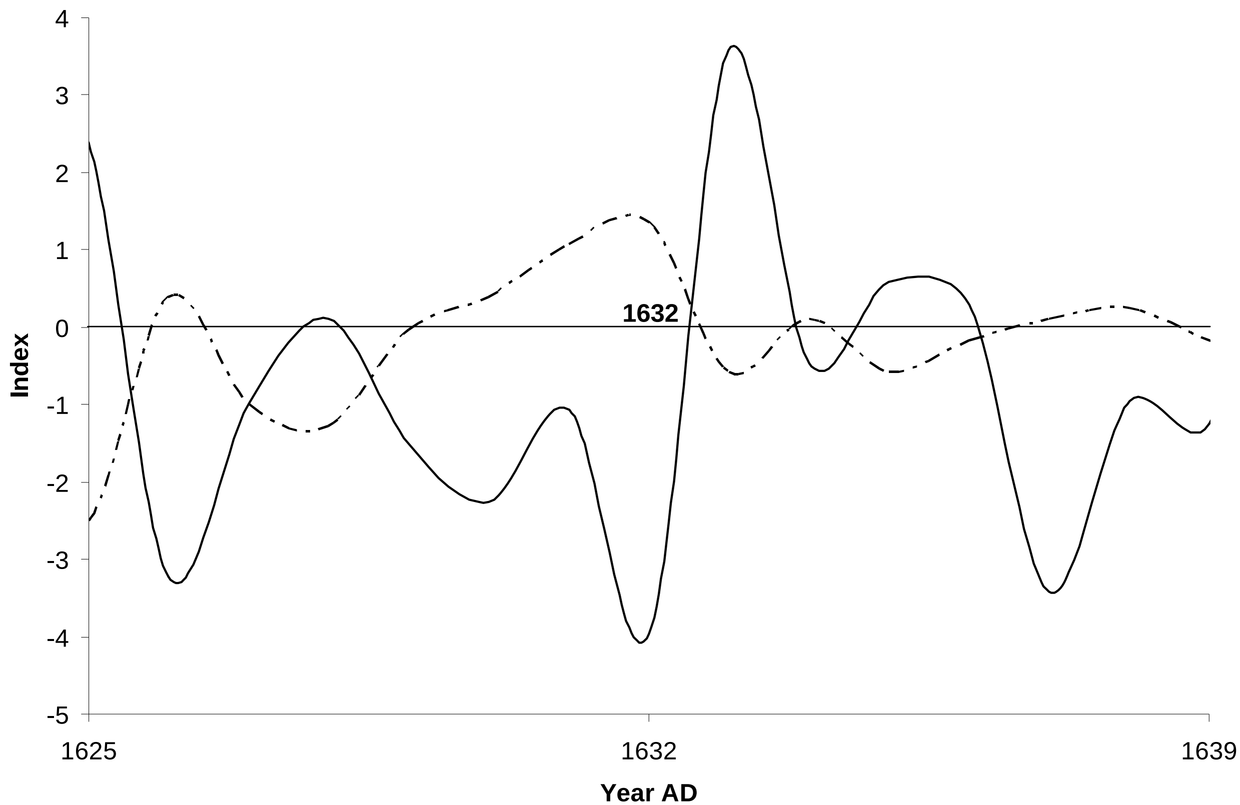

Figure 24. Multi-watershed fires in 1632 coincided with significantly warm (> 99.9% CL) July temperature (Biondi *et al.* 1999/2006, dashed line) and significantly dry (>99.9% CL) summer PDSI (Cook *et al.* 2004, solid line).

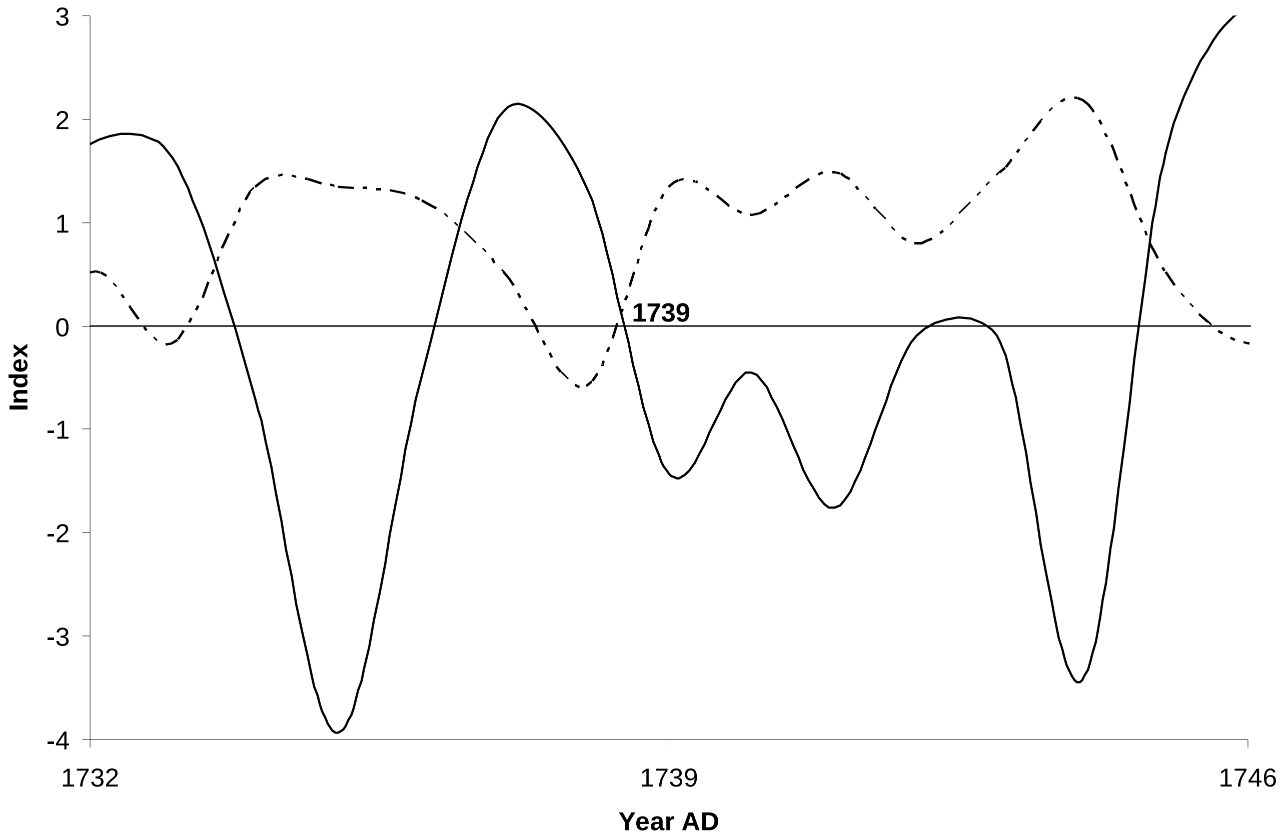

Figure 25. The single-watershed fire of 1739 coincided with significantly warm (>99.9% CL) July temperature (Biondi *et al.* 1999/2006, dashed line) and significantly dry (>99% CL) summer PDSI (Cook *et al.* 2004, solid line).

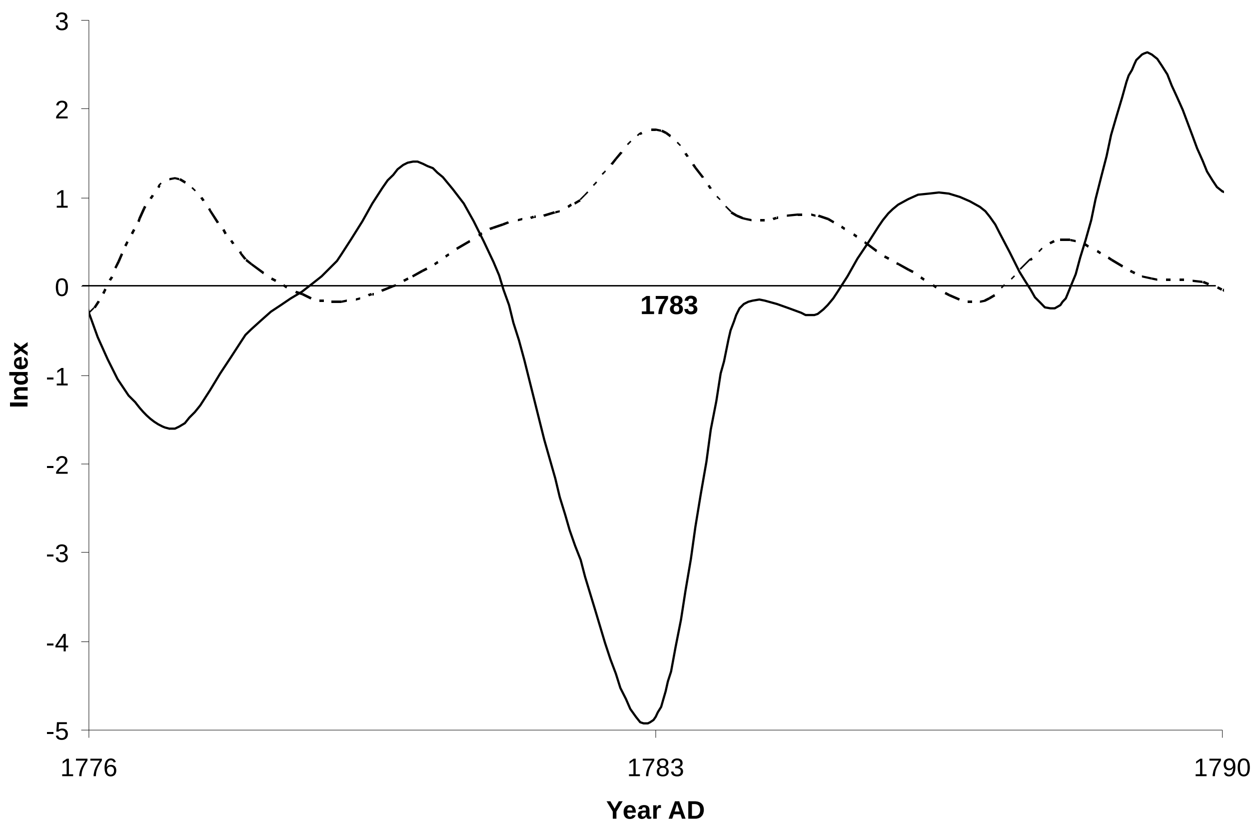

Figure 26. The single-watershed fire of 1783 coincided with significantly warm (>99.9% CL) July temperature (Biondi *et al.* 1999/2006, dashed line) and significantly dry (>99.9% CL) summer PDSI (Cook *et al.* 2004, solid line).

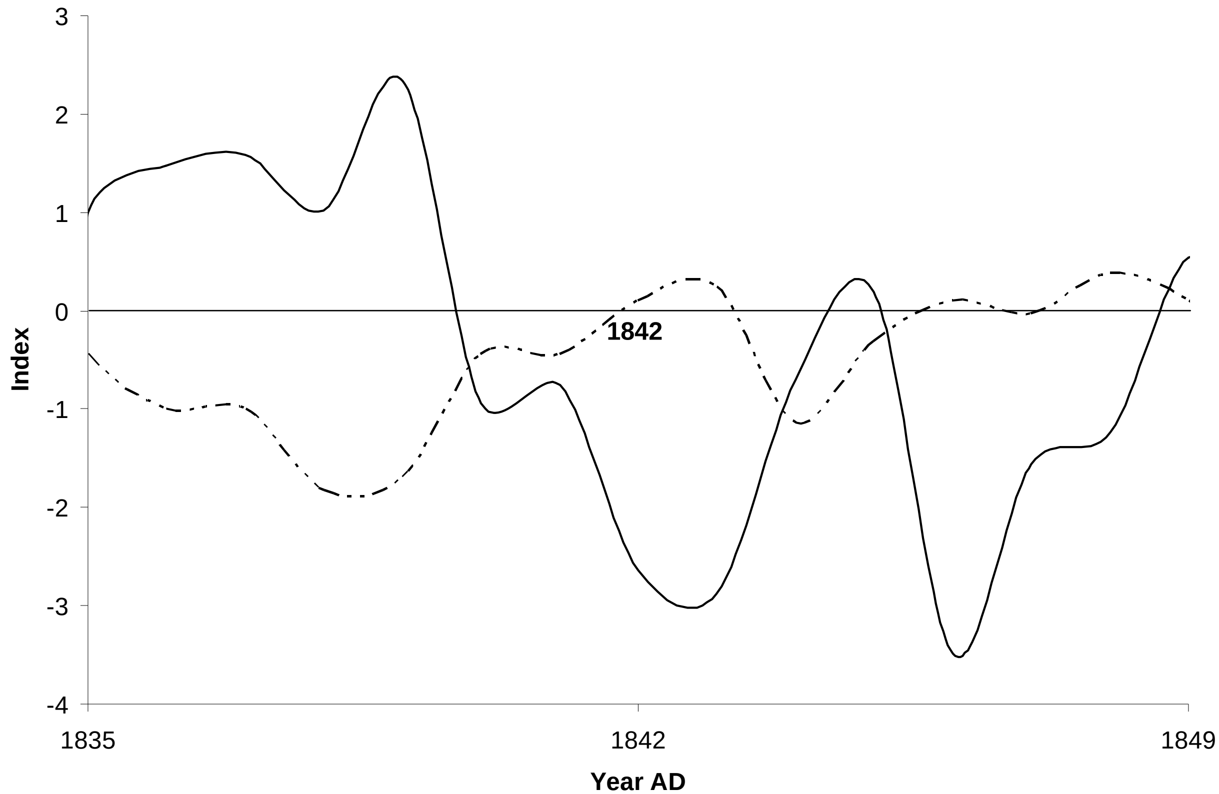

Figure 27. Multi-watershed fires in 1842 coincided with anomalously (but not significantly) warm July temperature (Biondi *et al.* 1999/2006, dashed line) and significantly dry (>99.9% CL) summer PDSI (Cook *et al.* 2004, solid line).

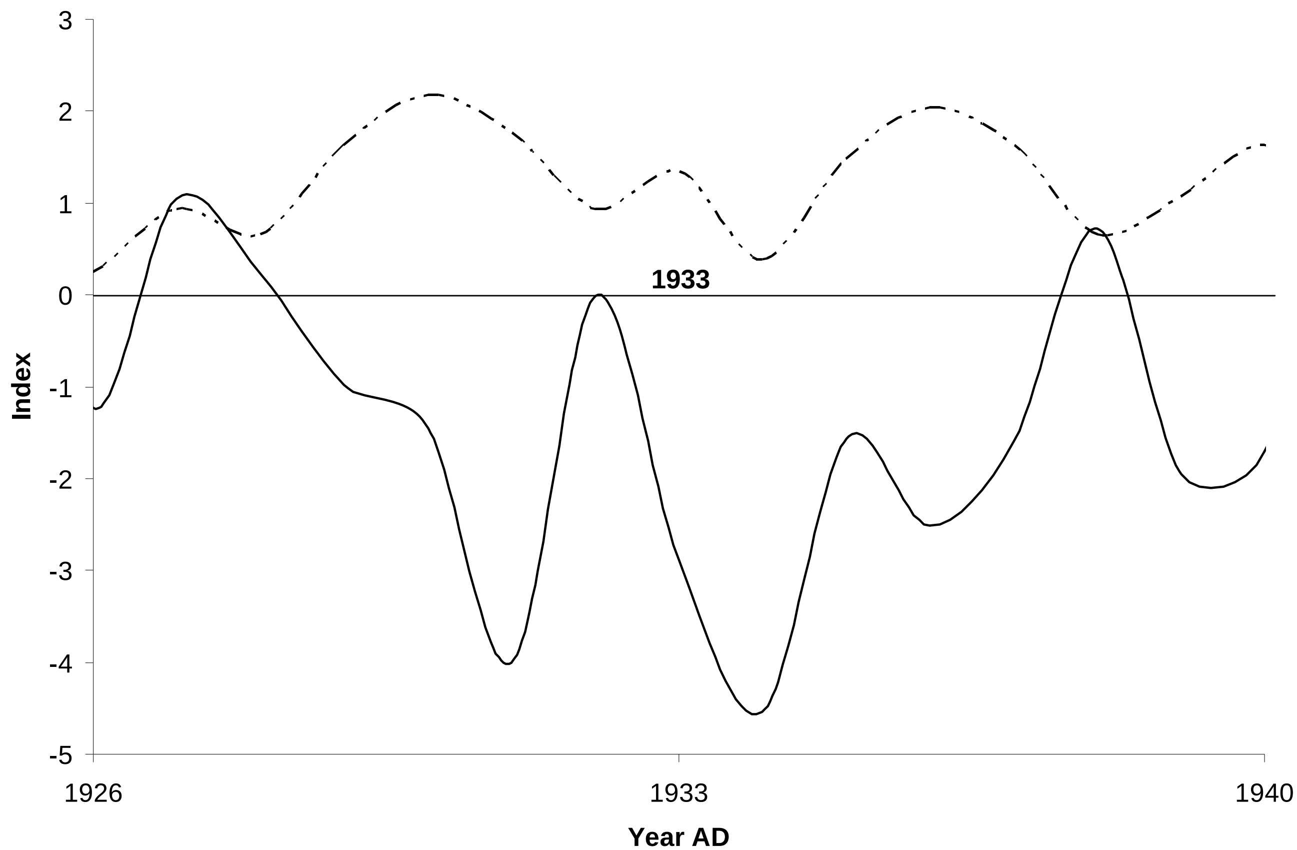

Figure 28. The single-watershed fire of 1933 coincided with significantly warm (>99.9% CL) July temperature (Biondi *et al.* 1999/2006, dashed line) and significantly dry (>99.9% CL) summer PDSI (Cook *et al.* 2004, solid line).

Sea Surface Temperature (SST) Oscillations

Spring PDO

Drought-induced fires did not coincide significantly with spring PDO the year of the fire, but did the year before (Figure 19). The relatively high first-order autocorrelation (0.6) in the spring PDO reconstruction lowers the annual precision of the comparison in SEA, meaning a multiannual perspective is useful in interpreting the connection with drought-induced fire. Figure 20 provides this multiannual perspective by juxtaposing observed values of spring PDO (black bars) with expected values, generated from 1000 random simulations in SEA (gray bars). Comparison of the observed with the expected indicates that drought-induced fires burned at the tail end of a positive surge in spring PDO. The significant anomaly the year before the fire (the vertical perspective) and the positive surge leading up to the fire (the horizontal perspective) imply a lagged, multi-year connection between spring PDO and drought-induced fire. Such a lagged connection might help explain significantly dry and warm anomalies the year after the fire (figures 14 and 16).

Combined Phases of Spring PDO and Decadal AMO

Drought-induced fires that burned during combined positive phases of the AMO Index and spring PDO (8 of 11) coincided significantly with positive spring PDO the year of the fire and the year before (Figure 21). This is not to suggest that the positive phase of the AMO intensifies spring PDO, but rather that drought-induced fires tended to burn during years with a climatic one-two punch of significantly positive spring PDO (which likely resulted in early snowmelt and a longer summer drying season) and a positive AMO Index (which likely intensified summer drought). Intervals of high fire-frequency at 1782/83 and 1930/33 coincide with positive 20-year peaks in both spring PDO and the AMO (Figure 29).

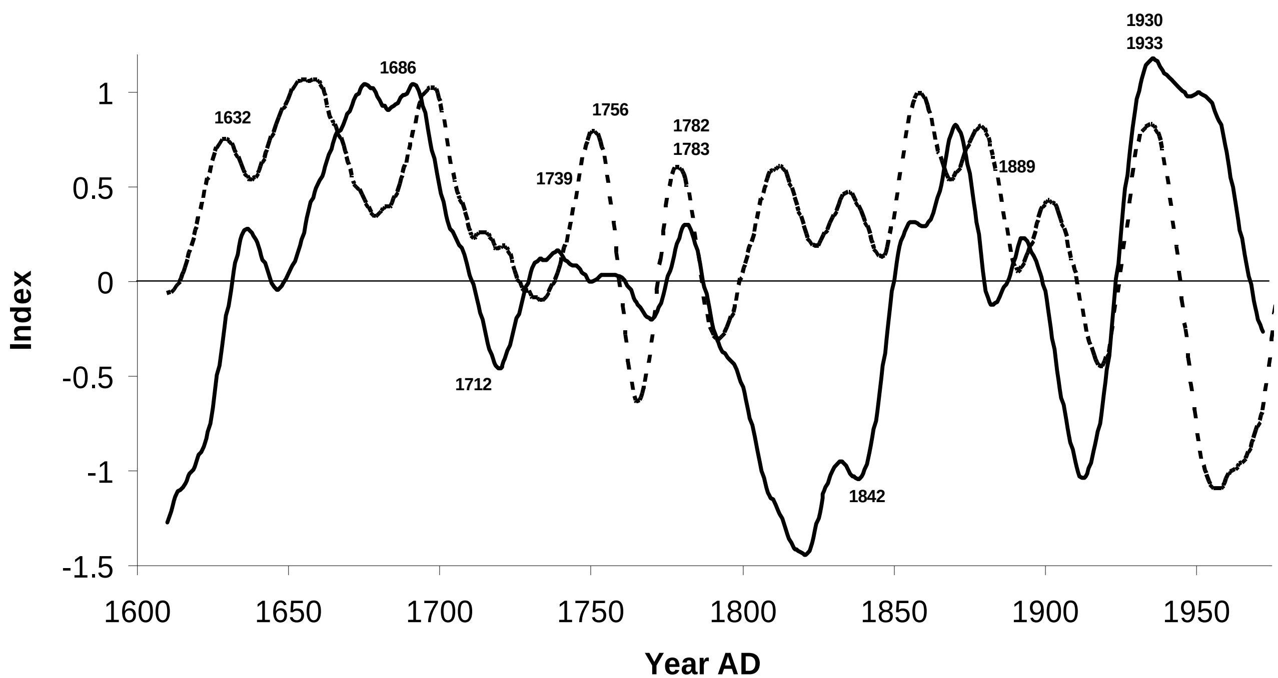

Figure 29. Spring PDO (dashed line, D'Arrigo and Wilson 2006) and AMO anomalies (solid line, Gray *et al.* 2004) on center-weighted, 20-year moving averages. Dates are years of annually resolved fires that burned during significant drought.

<u>Constructive Synergy between Seven-Year PDO and Winter Niño-3</u>

Four of 11 drought-induced fires that burned during combined negative phases of seven-year PDO and winter Niño-3 coincided with significantly negative winter Niño-3 the year of the fire (Figure 23). This suggests that during some years drought in the Sawtooth Valley (central Rocky Mountains) was intensified by combined phases of the Pacific oscillations in a manner similar to that of the southern Rockies, where fires tend to burn during combined negative phases of annual PDO and winter Niño-3 (Sibold and Veblen 2006). Three of the four fires in the Sawtooth Valley that burned during combined negative phases are known to have been stand-replacing (1632, 1739, 1842), and two of the three stand-replacing fires burned in multiple watersheds (1632, 1842). Thus the importance of this finding is that it identifies one mechanism linking the largest, most intense fires with combined phases of Pacific variability.

Drought-induced fires tended not to burn during combined positive phases of seven-year PDO and winter Niño-3. Gergis and Fowler (2009), however, reconstructed 1712 as a “weak” El Niño event, 1783 as a “moderate” El Niño event, 1889 as a “weak” El Niño event (though D’Arrigo *et al.* 2005 reconstructed winter Niño-3 at +1.1, exceeding the 99.9% confidence level), 1930 as a “moderate” El Niño event, and 1933 as a “weak” El Niño event. Glancing at Table 3, it is striking how many fire years—13 of 14 (93%)—were reconstructed as either a La Niña or El Niño event. It is particularly striking given that only 36% of the years between 1525 and 2002 were reconstructed as event years (Gergis and Fowler 2009). Fires in Idaho and western Montana across a variety of forest types burned during both El Niño and La Niña years (Morgan *et al.* 2008). This tendency for fires in central Idaho to burn during ENSO events, regardless of sign, might explain the lack of a significant coincidence between drought-induced fires and winter Niño-3 during all possible phase combinations (Figure 22), as SEA tests for departures in only one sign (i.e., a relationship involving both plus and minus cancels out in SEA). The temporal progression of ENSO event years in Table 3 suggests a transition in 1782/83 from fires associated with La Niña events to fires associated with El Niño events.

Periods of Low Fire Frequency

Between the 1630s and 1790s no more than two consecutive decades passed without fire (Figure 30, gray bars). The four decades between the low-intensity fire of 1799 and the stand-replacing fires of 1842 were fire-free in this study. This period coincided with a multidecadal negative phase of the AMO and cool July temperatures in central Idaho (Figure 30). Tree-rings from the Columbia Ice Field (Alberta, Canada, northern Rocky Mountains) indicate that the periods from 1819 to 1838 and 1799 to 1818 were the second and tenth coldest 20-year summer periods, respectively, since 950 AD (Luckman and Wilson 2005). Fire frequencies during this time were low in Rocky Mountain National Park (Sibold and Veblen 2006) and other locations in the western United States (Heyerdahl *et al.* 2002; Brown *et al.* 2008). An unidentified volcanic eruption in 1809 and the 1815 eruption of Tambora (Indonesia) apparently combined to make the 1810s the coldest decade of the past 600 years in the northern hemisphere (Briffa *et al.* 1998). The Dalton solar minimum dates between ~1800 and 1825 (Luckman and Wilson 2005). Low fire frequency in northern Patagonia (Argentina) in the first half of the 1800s was attributed in part to lower amplitudes or frequencies of ENSO events (Kitzberger *et al.* 2001).

The four decades between the fires of the 1880s and 1930s appear to have been a second fire-free period (Figure 30). In the early 20th century the AMO and July temperature in central Idaho were again in a trough (Figure 30). Spring PDO was in a negative phase between ~1910 and 1925 (Figure 29), suggesting cooler springs and a persistence of snowpack, providing a shorter drying season for fuels. A cluster of volcanic eruptions—Santa Maria (Guatemala, 1902), Ksudach (Kamchatka, 1907), and Novarupta (Alaska, 1912)—likely contributed to northern hemispheric cooling (Briffa *et al.* 1998).

Fire frequency across a variety of forest types in Idaho and western Montana was low in the mid 20th century (~1940 to 1980, Morgan *et al.* 2008), likely due in part to a multidecadal negative phase of spring PDO (Figure 29). Figures 29 and 30 suggest that fire weather in the Sawtooth Valley is supported by a climatic foundation composed of positive to neutral multidecadal phases of the AMO and spring PDO. Multidecadal periods when one or both oscillations fall into a negative phase tend to be characterized by low fire frequency. July temperature in central Idaho closely parallels the AMO on a 10-year moving average (Figure 30), though it is unknown whether or to what extent temperature is driven by the AMO.

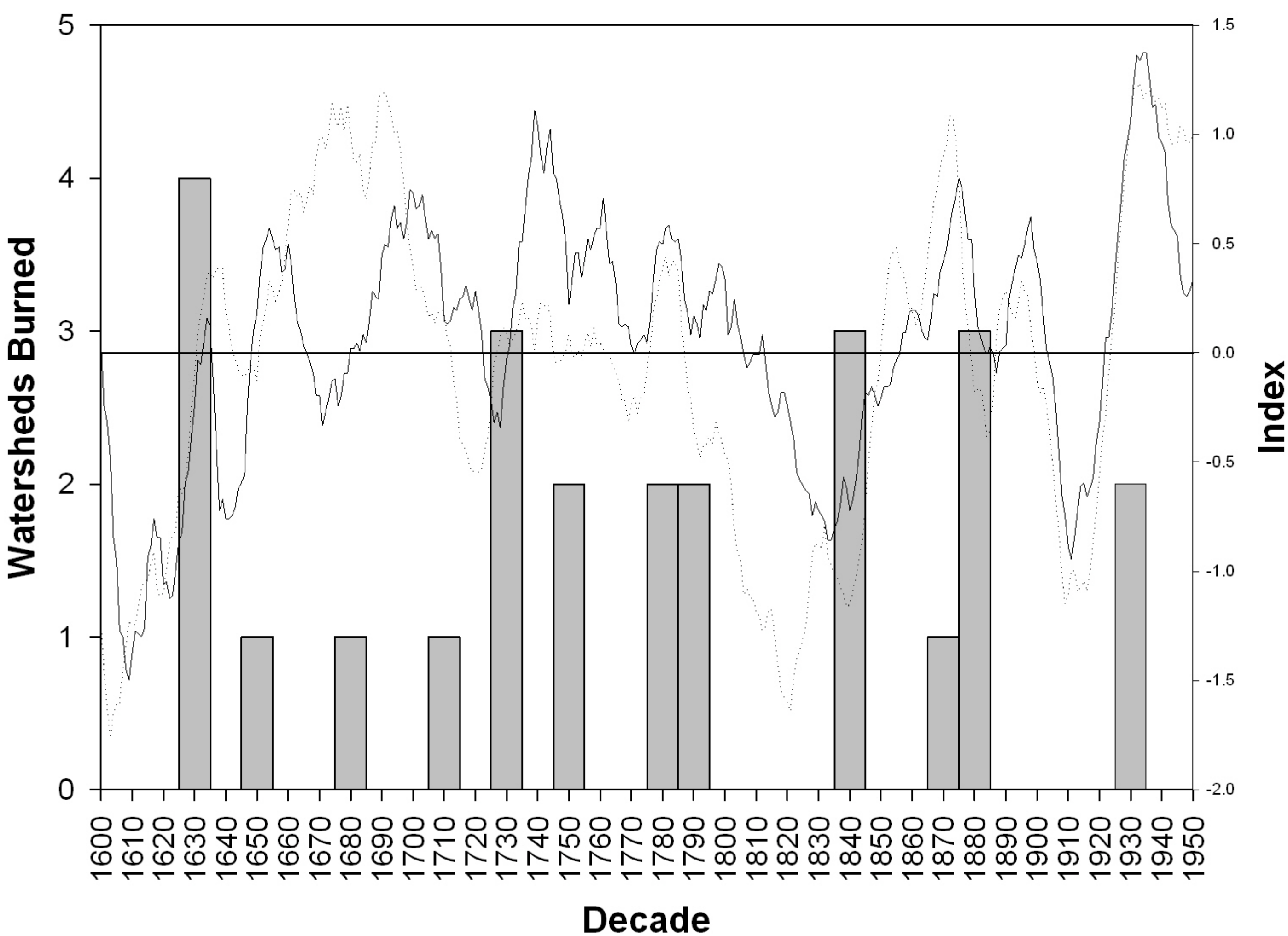

Figure 30. Gray bars represent the number of watersheds burned by decade for the set of all fires (n = 20). July temperature for central Idaho (Biondi *et al.* 1999/2006, solid line) and the AMO (Gray *et al.* 2004, dotted line) are shown on centered, 10-year moving averages.

Stand-Replacing vs. Low-Intensity Fires

Fires known to have been stand-replacing (1632, 1739, 1783, 1842, 1933) burned during years that were severely dry (average PDSI = -3.2), whereas low-intensity fires (1799, 1844, 1889) burned under a variety of drought conditions (Table 3). The fire of 1799 burned during a significantly wet year (PDSI = +2.6, > 99.9% CL); the fire of 1844 burned during a year of mild, non-significant drought (PDSI = -0.71); the fire of 1889 burned during a year of extreme drought (PDSI = -4.7). Average PDSI for low-intensity fires was -0.94, which does not exceed the SEA 95% confidence threshold of -1. The difference in average PDSI between stand-replacing and low-intensity fires implies that low-intensity fires depended on age-structure, fuel accumulation, or some other variable in addition to climate (Turner and Romme 1994). Intriguingly, all three low-intensity fires burned during reconstructed El Niño events (Table 3).

Average elevation of trees recording stand-replacing fires was 2180 m; average elevation of trees recording low-intensity fires was 2056 m. One explanation for the difference in elevation could be the proximity of low-intensity sites to the valley (Figure 10), from which brush fires might have spread into the forest and burned surface fuels and scarred trees during years unfavorable (climatically or structurally) to crown fire. Cryptically, all three low-intensity fires burned in the lower Decker Watershed. Low-elevation stands near the Ranger Station (Figure 9) were scouted as intensively for fire-scarred lodgepole as the Decker watershed, yet none was found. A fire-scarred Douglas-fir (DFCF10) near the Ranger Station records a fire in ~1799 (Figure 9), so the possibly of low-intensity fire in that area cannot be excluded.

Stand-Replacing Fires: Climatic Nuts and Bolts

The multi-watershed fires of 1632 burned in four (possibly five or more) watersheds during a year of significantly warm reconstructed July temperature (Figure 24). Extreme summer drought (PDSI = -4) in 1632 was preceded by multi-year drought in 1631 (PDSI = -1.1), 1630 (PDSI = -2.3), and 1629 (PDSI = -1.5, Cook *et al.* 2004). Drought was severe to extreme in 1632 across most of the United States (Figure 31, Cook *et al.* 2004). "Regional fire" in 1632 was reconstructed in five forests across Utah (Brown *et al.* 2008) and at Devils Tower National Monument in Wyoming (Fisher and Jenkins 1987). "Extensive fire" was dated to 1631 and 1632 in the Bitterroot Valley of western Montana (Arno 1976). Stand-age evidence from Yellowstone National Park indicates a large fire in ~1630 (Romme 1982). A "small fire" was reconstructed in the Sierra Nevada in 1632 (Kilgore and Taylor 1979).

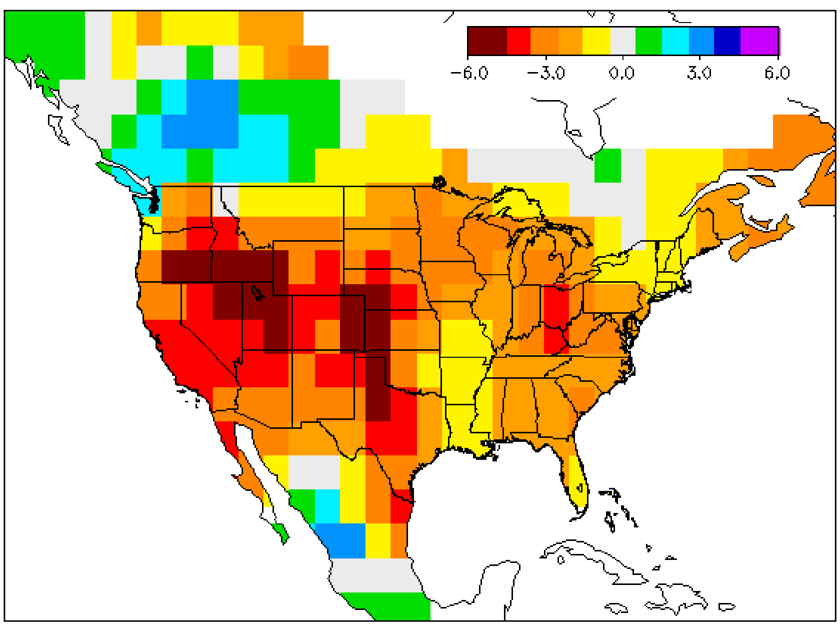

Figure 31. Reconstructed PDSI for the United States in 1632 (http://www.ncdc.noaa.gov/cgi-bin/paleo/pd04plot.pl).

Spring PDO in 1631 and 1632 was significantly positive (> 99.9% and 99% CL, respectively, Table 3), suggesting warm springs and early snowmelts. The AMO Index was positive in 1632, indicating a drought-intensifying connection with spring PDO. Annual PDO (Shen *et al.* 2006) was -1.2, exceeding the 99.9% confidence level. Assuming that spring PDO (D'Arrigo and Wilson 2006) and annual PDO (Shen *et al.* 2006) are both reconstructed accurately, 1632 must have been a year of extreme variability in the PDO. Seven-year PDO and winter Niño-3 were both negative, suggesting a drought-intensifying synergy. Gergis and Fowler (2009) reconstructed 1632 as an "extreme" La Niña event (1 of only 12 for the period between 1525 and the present). Gergis and Fowler (2009) also reconstructed protracted La Niña events, defined as events lasting three years or longer; the longest protracted La Niña event (11 years) lasted from 1622 to 1632. The period between ~1600 and 1630 was reconstructed in central Idaho as cool (Figure 30), which perhaps facilitated development of dense forests. One interpretation of the fires of 1632 would be that a protracted La Niña resulted in multi-year drought in the late 1620s and early 1630s, and that significantly warm July temperatures (Biondi *et al.* 1999/2006) and significantly positive spring PDO (D'Arrigo and Wilson 2006) in 1631 and 1632 intensified drought the year of the fire.

The single-watershed fire of 1739 burned a large portion of the Decker watershed, from the valley up to at least Decker Lake (Figure 8), during a year that was significantly warm and dry (Figure 25). The year before the fire was significantly wet (PDSI = +1.4, Table 3). A large fire in 1739 was reconstructed in lodgepole pine in Yellowstone National Park (Romme 1982). Spring PDO was positive, but not significantly, and the AMO Index was only slightly positive. The AMO anomaly, however, was significantly positive (> 99.9% CL, Gray *et al.* 2004), meaning a drought-intensifying synergy between spring PDO and the AMO cannot be excluded. Annual PDO reconstructed from eastern Pacific records (D'Arrigo *et al.* 2001) was significantly negative, exceeding the 99.9% confidence level; the Shen *et al.* (2006) annual PDO, reconstructed from western Pacific records, was only slightly negative. Seven-year PDO was negative, winter Niño-3 was significantly negative (> 99% CL), and 1739 was reconstructed as a "very strong" La Niña event. The minus-minus-plus phase combination of annual PDO, winter Niño-3, and the AMO is the combination most significantly associated with fire in the southern Rocky Mountains (Sibold and Veblen 2006; Schoennagel *et al.* 2007). Drought in 1739 was reconstructed as mild to severe across the western United States (Figure 32, Cook *et al.* 2004).

In addition to the 1739 fire, a fire-scarred Douglas-fir (DFCF12) in the Decker watershed records a fire in 1632 (Figure 8). The absence of survivors from the 1632 lodgepole cohort suggests the fire of 1739 burned with high intensity. DFCF12 also records fires in ~1500 and ~1428; assuming all these fires were stand-replacing, the Decker watershed appears to have burned once every 70 to 130 years. As of 2009, it has been 270 years since the last stand-replacing fire. The lower part of the watershed has been characterized by low-intensity fire since 1799.

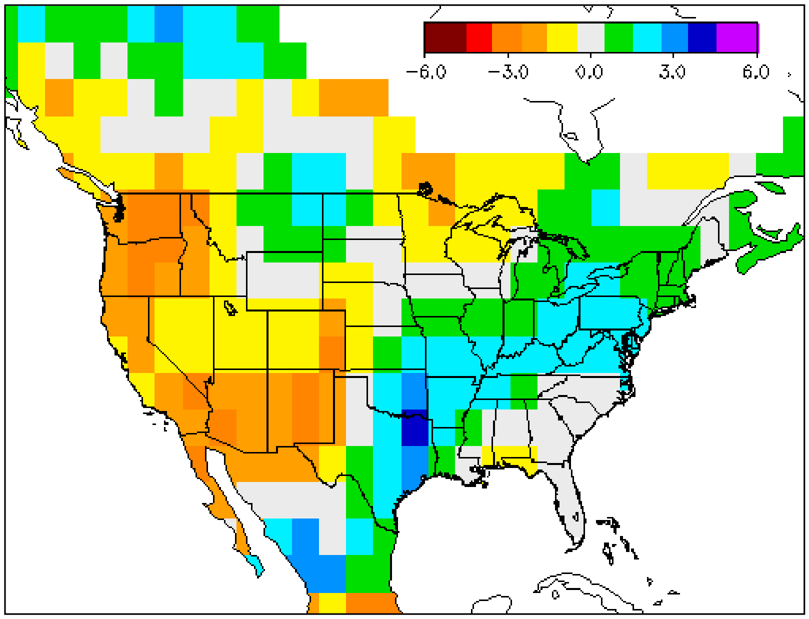

Figure 32. Reconstructed PDSI for the United States in 1739 (http://www.ncdc.noaa.gov/cgi-bin/paleo/pd04plot.pl).

The single-watershed fire of 1783 coincided with extreme drought (PDSI = -4.9, Table 3) and significantly warm (> 99.9% CL) July temperature (Figure 26). PDSI the year before the fire also was significantly dry (-2.9, > 99.9% CL) and coincided with the single-point fire of 1782. Drought in 1783 was severe to extreme in Idaho, Oregon, and Washington, while much of the southwest was neutral to wet (Figure 33, Cook *et al.* 2004). “Multi-drainage fires” in the Sierra Nevada (Kilgore and Taylor 1979) and a “regional-fire year” in Idaho and western Montana (Heyerdahl *et al.* 2008) were reconstructed in 1783. Spring PDO was significantly positive the year of the fire and the year before (> 99.9% CL both years), and the AMO Index was positive, indicating a drought-intensifying connection. Gergis and Fowler (2009) reconstructed 1783 as a “moderate” El Niño event, but seven-year PDO was negative, suggesting no drought-intensifying synergy.

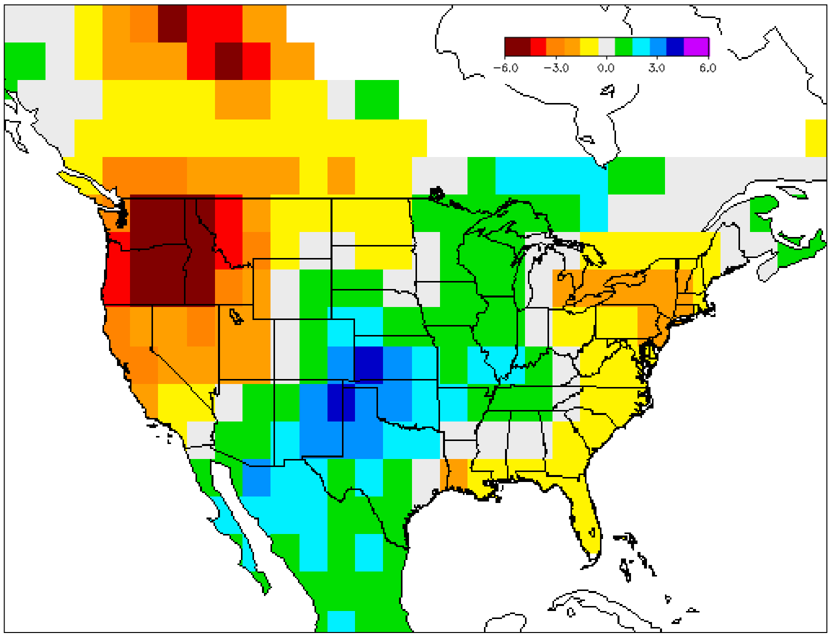

Figure 33. Reconstructed PDSI for the United State in 1783 (http://www.ncdc.noaa.gov/cgi-bin/paleo/pd04plot.pl).

The fires of 1842, which burned in at least two watersheds, coincided with significant drought (> 99.9% CL) and anomalously (but not significantly) warm July temperature (Figure 27). As with the multi-watershed fires of 1632, the fires of 1842 were preceded by a multidecadal cool period (Figure 30). Spring PDO was positive (but not significantly) and the AMO Index was strongly negative (Table 3), suggesting no drought-intensifying connection. Seven-year PDO was negative and winter Niño-3 was significantly negative (> 99% CL), suggesting a drought-intensifying synergy. Severe to extreme drought extended from the southern to the northern Rocky Mountains in 1842 (Figure 34, Cook *et al.* 2004). A "stand-replacing" fire in an upper-montane forest of northern New Mexico (Margolis *et al.* 2007) and a "high severity" fire in Rocky Mountain National Park (Buechling and Baker 2004) were reconstructed in 1842, as well as "small fires" on the Bitterroot National Forest (Arno 1976) and a "local-fire year" in Idaho and western Montana (Heyerdahl *et al.* 2008).

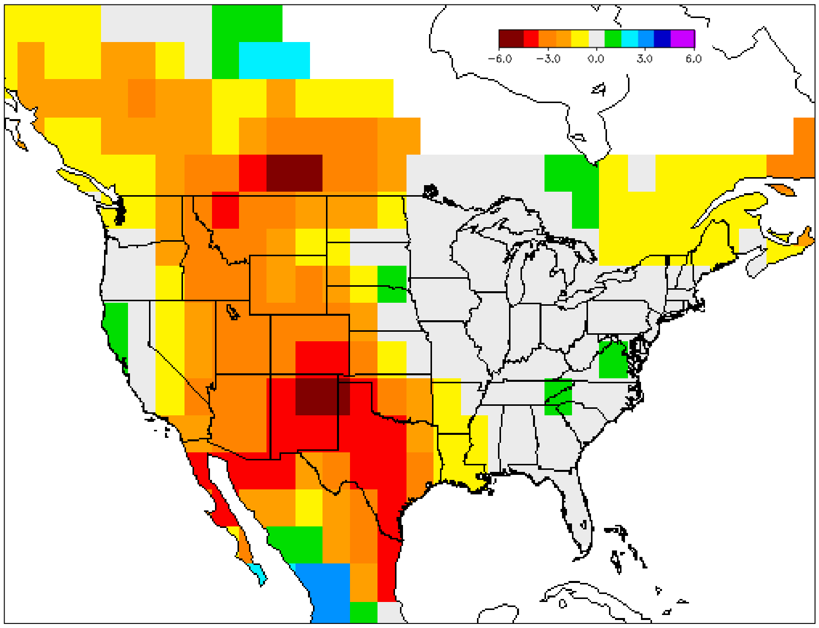

Figure 34. Reconstructed PDSI for the United States in 1842 (http://www.ncdc.noaa.gov/cgi-bin/paleo/pd04plot.pl).

The single-watershed fire of 1933 burned in the upper part of the Bench Lakes Watershed (Figure 6) during a year that was significantly warm and dry (Figure 28). Drought in 1933 was moderate to severe in the central Rocky Mountains, in much of the southern Rockies, and the Great Basin, but New Mexico and Arizona were wet (Figure 35, Cook *et al.* 2004). Seven-year PDO was positive, but winter Niño-3 was negative (Table 3), suggesting no drought-intensifying synergy. Spring PDO was positive (but not significantly) the year of the fire and significantly positive (> 99.9% CL) the year before. In 1933 the AMO index was strongly positive, and the AMO anomaly (Gray *et al.* 2004) was significantly positive (> 99.9% CL), suggesting drought was driven primarily by the AMO, likely involving a lagged response from Spring PDO.

The early 1930s, time of the Dust Bowl drought, appear to have been at least as climatically favorable to large, stand-replacing fire in central Idaho as the early 1630s (Briffa *et al.* 1992; Cook *et al.* 2004). The fires of 1632 were the most extensive reconstructed in this study. In contrast, 1930 was a point fire (the historical fire atlas contains numerous point fires in the Sawtooth Valley during the 1930s), and the 1933 fire burned only a small area (<100 ha). Given the climatic favorability to fire in both decades, what could explain the great difference in area burned? The large extents of the 1988 Yellowstone fires and the 2005 Valley Road Fire suggest that fire suppression in a stand-replacing forest type will not be effective under extreme drought conditions. Thus it seems unlikely that fire suppression accounts for the low area burned during the 1930s. An alternative hypothesis might be that the forest differed in age structure between the 1630s and the 1930s as a result of variations in mountain pine beetle activity, and that differences in age structure affected the spread of crown fire. It is unknown (and probably unknowable) how windy it was in central Idaho was in the summer of 1632.

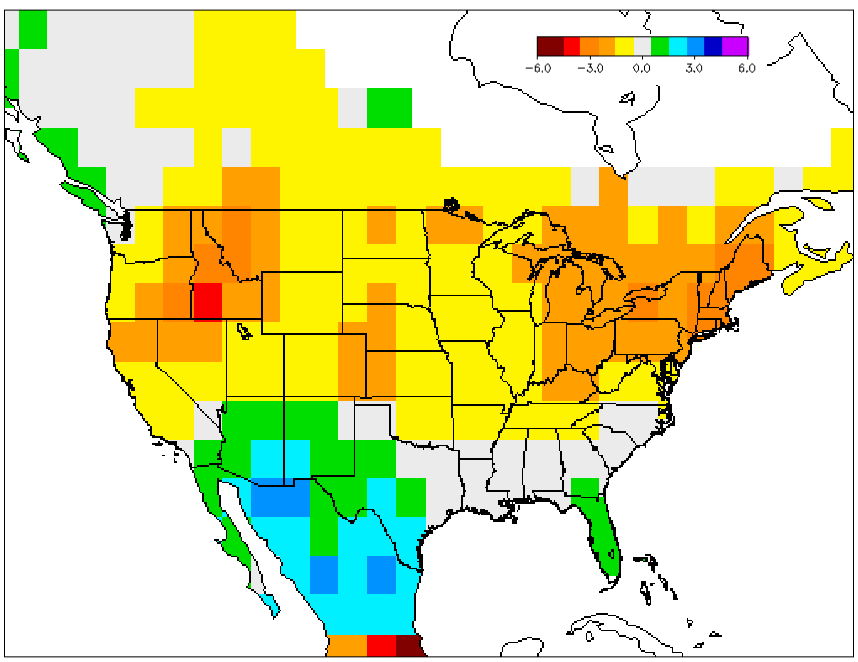

Figure 35. Reconstructed PDSI for the United States in 1933 (http://www.ncdc.noaa.gov/cgi-bin/paleo/pd04plot.pl).

The Valley Road Fire, which burned ~17,000 ha on the east side of the Sawtooth Valley in early September of 2005 (Figure 2), was the latest multi-watershed, stand-replacing fire, the first since 1842. Dead needles and small branches (1-hour fuels) would have been plentiful in the trees and on the ground as a result of the on-going pine-beetle epidemic (Page and Jenkins 2007a). The Valley Road Fire was preceded by multi-year drought: reconstructed Summer PDSI (point 69, Cook *et al.* 2004) was -1.9 in 2000, -2.7 in 2001, -1.6 in 2002, and -2.2 in 2003. Data from the weather station in Stanley, ID, at the northern end of the study area (Western Regional Climate Center 2009, http://www.wrcc.dri.edu/cgi-bin/cliMAIN.pl?id8676) indicate that between September 2003 and August 2004 the Sawtooth Valley received 43% of normal precipitation. (Because data for May of 2004 were missing, I inserted the instrumental average for May.) Much of the western United States was under moderate to extreme drought conditions at the end of August 2004 (Figure 36). Between September 2004 and August 2005 the Sawtooth Valley received 62% of normal precipitation. (Because data for April and May of 2005 were missing, I inserted the instrumental averages for April and May; actual precipitation, therefore, likely was less than 62% of normal for 2005.) At the end of August 2005, drought was severe in central Idaho and parts of the northwest, but the southwest (including the southern Rockies) was wet (Figure 37).

July maximum temperature in the Sawtooth Valley was 4.9% above average in 2000, 1% above average in 2001, 6.3% above average in 2002, 8.4% above average in 2003, 1.3% above average in 2004, and 3.7% above average in 2005. Spring maximum temperature (March, April, May) in 2005 was 2% above average and coincided with a strongly positive spring PDO anomaly of 1.4 (Mantua *et al.* 1997); the AMO had been in a positive phase since 1997 (Enfield *et al.* 2001). Warm temperatures, multi-year drought, strongly positive Spring PDO, and positive decadal AMO also characterized the multi-watershed fires of 1632. But whereas the fires of 1632 appear to have burned in the context of a prolonged La Niña, in 2005 winter Niño-3 was positive (0.46, Kaplan *et al.* 1998) and seven-year PDO was positive (Mantua *et al.* 1997).

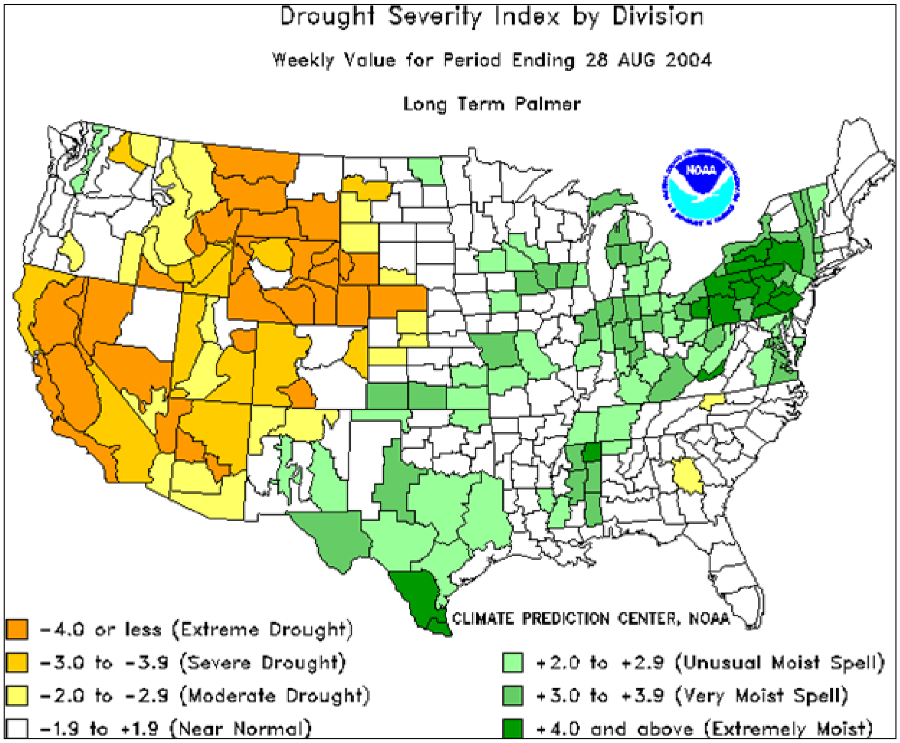

Figure 36. PDSI for the United States at the end of August 2004 (http://www.cpc.ncep.noaa.gov/ products/analysis_monitoring/regional_monitoring/palmer/2004/08-28-2004.gif).

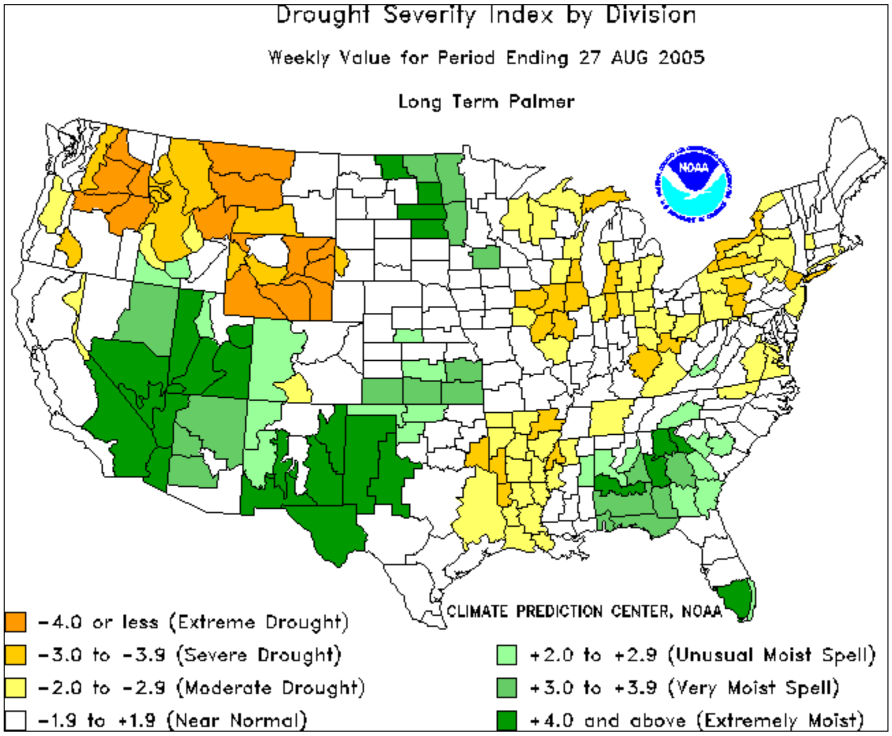

Figure 37. PDSI for the United States at the end of August 2005 (http://www.cpc.ncep.noaa.gov/ products/analysis _monitoring/ regional_monitoring/palmer/2005/08-27-2005.gif).

CHARCOAL: RESULTS AND DISCUSSION

Sixteen charcoal samples were radiocarbon dated. The 11 charcoal sites (Figure 38) are categorized into four environments: incised alluvial-fan (1 site), incised floodplain (1 site), soil in-situ (5 sites), and soil depositional (4 sites). The depositional environment for each sample is reported under the "site description" heading in Table 6 (Appendix B).

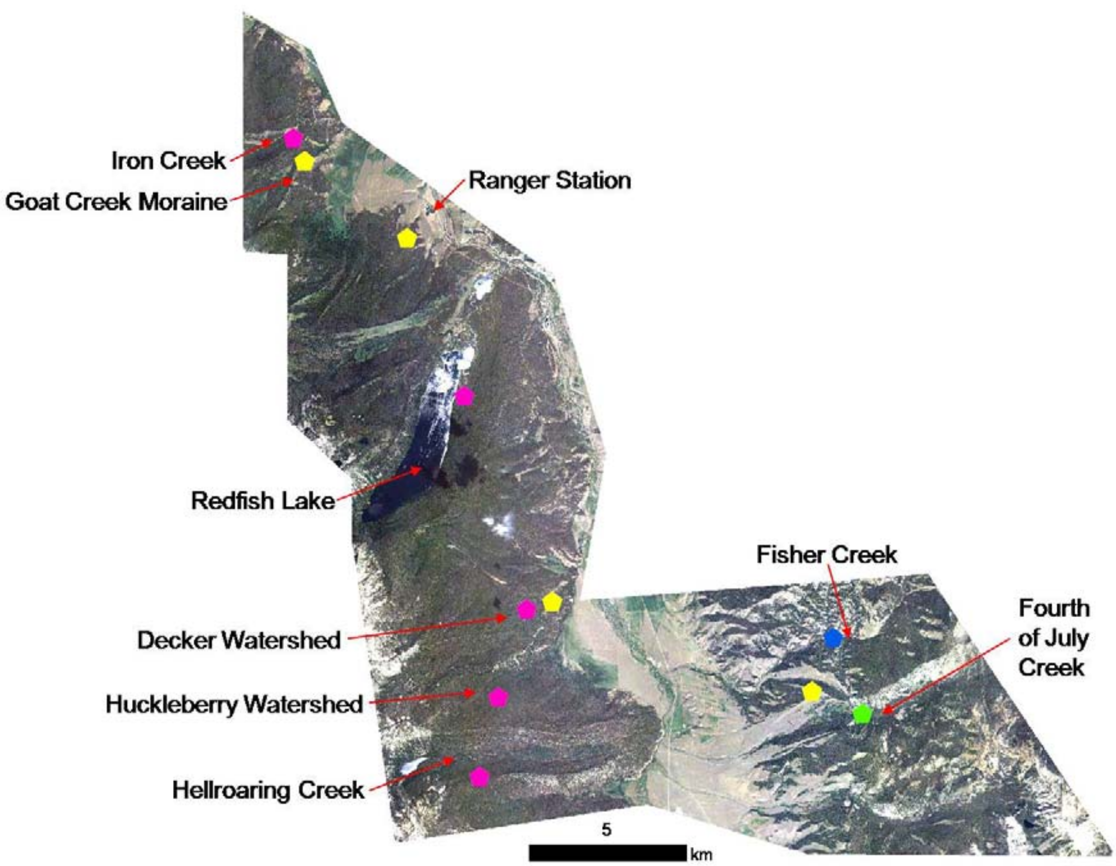

Figure 38. Charcoal sites in the Sawtooth Valley: blue = incised fan, green = incised floodplain, pink = soil in-situ, yellow = soil depositional.

Incised Alluvial Environments

The incised alluvial fan (Figure 39, Table 4, samples IFC08 and IFC10b) is composed of stratigraphically distinct hyperconcentrated-flow deposits at the mouth of a small watershed. The incised floodplain (Figure 39, Table 4, samples SC04, SC05, SC06b, SC07b) is composed largely of silt (cut by a meander bend during high water), containing charcoal-rich deposits.

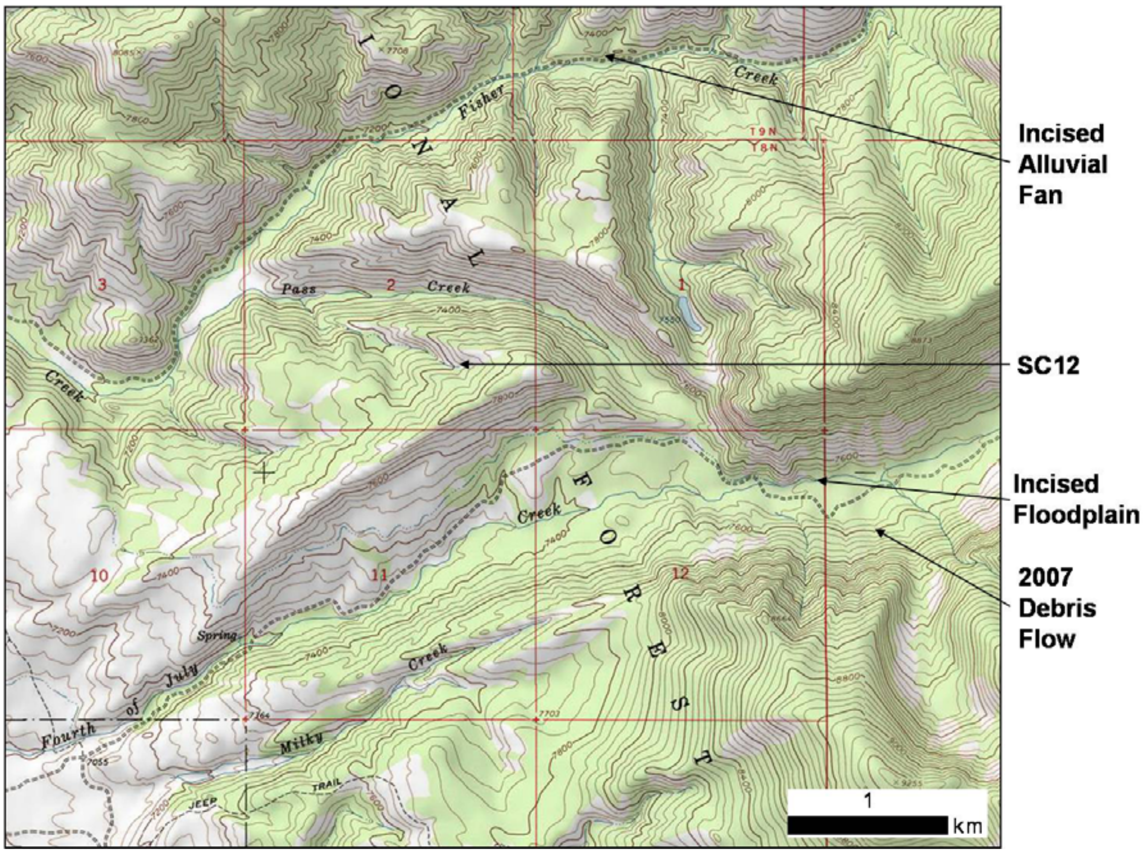

Figure 39. Both incised alluvial charcoal sites and one depositional soil-charcoal site (SC12) are on the east side of the Sawtooth Valley. The map was created using the National Geographic TOPO program.

Soil Charcoal

Soil in-situ sites are erosional environments, where older charcoal has been exposed. In-situ sites might be at high elevations relative to the valley floor (Plot 4, Figure 40), on hillsides at various elevations (plots 5 and 17, figures 40 and 41, respectively), or near lakes, where the shore has eroded into the lake (Plots 3 and 13, Figure 40). Soil-depositional sites are at low elevations relative to neighboring topography, but are not necessarily low in elevation relative to the valley floor. Soil-depositional sites might be at the edge of a valley (SC15.1, Figure 41), on saddles on moraines (SC12 and SC09, figures 39 and 41, respectively), or where steep topography is flattening out (SC14 and SC16, Figure 40). After a fire, runoff during heavy rainstorms can wash surface charcoal from in-situ to depositional sites. Some charcoal remains at in-situ sites, particularly in micro-depositional environments (e.g., on the uphill side of a large rock), and eventually is buried as a burned surface by loess and organic matter. During particularly torrential rainstorms older charcoal might be eroded from in-situ sites to depositional sites. If a site is categorized (based on topographic position) as depositional, however, it does not follow that all charcoal will have been deposited as a result of erosion from in-situ sites, because a burned surface can be left after a fire at either site. The possibility of erosion and deposition of older charcoal on top of younger burned surfaces suggests that stratigraphies could be inverted at depositional sites.

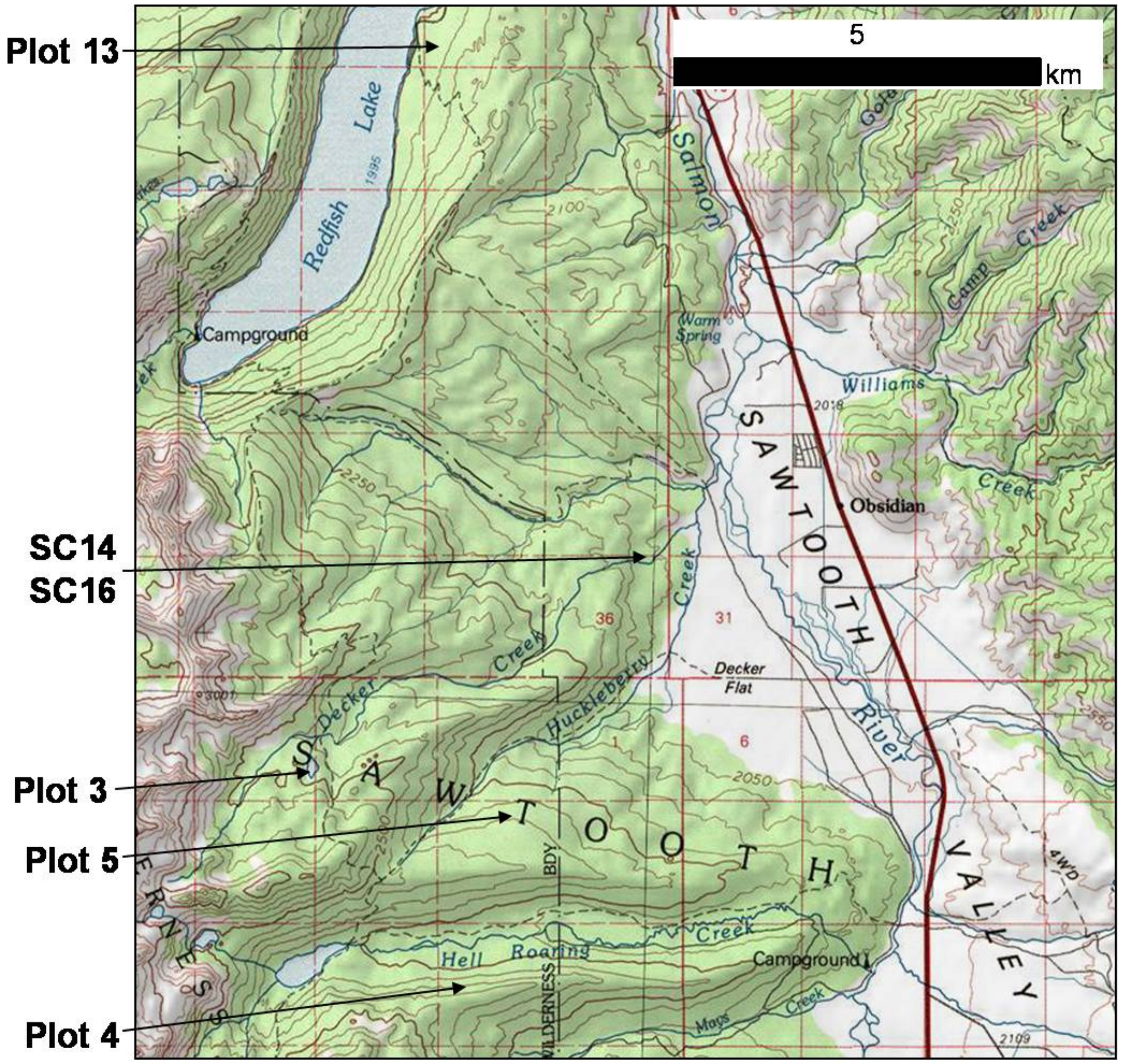

Figure 40. Soil-charcoal sites in the southwestern corner of the study area. The map was created using the National Geographic TOPO program.

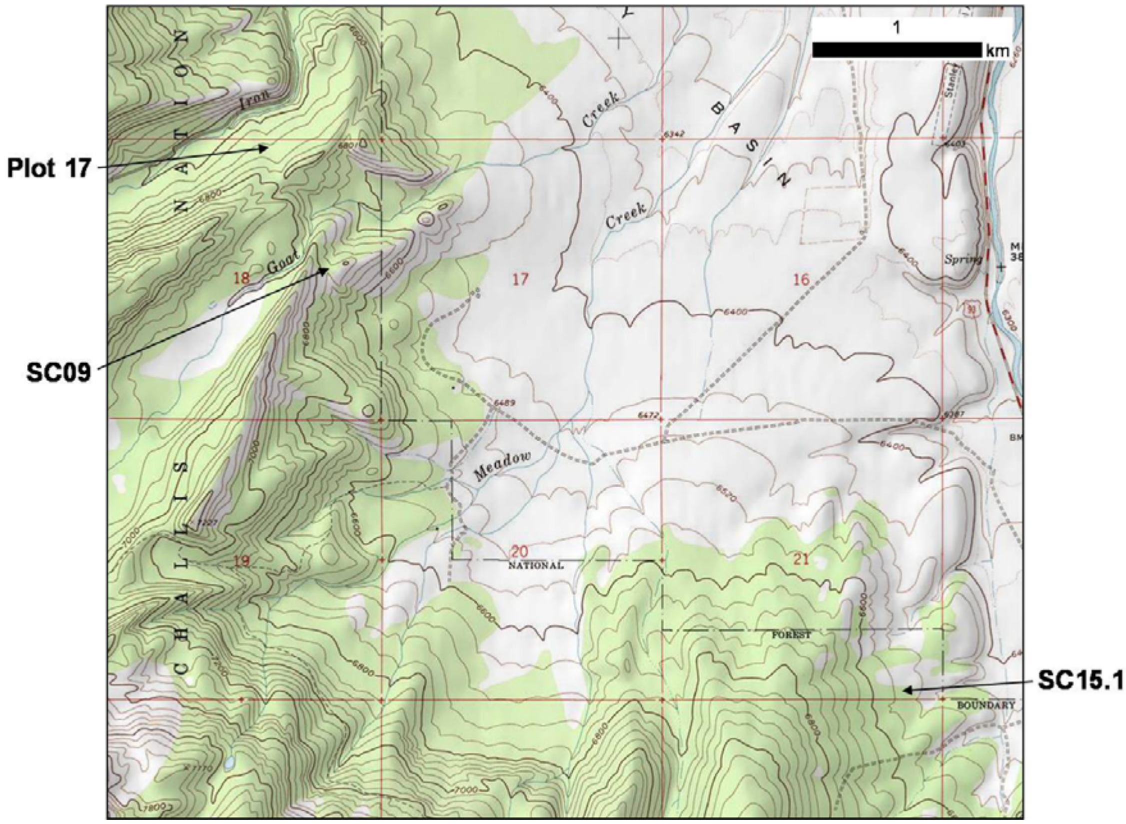

Figure 41. Soil-charcoal sites in the northern section of the study area. The map was created using the National Geographic TOPO program.

Table 4. Radiocarbon ages and calibrated dates from 16 charcoal samples (11 sites) in the Sawtooth Valley. **(Table continues on page 78.)**

Site	Sample	Depth (cm)	14C Age	Error	2-Sigma Range		% Area	Notes
Fisher Creek	IFC08	13	1276	41	839 AD	864 AD	4	
					659 AD	827 AD	96	
	IFC10b	28	1520	34	432 AD	610 AD	100	
4th July Creek	SC04	32--40	262	32	1942 AD	1951 AD	2	
					1778 AD	1799 AD	11	
					1617 AD	1672 AD	52	~1654 fire scar
					1514 AD	1599 AD	35	
	SC05	60--62	862	33	1148 AD	1258 AD	81	
					1121 AD	1139 AD	5	
					1046 AD	1090 AD	14	
	SC06b	96--99	1108	36	866 AD	1018 AD	99	
					828 AD	838 AD	1	
	SC07b	102--104	1290	34	794 AD	801 AD	1	
					657 AD	779 AD	99	
Decker Lake	Plot 3	21	7094	45	7839 BP	8003 BP	100	
Hellroaring Cr	Plot 4	15	3559	68	3644 BP	3660 BP	1	
					3686 BP	3996 BP	95	
					4036 BP	4078 BP	4	
Huckleberry	Plot 5	16	3176	38	3339 BP	3470 BP	100	
East Redfish	Plot 13	10	2402	35	2344 BP	2501 BP	85	
					2595 BP	2613 BP	3	
					2637 BP	2695 BP	13	

Table 4. Continued.

Site	Sample	Depth (cm)	14C Age	Error	2-Sigma	Range	% Area	Notes
Iron Creek	Plot 17	8--12	1428	34	570 AD	659 AD	100	
4th July moraine	SC12	13	157	32	1910 AD	1953 AD	19	
					1831 AD	1888 AD	16	~1873 fire scar
					1793 AD	1827 AD	12	
					1718 AD	1785 AD	35	1734, 1756 fire scars
					1665 AD	1708 AD	18	
Lower Decker	SC16	7	391	34	1558 AD	1631 AD	31	inverted age; 2 mm sizes (reworked?)
					1440 AD	1524 AD	69	~1500 fire scar
	SC14	13	185	33	1917 AD	1952 AD	19	1 cm sizes; depth/age similar to SC12
					1851 AD	1877 AD	3	
					1836 AD	1845 AD	1	
					1726 AD	1814 AD	55	1739 fire scar
					1649 AD	1696 AD	22	
Near Plot 15.1	SC15.1	8	996	35	1076 AD	1154 AD	37	
					982 AD	1058 AD	63	
Goat Creek	SC09	9	311	33	1483 AD	1649 AD	100	

^{14}C Ages and Calibrated Dates

Radiocarbon dating of charcoal provides a conservative estimate of fire (i.e., some fires are missed), meaning there likely is little to be inferred by comparing relative heights of peaks on summed-probability curves, particularly given the small sample size (n = 16). Peaks can shift by a decade or more, depending on the type of moving average applied to the probabilities, and therefore should be viewed as representing a multidecadal period rather than a single year or decade. Radiocarbon ages younger than 300 ^{14}C yr BP have wide calibrated date ranges because consistently low levels of ^{14}C were produced in the atmosphere during that time (Trumbore 2000). Probabilities from samples SC12 and SC14 (Table 4), with ^{14}C ages of 157 (± 32) and 185 (± 33), respectively, are smeared out over several intersections of the radiocarbon ages with the calibration curve. The result is intensified noise and weakened signal between ~1650 and

1950 AD in the summed probabilities. The age range for SC12 can arguably be narrowed to the interval between 1718 and 1785 AD (the range with the greatest area under the probability curve) by association with nearby fire scars, dating to 1734 and 1756 (Tables 1 and 4). Similarly, the age range for SC14 might be narrowed to the interval between 1726 and 1814 (the range with the greatest area under the probability curve) by association with a fire scar in the same watershed dating to 1739.

When a calibrated date range of an individual sample is reported in the text, it is the range with the highest percentage of area under the 2-sigma region of the probability curve (Table 4). Areas of reported ranges vary from 100% (the radiocarbon age intersected the calibration curve at only one point in calendar time) to 52% (the radiocarbon age intersected the calibration curve at four points in calendar time).

Graphical Analyses of Summed Probabilities

Probabilities from calibrated radiocarbon dates were summed, based on the assumption that peaks in the sum of probabilities represent single fires large in area or periods of high fire-frequency. Dates are reported in calendar years before present (1950 AD) or calendar years AD. Summed probabilities provide a record of fire for much of the Holocene (Figure 42). The two highest probability peaks on a 100-year moving average date to ~1230 cal yr BP (~720 AD) and ~325 cal yr BP (~1630 AD). The ~1230 cal yr BP peak tops an interval of relatively high fire probabilities from ~1500 to 700 cal yr BP (~450 to 1250 AD). The ~325 cal yr BP peak tops a second interval of relatively high fire probabilities from ~530 to 150 cal yr BP (~1420 to 1800 AD).

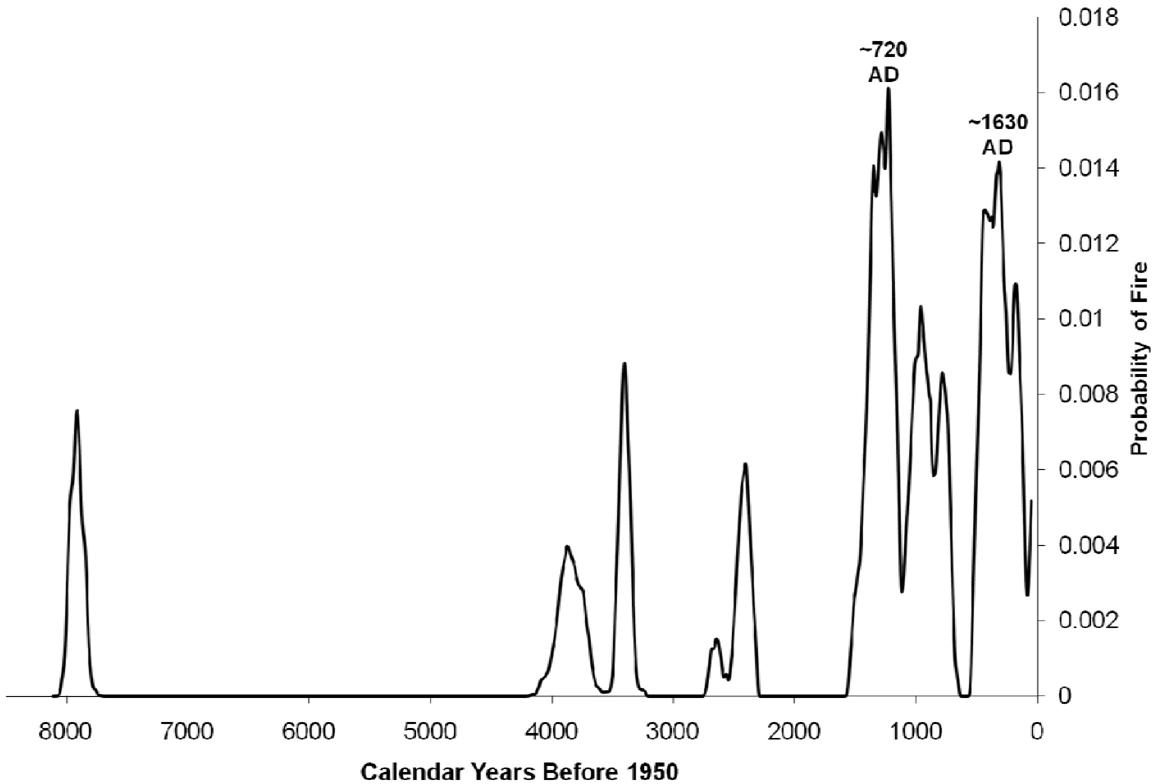

Figure 42. Summed probabilities of fire from radiocarbon dating of charcoal on a 100-year, centered moving average (n = 16).

Because sample depth in the Sawtooth Valley is shallow prior to ~1500 cal yr BP or ~450 AD (n = 4, Table 4), it is difficult to draw conclusions about the early and middle Holocene. Accordingly, discussion will focus on the past ~1500 years. To identify periods of above or below average probabilities between ~450 AD and the present, I calculated the mean and 99.9% confidence interval on a 50-year, center-weighted moving average (Figure 43). Fire probabilities are above average from ~550 to 780 AD (peaking at ~ 625, 695, and 750 AD), ~900 to 1040 AD (peaking at ~1020 AD), ~1165 to 1210 AD (peaking at ~1185 AD), ~1460 to 1685 AD (peaking at ~1535 and 1645 AD), and ~1735 to 1800 AD (peaking at ~1780 AD). Fire probabilities are below average from ~785 to 895 AD, ~1050 to 1155 AD, ~1220 to 1450 AD, ~1690 to 1730 AD, and ~1810 AD to the present.

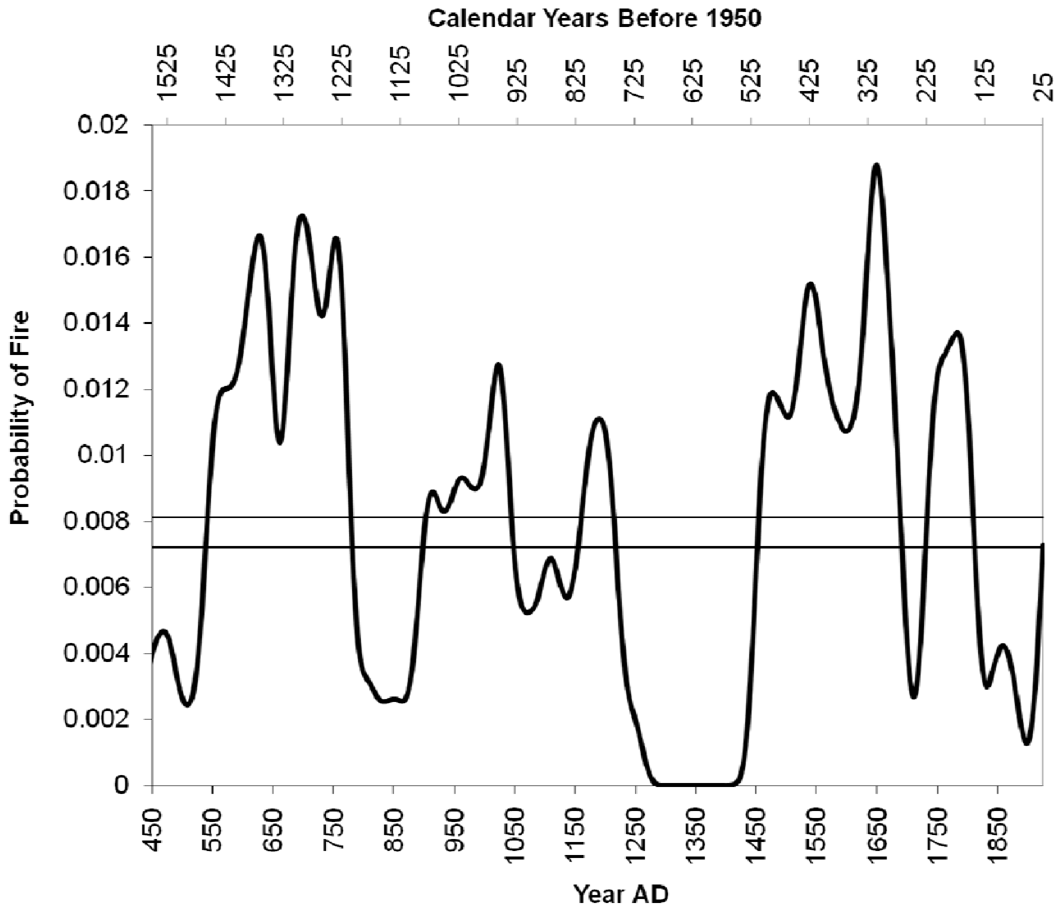

Figure 43. Fire probabilities between 450 AD and the present on a 50-year, center-weighted moving average (n = 12). Horizontal lines represent the 99.9% confidence interval of the mean.

Probability of Fire and Reconstructed July Temperature in central Idaho

Results from dendrochronology indicate that fires burned during years with significantly warm July temperature (Figure 16). On a 10-year moving average (Figure 30) the coincidence of high fire frequency with warm temperatures is less salient than the coincidence of low fire frequency with cool temperatures. This is not surprising, given that anomalously warm temperatures are necessary, but not sufficient, for the spread of stand-replacing fires, which are caused not by warm temperatures, but by an ignition (human or lightning), possibly facilitated by a favorable age structure or fuel level (e.g., abundant dead needles during a pine-beetle epidemic) in addition to temperature. During periods of anomalously cool temperatures, however, fuels likely would be too wet for the spread of fire regardless of other variables.

Summed probabilities from radiocarbon dating are juxtaposed with reconstructed July temperature for central Idaho (Biondi *et al.* 1999/2006) to examine the relationship between fire and temperature on a fifty-year moving average (Figure 44). As with the 10-year average from dendrochronology, the most salient coincidence is between low fire probability and cool temperatures. A drop in fire probabilities to zero or nearly zero from ~1280 to 1410 AD coincides with a period of cool July temperature from ~1250 to 1380 AD, which includes the coldest reconstructed period of the past 800 years, ~1280 to 1350 AD. The ~1280 to 1350 AD cold period coincides with the Wolf solar minimum, and the intervals from 1310 to 1317 AD and 1340 to 1350 AD were punctuated by volcanic eruptions (Bridgman and Oliver 2006). The Greenland Ice Sheet Project (reported by Vail 1998) reconstructed cold periods from 1308 to 1318 AD, 1324 to 1329 AD, 1343 to 1362 AD, and 1380 to 1384 AD; these cold periods coincide with zero fire probability in the Sawtooth Valley from ~1310 to 1385 AD. Tree rings from the Columbia Ice Field (Alberta, Canada, northern Rocky Mountains) indicate that the periods from 1275 to 1294 AD and 1311 to 1330 AD were the fifth and eleventh coldest 20-year periods, respectively, since 950 AD (Luckman and Wilson 2005). Documentary records indicate unusually cold winters in Europe between 1303 and 1328 AD (Pfister *et al.* 1996).

Fires in northwestern Minnesota reconstructed from varved lake sediments and fire-scarred trees were found to have been less frequent between 1240 and 1440 AD and during the Little Ice Age (LIA, ~1550 to 1850 AD) and more frequent in the 1400s and 1500s (Clark 1990). The 1500s, the warmest period of the past ~800 years reconstructed in central Idaho, coincides with a peak in fire probability in the Sawtooth Valley in ~1535 AD (Figure 44), though other peaks in fire probability do not coincide with temperature peaks.

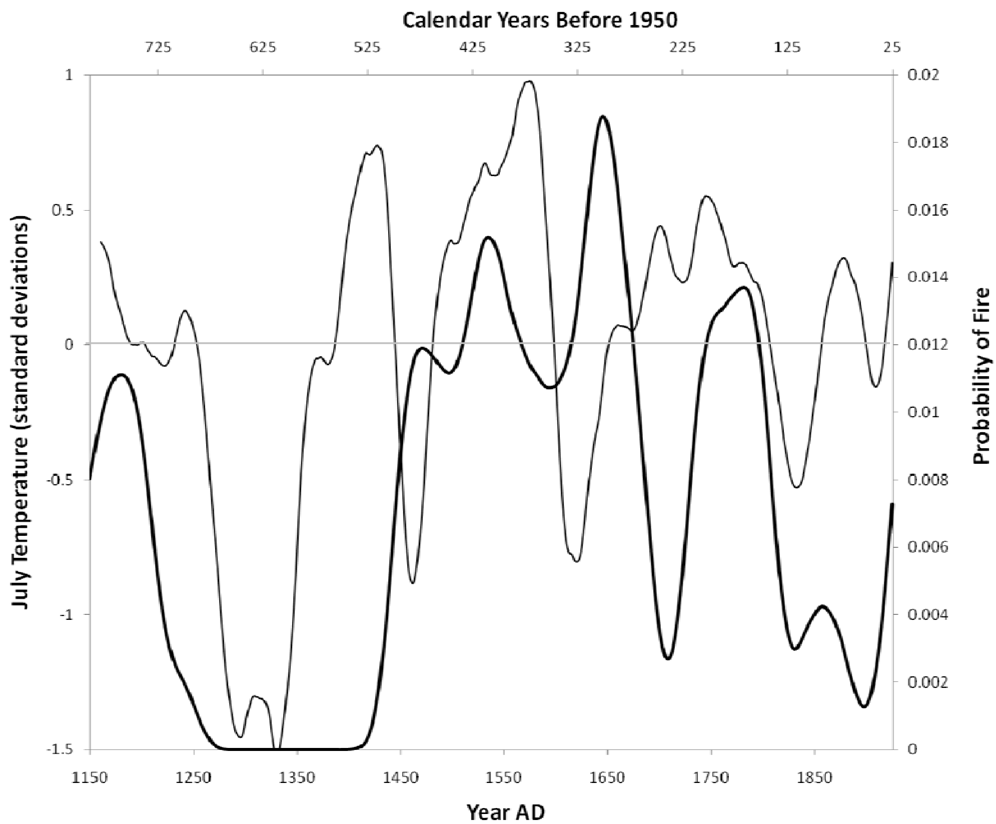

Figure 44. Probability of fire in the Sawtooth Valley (bold line) and reconstructed July temperature for central Idaho (Biondi *et al.* 1999/2006, thin line) on 50-year, center-weighted moving averages.

The highest peak in fire probability in the Sawtooth Valley during the past ~800 years is at ~1645 AD (Figure 44). A single-point fire was reconstructed from tree rings in ~1654 AD (tables 1 and 4) on the east side of the valley, and stand-replacing, multi-watershed fires were reconstructed on the west side of the valley in 1632 AD, a year of extreme drought and significantly warm (> 99.9% CL) July temperature (Figure 24). The

1632 AD fires burned in the context of a 50-year trough in July temperature (which bottomed out in ~1625 AD, Figure 44), indicating that a short burst of significantly warm temperature (1631 and 1632 AD, Biondi *et al.* 1999/2006) during a prolonged cool period can dry fuels sufficiently for a large, stand-replacing fire. This suggests that the cold period between ~1280 and 1350 AD, during which fire probability fell to zero or nearly zero, was punctuated by no short bursts of significantly warm temperatures. Annually resolved anomalies of July Temperature (Biondi *et al.* 1999/2006) between 1280 and 1350 AD confirm that no year was reconstructed as warm.

The ~1280 to 1350 AD cold period (Biondi *et al.* 1999/2006) coincides on a fifty-year moving average with anomalously wet conditions reconstructed between ~1280 and 1360 AD (Figure 45, Cook *et al.* 2004). This wet period was the longest, though not the highest in amplitude, reconstructed for the past ~1000 years, implying an effective wetness due to low temperatures rather than large volumes of precipitation.

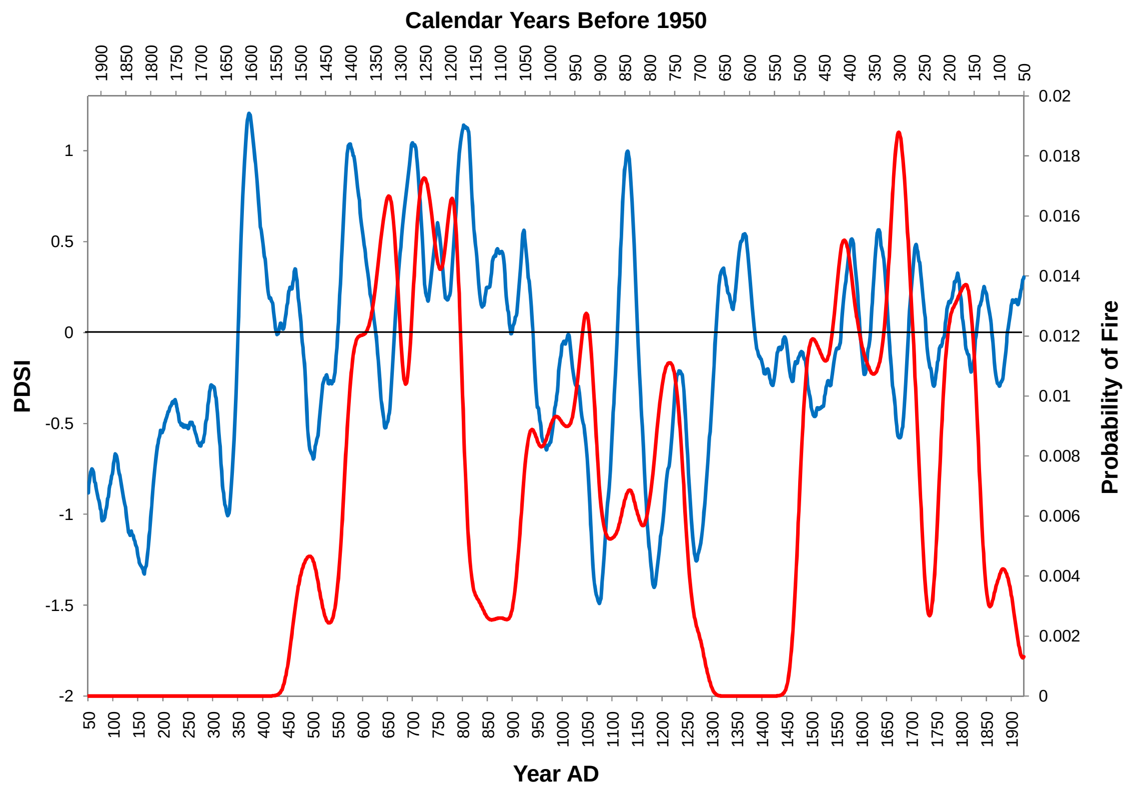

Figure 45. Probability of fire in the Sawtooth Valley (red line) and reconstructed summer PDSI for central Idaho (point 69, Cook *et al.* 2004, blue line) on 50-year, center-weighted moving averages. Negative PDSI values indicate drought; positive values indicate wetness.

Fire Probabilities from Opposite Sides of the Sawtooth Range Compared

The South Fork of the Payette (SFP) watershed on the opposite (west) side of the Sawtooth Range is lower in base elevation and warmer than the Sawtooth Valley, with ponderosa pine (*Pinus ponderosa*) at lower elevations and mixed-conifer forests at higher elevations. Despite that the SFP and Sawtooth Valley represent two distinct forest types (montane and subalpine, respectively), fire probabilities from SFP charcoal (collected from incised alluvial fans, Pierce *et al.* 2004) show a similar pattern to those of the Sawtooth Valley over the Holocene (Figure 46). Both forest types show small peaks in the early Holocene (~7000 cal yr BP on the SFP, ~8000 cal yr BP in the Sawtooth Valley), relatively low probabilities from ~6500 to 4000 cal yr BP (middle Holocene), relatively high probabilities from ~1400 to 740 cal yr BP (~550 to 1210 AD), a modest trough in ~1100 cal yr BP (~850 AD), a deeper trough in ~650 cal yr BP (~1300 AD), and relatively high probabilities from ~500 to 150 cal yr BP (~1450 to 1800 AD).

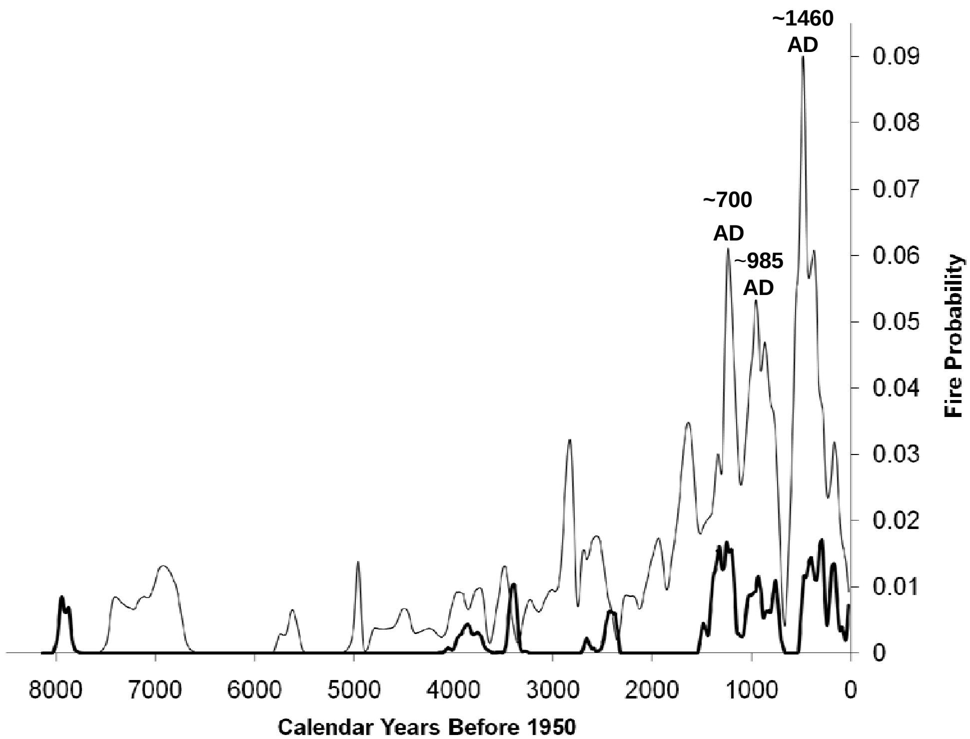

Figure 46. Probability of fire for the Sawtooth Valley (bold line, n = 16) and South Fork of the Payette (SFP, Pierce *et al.* 2004, thin line, n = 91) on 50-year, centered moving averages. Probabilities are higher for the SFP because more charcoal samples were dated for that study.

Drought, Fire Probabilities, and Erosion over the past ~1500 Years

Above-average fire probabilities in the Sawtooth Valley between ~550 and 780 AD coincide with reconstructed wet conditions on a 50-year moving average, with the exception of a combined drought/fire peak in ~625 AD (Figure 45, Cook *et al.* 2004). Lake levels were high in the Carson Sink (Nevada) at some point between ~431 and 642 AD, indicating a period of anomalous wetness in the larger region (Adams 2003). The ~695 and ~750 AD fire peaks in the Sawtooth Valley occur in a context of high-amplitude wet peaks in ~675 and ~785 AD (Figure 49). Alluvial-fan deposits in the

South Fork of the Payette (SFP) between ~550 and 800 AD were dominated by "small events" (implying fires of low intensity during wetter periods), but some deposits were categorized as "large events" (implying fires of higher intensity during drier periods, Pierce *et al.* 2004). In the Sawtooth Valley, most of the fire probability during this period is associated with the two incised alluvial sites, which include signals of both fire (drought) and erosion (wetness). Both deposits in the incised alluvial-fan date to this ~550 to 780 AD period, the older between 432 and 610 AD (100% of the area under the probability curve, Table 4, IFC10b), the younger between 659 and 827 AD (96% of the area under the probability curve, Table 4, IFC08). The lowest charcoal-bearing deposit in the incised floodplain dates between 657 and 779 AD (99% of the area under the probability curve, Table 4, SC07b). The deposits dating from 657 to 779 AD and 659 to 827 AD (from the adjacent Fourth of July and Fisher watersheds, respectively, Figure 39) likely date the same large fire, which would have burned during an interval reconstructed as wet on a 50-year moving average (Figure 45). The coincidence of high probabilities of fire-induced erosion and low-frequency, high-amplitude peaks in wetness implies a period of anomalously high precipitation, interrupted by short bursts of significantly warm temperatures and drought during which large fires could burn. Reconstructed temperature does not extend back to the ~550 to 780 AD period. Annual anomalies of summer PDSI (Cook *et al.* 2004) indicate that the average dry period (arbitrarily defined in this study as two or more consecutive years of negative PDSI) between 640 and 780 AD, when high probabilities of fire-induced erosion coincided with high-amplitude reconstructed wetness on a 50-year moving average (Figure 45), was 2.5 years. This implies that significantly warm temperatures at least on a multiannual timescale would have been required to dry the forest sufficiently for the spread of a stand-replacing fire. In the decade following fire, torrential or prolonged rains would have provided the erosion, depositing sediments on alluvial fans, though the sequence of fire and erosion could have been completed within a single year (hot, dry summer, warm, wet winter).

Large fire-induced debris-flow deposits on the SFP dating to the Medieval Climatic Anomaly (MCA, ~900 to 1250 AD) indicate stand-replacing fires in that ponderosa-pine and mixed-conifer forest (Pierce *et al.* 2004). These fires likely burned during multidecadal droughts (Figure 47, Cook *et al.* 2004). In the Sawtooth Valley, two of four charcoal-bearing deposits in the incised floodplain date to the MCA, the older between 866 and 1018 AD (99% of the area under the probability curve, Table 4, SC06b), the younger between 1148 and 1258 AD (81% of the area under the probability curve, Table 4, SC05). Because mountain floodplains are distant from the sources of fire-induced erosion, charcoal deposits likely record only the largest, most intense fires or the most torrential rainstorms. The similarity of fire regimes in the SFP and Sawtooth Valley during the MCA indicates that extreme climatic conditions can drive fire-induced erosion across forest types.

A peak in fire probabilities in the Sawtooth Valley in ~1020 AD occurred in the context of ~170 years of reconstructed drought (Cook *et al.* 2004) and anomalously warm reconstructed Northern Hemisphere temperature (Esper *et al.* 2002, Figure 47). Cook *et al.* 2004b caution, however, that reconstructed Northern Hemisphere temperature before 1200 AD is “more tenuous” than in following centuries because of fewer chronologies and lower within-chronology replication. Tree rings from the Columbia Ice Field (Alberta, Canada, northern Rocky Mountains) indicate that the period from 1009 to 1028

AD was the fourth warmest 20-year period reconstructed since 950 AD (Luckman and Wilson 2005). The drought peak in ~1050 AD, the highest in amplitude reconstructed during the past 2000 years, was followed by a wet peak in ~1110 AD, the largest in amplitude reconstructed during the past 1100 years (Figure 47, Cook *et al.* 2004). During the ~1085 to 1125 AD wet period, which coincided with slightly below-average fire probabilities in the Sawtooth Valley (Figure 47), forests would have regenerated, perhaps to burn again during a second multidecadal drought between ~1125 and 1280 AD, which coincided with a peak in fire probability in the Sawtooth Valley in ~1185 AD. During the second drought period, Northern Hemisphere temperature appears to have been on a cooling trend (Esper *et al.* 2002), which might explain the simultaneous drop-off of fire probabilities with increasing drought between ~1210 and 1250 AD (Figure 47) as the ~1280 to 1350 AD cold period (Figure 44) approached. Tree rings from the Columbia Ice Field (Alberta, Canada, northern Rocky Mountains) indicate that the periods from 1221 to 1240 AD and 1247 to 1266 AD were the ninth and seventh coldest 20-year periods, respectively, reconstructed since 950 AD (Luckman and Wilson 2005).

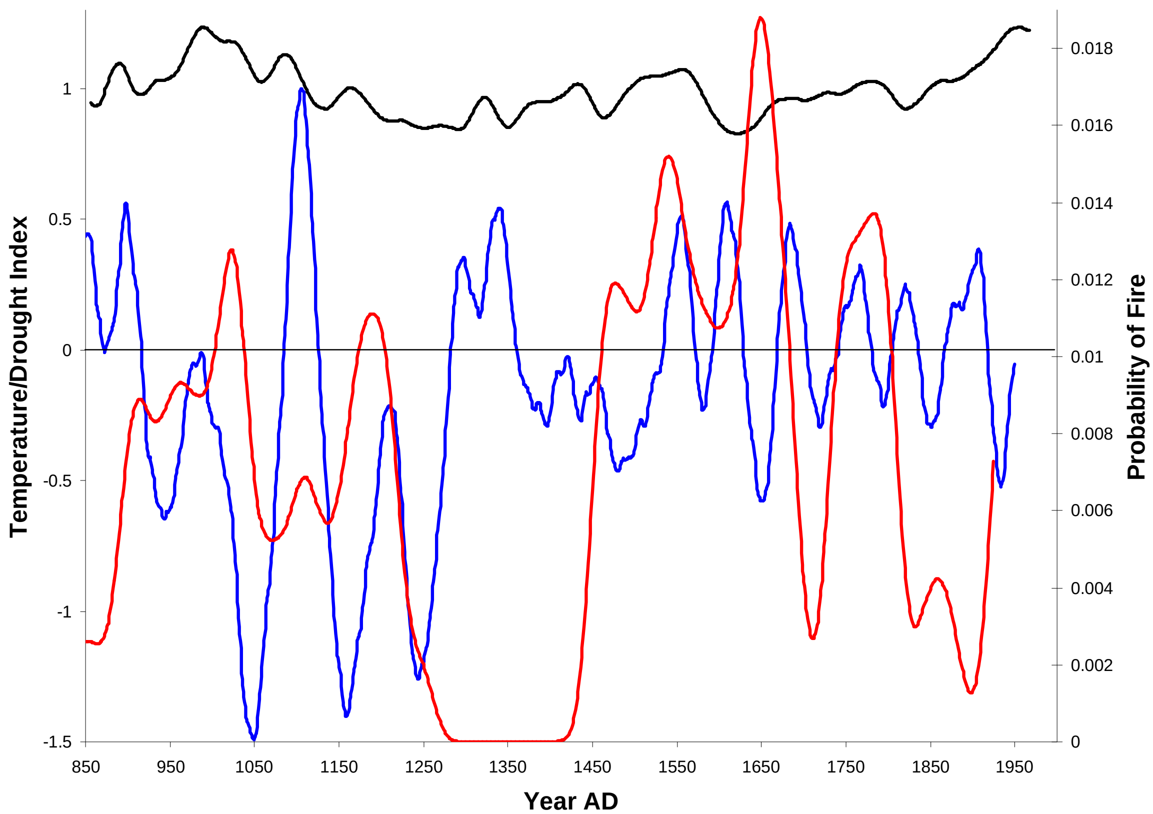

Figure 47. Probability of fire in the Sawtooth Valley (red line), reconstructed summer PDSI for central Idaho (point 69, Cook *et al.* 2004, blue line), and reconstructed Northern Hemisphere temperature (Esper *et al.* 2002, black line, in degrees Celsius) on 50-year, center-weighted moving averages. Negative PDSI values indicate drought; positive values indicate wetness.

In the Sawtooth Valley five of six deposits from the two incised alluvial sites date between ~550 and 1200 AD (Tables 4 and 6), a time span characterized by reconstructed multidecadal, high-amplitude oscillations between dry and wet conditions (Figure 45). Whereas incised alluvial sites necessarily record a coupled drought-erosion signal, depositional soil-charcoal sites record signals of drought, but not necessarily of erosion, and in-situ soil-charcoal sites record an uncoupled drought signal. Only two of 10 soil-charcoal samples contribute to fire probabilities during the ~550 to 1200 AD period. One sample (in-situ) dates between 570 and 659 AD (100% of the area under the probability curve, Table 4, Plot 17) and appears to be the main contributor to the ~625 AD peak in fire probability, which coincides with a reconstructed drought peak (Cook *et al.* 2004,

Figure 45) in an otherwise wet period. The other soil-charcoal sample (depositional) dates between 982 and 1058 AD (63% of the area under the probability curve, Table 4, SC15.1), a period of reconstructed multidecadal drought (Figure 47).

Soil charcoal from in-situ sites accounts for probability peaks up to ~1330 cal yr BP (620 AD), whereas soil charcoal from depositional sites accounts for peaks starting in ~980 cal yr BP (970 AD, Figure 48). Does the timing of this peak shift in soil-charcoal environment indicate an interval of widespread fire-induced erosion between ~1330 and 980 cal yr BP (~620 and 970 AD), when anomalously large amounts of charcoal were eroded from topographically high in-situ environments and re-deposited in depositional environments? If so, can an interval be identified when fire-induced erosion was most intense? The four largest peaks in incised alluvial charcoal (with coupled fire-erosion signals, Figure 48) date to ~1380 cal yr BP (~570 AD, reconstructed as wet in Figure 45), ~1230 cal yr BP (~720 AD, reconstructed as wet in Figure 45), ~1015 cal yr BP (~935 AD, reconstructed as dry in Figure 45), and ~750 cal yr BP (~1200 AD, reconstructed as dry in Figure 45). Peaks in fire-induced erosion thus appear to have coincided with both wet and dry periods on a 50-year moving average. The shift in environment in soil-charcoal probability peaks between ~1330 and 980 cal yr BP (~620 and 970 AD) from in-situ to depositional brackets the highest (~1230 cal yr BP or ~720 AD) and second highest (~1015 cal yr BP or ~935 AD) peaks in incised alluvial charcoal, implying that the most intense interval of fire-induced erosion occurred between ~1230 and ~1015 cal yr BP (~720 and 935 AD). Because fire probabilities are low across charcoal categories during the 800s AD (Figure 47), I suggest that the 700s AD or 900s AD were centuries characterized by anomalously large volumes of fire-induced erosion. This hypothesis is supported by peaks in the probability of fire-induced erosion on the nearby SFP in ~700 and ~985 AD (Figure 46).

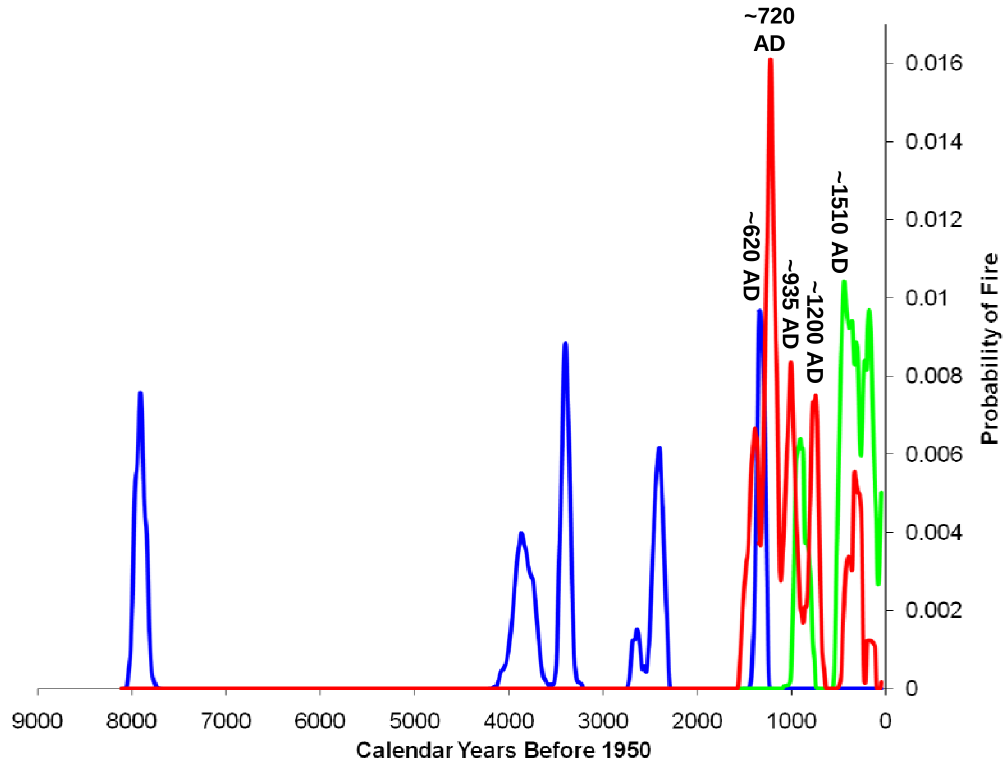

Figure 48. Fire probabilities for the Sawtooth Valley by charcoal category on centered, 100-year moving averages. Blue is in-situ soil charcoal (n = 5), green is depositional soil charcoal (n = 5), and red is incised alluvial charcoal (n = 6).

During the Little Ice Age (LIA, ~1550 to 1850 AD) reconstructed July temperature was warmer and more variable than during the ~1280 to1350 AD cold period (Figure 44), and fire probabilities were relatively high in both the SFP and Sawtooth Valley (Figure 46). LIA alluvial-fan deposits classified as “small events” on the SFP suggest fires of lower intensity than during the MCA, in turn suggesting that droughts were shorter or less intense during the LIA. In the Sawtooth Valley, neither of the alluvial sites (which record coupled fire-erosion signals) contained a deposit with highest probability more recent than the 1600s AD (Table 4), whereas five of six deposits date to the ~550 to 1200 AD period. Furthermore, the deposit in the incised floodplain that dates with the highest probability to the 1600s AD (SC04, Table 4) was the least distinct (smaller pieces, lower abundance) of the four deposits in that section, suggesting the fire was smaller in area or less intense or that erosive powers were decreased compared with the ~550 to 1200 AD period. Reconstructed PDSI for central Idaho during the LIA was higher in frequency and lower in amplitude than during the ~550 to 1200 AD period (Figure 45), indicating a more moderate climate with shorter, less intense droughts and wet periods. Large (multi-watershed), stand-replacing fires reconstructed from tree rings in the Sawtooth Valley during the LIA were infrequent; the fires of 1632 burned in at least four watersheds, and the fires of 1842 burned in at least two watersheds, with all other fires since 1600 restricted to a single watershed (Table 2). Fire and climate during the LIA coincided significantly on interannual timescales, indicating that fires burned during significantly warm, dry years in a context of cool, effectively wet conditions (figures 24 through 28). Fire probabilities after ~1800 AD likely were dampened by multidecadal cool periods (Figure 30), but likely also are a result of bias during the processing of the charcoal, when it was decided that samples from depths shallower than 7 cm would not be dated to avoid the possibility of dating contemporary fires.

Contemporary Analogues

Large, stand-replacing fires in central Idaho since the mid 1980s have been accompanied by fire-induced erosion. The 1989 Lowman Fire on the SFP was followed in December 1996 by torrential rains on melting snow, which triggered large debris flows in north-facing watersheds after colluvium, no longer held in place by tree roots, became saturated (Meyer *et al.* 2001). The stand-replacing 2005 Valley Road Fire in the Sawtooth Valley was followed in July of 2007 by a torrential rainstorm, which triggered large debris flows as a result of runoff from soils with reduced infiltration (Figure 49). These fire-induced debris flows included drought and precipitation signals on subdecadal time scales, indicating that the multidecadal oscillations between drought and wetness that apparently characterized the MCA are not required for major episodes of fire-induced erosion in central Idaho.

Figure 49. The 2005 Valley Road Fire in the Sawtooth Valley decreased the capacity of the soil to absorb water. A torrential rainstorm in July of 2007 produced large volumes of runoff, which transported debris flows to an alluvial fan in the Fourth of July watershed, near the Champion Trail (Figure 39). This north-facing slope could erode more in the near future, when decaying roots are no longer able to hold the colluvium in place.

CONCLUSIONS

The record from dendrochronology indicates that multi-watershed, stand-replacing fires (paleoanalogues of the 2005 Valley Road Fire) burned the study area in the Sawtooth Valley roughly every 100 to 200 years between 1632 and 1933. Fires of various sizes and intensities burned in at least one watershed every 10 to 20 years. Periods of low fire-frequency from 1800 to 1841 and 1890 to 1929 coincided with multidecadal periods of cool July temperature, paralleled closely by troughs in the AMO.

Annually resolved fires burned during summers that were significantly warm and dry. A positive surge of spring PDO associated with drought-induced fires suggests that warm springs resulted in early snow melt, which extended the summer drying season. Reconstructed annual temperature for the central Rocky Mountains (Briffa *et al.* 1992) is correlated most strongly with the instrumental spring season. The significant coincidence of annual temperature with fires in the Sawtooth Valley suggests that spring temperature was warm during fire years. Most drought-induced fires burned during combined positive phases of spring PDO and decadal AMO, suggesting a climatic one-two punch of early snowmelt and summer drought. Fires burned during both El Niño and La Niña events. The multi-watershed fires of 1632, which burned in at least four watersheds and were the largest reconstructed in this study, were preceded by the longest protracted La Niña event (11 years) reconstructed since 1525.

Radiocarbon dating of charcoal indicates peaks in fire probability in ~720 AD (1230 BP) and in ~1630 AD (320 BP). Comparison of Sawtooth Valley and South Fork Payette fire probabilities indicates that climatic extremes drive fire regimes across forest types. Climatic extremes include the ~1280 to 1350 AD cold period (low fire probabilities on both sides of the Sawtooth Range) and the ~900 to 1250 AD (MCA) mega-droughts (large, stand-replacing fires on both sides of the Sawtooth Range).

WORKS CITED

Adams, K. D. 2003. Age and paleoclimatic significance of late Holocene lakes in the Carson Sink, NV, USA. *Quaternary Research* 60, 294-306.

Arno, S. F. 1976: The historical role of fire on the Bitterroot National Forest. *USDA Forest Service Research Paper INT-187*.

Barlow, M., Nigam, S. and Berbery, E. H. 2001. ENSO, Pacific decadal variability, and U. S. summertime precipitation, drought, and streamflow. *Journal of Climate* 14, 2105-2128.

Barrett, S. W. and Arno, S. F. 1988. Increment-borer methods for determining fire history in coniferous forests. *USDA Forest Service General Technical Report INT-244*.

Bessie, W. C. and Johnson, E. A. 1995. The relative importance of fuels and weather on fire behavior in subalpine forests. *Ecology* 76, 747-762.

Biondi, F., Perkins, D. L., Cayan, D. R. and Hughes M. K. 1999/2006. July temperature during the second millennium reconstructed from Idaho tree rings. *Geophysical Research Letters* 26, 1445-1448.

Bridgman, H. A. and Oliver, J. A. 2006: *The global climate system: patterns, processes, and teleconnections*. Cambridge University Press.

Briffa, K. R., Jones, P. D. and Schweingruber, F. H. 1992. Tree-ring density reconstructions of summer temperature patterns across western North America since 1600. *Journal of Climate* 5, 735-754.

Briffa, K. R., Jones, P. D., Schweingruber, F. H. and Osborn, T. J. 1998. Influence of volcanic eruptions on Northern Hemisphere summer temperature over the past 600 years. *Nature* 393, 450-455.

Brown, P. M., Heyerdahl, E. K., Kitchen, S. G. and Weber, M. H. 2008. Climate effects on historical fires (1630—1900) in Utah. *International Journal of Wildland Fire* 17, 28-39.

Brunelle, A., Whitlock, C., Bartlein, PJ. and Kipfmueller, K. 2005. Holocene fire and vegetation along environmental gradients in the Northern Rocky Mountains. *Quaternary Science Reviews* 24, 2281-2300.

Buechling, A. and Baker, W. L. 2004. A fire history from tree rings in a high-elevation forest of Rocky Mountain National Park. *Canadian Journal of Forest Research* 34, 1259-1273.

Clark, J. S. 1990. Fire and climate change during the last 750 Yr in northwestern Minnesota. *Ecological monographs* 60, 135-159.

Cochran, P. H. and Berntsen, C. M. 1973. Tolerance of lodgepole and ponderosa pine seedlings to low night temperatures. *Forest Science* 19, 272-280.

Cook, E. R., Woodhouse, C. A., Eakin, C. M., Meko, D. M., Stahle, D. W. 2004a. Long-term aridity changes in the western United States. *Science* 306, 1015-1018.

Cook, E. R., Esper, J. and D'Arrigo, R. D. 2004b. Extra-tropical Northern Hemisphere land temperature variability over the past 1000 years. *Quaternary Science Reviews* 23, 2063-2074.

D'Arrigo, R., Villalba, R. and Wiles, G. 2001. Tree-ring estimates of Pacific decadal climate variability. *Climate Dynamics* 18, 219-224.

D'Arrigo, R., Cook, E. R., Wilson, R. J., Allan, R., and Mann, M. E. 2005. On the variability of ENSO over the past six centuries. *Geophysical Research Letters* 32, LO3711 1-4.

D'Arrigo, R. and Wilson, R. 2006. On the Asian Expression of the PDO. *International Journal of Climatology* 26, 1607-1617.

DeBano, L. F. 2000. The role of fire and soil heating on water repellency in wildland environments: a review. *Journal of Hydrology* 231-232, 195-206.

Despain, D. G. 1990: *Yellowstone vegetation: consequences of environment and history in a natural setting.* Roberts Rinehart.

Enfield, D. B., Mestas-Nuñez, A. M. and Trimble, P. J. 2001. The Atlantic multidecadal oscillation and its relation to rainfall and river flows in the continental U. S. *Geophysical Research Letters* 28, 2077-2080.

Esper, J., Cook, E. R. and Schweingruber, F. H. 2002. Low-frequency signals in long tree-ring chronologies for reconstructing past temperature variability. *Science* 295, 2250-2253.

Fisher, R. F. and Jenkins, M. J. 1987. Fire and the prairie-forest mosaic of Devils Tower National Monument. *American Midland Naturalist* 117, 250-257.

Gavin, D. G. 2001. Estimation of inbuilt age in radiocarbon ages of soil charcoal for fire history studies. *Radiocarbon* 43, 27-44.

Gergis, J. L. and Fowler, A. M. 2009. A history of ENSO events since A. D. 1525: implications for future climate change. *Climatic Change* 92, 343-387.

Gershunov, A. and Barnett, T. P. 1998. Interdecadal modulation of ENSO teleconnections. *Bulletin of the American Meteorological Society* 79, 2715-2725.

Gray, S. T., Graumlich, L. J., Betancourt, J. L. and Pederson, G. T. 2004. A tree-ring based reconstruction of the Atlantic Multidecadal Oscillation since 1567 A. D. *Geophysical Research Letters* 31, L12205 1-4.

Grissino-Mayer, H. D. 2001. Evaluating crossdating accuracy: a manual and tutorial for the computer program Cofecha. *Tree-Ring Research* 57, 205-221.

Grove, J. M. 1988: *The little ice age*. Methuen.

Heyerdahl, E. K., Brubaker, L. B. and Agee, J. K. 2002. Annual and decadal climate forcing of historical fire regimes in the interior Pacific Northwest, USA. *The Holocene* 12, 597-604.

Heyerdahl, E. K., Morgan, P., and Riser II, J. P. 2008. Multi-season climate synchronized historical fires in dry forests (1650—1900), Northern Rockies, USA. *Ecology* 89, 705-716.

Holmes, R. L. 1983. Computer-assisted quality control in tree-ring dating and measurement. *Tree-Ring Bulletin* 43, 69-78.

Kaplan, A., Cane, M. A., Kushnir, Y., Clement, A. C., Blumenthal, M. B. and Rajagopalan, B. 1998. Analyses of global sea surface temperature. *Journal of Geophysical Research* 103, 18,567-18,589.

Kilgore, B. M. and Taylor, D. 1979. Fire history of a sequoia-mixed conifer forest. *Ecology* 60, 129-142.

Kipfmueller, K. F. and Baker, W. L. 1998. A comparison of three techniques to date stand-replacing fires in lodgepole pine forests. *Forest Ecology and Management* 104, 171-177.

Kipfmueller, K. F. and Baker, W. L. 2000. A fire history of a subalpine forest in south-eastern Wyoming, USA. *Journal of Biogeography* 27, 71-85.

Kipfmueller, K. F. and Swetnam, T. W. 2000. Fire-climate interactions in the Selway-Bitterroot Wilderness area. USDA Forest Service Proceedings RMRS-P-15-Vol-5, 270-275.

Kitzberger, T., Swetnam, T. W. and Veblen, T. T. 2001. Inter-hemispheric synchrony of forest fires and the El Niño-Southern Oscillation. Global Ecology and Biogeography 10, 315-326.

Kunkel, M. L. and Pierce, J. L. 2010. Reconstructing snowmelt in Idaho's watershed using historic streamflow records. *Climate Change* 98, 155-176.

Luckman, B. H. and Wilson, R. J. S. 2005. Summer temperatures in the Canadian Rockies during the last millennium: a revised record. Climate Dynamics 24, 131-144.

Mantua, N. J., Hare, S. R., Zhang, Y., Wallace, J. M. and Francis, R. C. 1997. A Pacific interdecadal climate oscillation with impacts on salmon production. *Bulletin of the American Meteorological Society* 78, 1069-1079.

MacDonald, G. M. and Case, R. A. 2005. Variations in the Pacific Decadal Oscillation over the past millennium. *Geophysical Research Letters* 32, LO8703 1-4.

McCabe, G. J. and Dettinger, M. D. 2002. Primary modes and predictability of year-to-year snowpack variations in the western United States from teleconnections with Pacific ocean climate. *Journal of Hydrometeorology* 3, 13-25.

McCabe, G. J., Palecki, M. A. and Betancourt, J. L. 2004. Pacific and Atlantic ocean influences on multidecadal drought frequency in the United States. *PNAS* 101, 4136-4141.

Margolis, E. Q., Swetnam, T. W. and Allen, C. D. 2007. A stand-replacing fire history in upper montane forests of the southern Rocky Mountains. *Canadian Journal of Forest Research* 37, 2227-2241.

Meyer, G. A., Wells, S. G. and Jull, A. J. T. 1995. Fire and alluvial chronology in Yellowstone National Park: climatic and intrinsic controls on Holocene geomorphic processes. *GSA Bulletin* 107, 1211-1230.

Meyer, G. A. and Wells, S. G. 1997. Fire-related sedimentation events on alluvial fans, Yellowstone National Park, U. S. A. *Journal of Sedimentary Research* 67, 776-791.

Meyer, G. A., Pierce, J. L., Wood, S. H. and Jull, A. J. T. 2001. Fires, storms, and erosional events in the Idaho Batholith. *Hydrological processes* 15, 3025-3038.

Minobe, S. 1997. A 50—70 year climatic oscillation over the North Pacific and North America. *Geophysical Research Letters* 24, 683-686.

Minobe, S. 2000. Spatio-temporal structure of the penta-decadal variability over the North Pacific. *Progress in Oceanography* 47, 381-408.

Mitchell, R. G., Martin, R. E. and Stuart, J. 1983. Catfaces on lodgepole pine—fire scars or strip kills by the mountain pine beetle? *Journal of Forestry* 81, 598-613.

Morgan, P., Heyerdahl, E. K. and Gibson, C. E. 2008. Multi-season climate synchronized forest fires throughout the 20th century, northern Rockies, U. S. A. *Ecology* 89, 717-728.

Page, W. G. and Jenkins, M. J. 2007a. Predicted fire behavior in selected mountain pine beetle-infested lodgepole pine. *Forest Science* 53, 662-674.

Page, W. G. and Jenkins, M. J. 2007b. Mountain pine beetle-induced changes to selected lodgepole pine fuel complexes within the Intermountain Region. *Forest Science* 53, 507-518.

Palmer, W. C. 1965. Meteorological drought. *U. S. Weather Bureau, Office of Climatology, research paper No. 45*.

Perkins, D. L. and Swetnam, T. W. 1996. A dendroecological assessment of whitebark pine in the Sawtooth-Salmon River region, Idaho. *Canadian Journal of Forest Research* 26, 2123-2133.

Pierce, J. L., Meyer, G. A. and Jull, A. J. T. 2004. Fire-induced erosion and millennial-scale climate change in northern ponderosa pine forests. *Nature* 432, 87-90.

Pfister, C., Schwarz-Zanetti, G. and Wegmann, M. 1996. Winter severity in Europe: the Fourteenth century. *Climatic Change* 34, 91-108.

Romme, W. H. 1982. Fire and landscape diversity in subalpine forests of Yellowstone National Park. *Ecological Monographs* 52, 199-221.

Schoennagel, T., Veblen, T. T., and Romme, W. H. 2004. The interaction of fire, fuels, and climate across Rocky Mountain forests. *Bioscience* 54, 661-676.

Schoennagel, T., Veblen, T. T., Romme, W. H., Sibold, J. S. and Cook, E. R. 2005. ENSO and PDO variability affect drought-induced fire occurrence in Rocky Mountain subalpine forests. *Ecological Applications* 15, 2000-2014.

Schoennagel, T., Veblen, T. T., Kulakowski, D. and Holz, A. 2007. Multidecadal climate variability and climate interactions affect subalpine fire occurrence, western Colorado (USA). *Ecology* 88, 2891-2902.

Serreze, M. C., Clark, M. P., Armstrong, R. L., McGinnis, G. A. and Pulwarty, R. S. 1999. Characteristics of the western United States snowpack from snowpack telemetry (SNOTEL) data. *Water Resources Research* 35, 2145-2160.

Shen, C., Wang, W., Gong, W. and Hao, Z. 2006. A Pacific Decadal Oscillation record since 1470 AD reconstructed from proxy data of summer rainfall over eastern China. *Geophysical Research Letters* 33, LO3702, 1-4.

Shuman, B., Henderson, A. K., Colman, S. M., Stone, J. R., Fritz, S. C., Stevens, L. R., Power, M. J. and Whitlock, C. 2009. Holocene lake-level trends in the Rocky Mountains, U. S. A. *Quaternary Science Reviews* 28, 1861-1879.

Sibold, J. S. and Veblen, T. T. 2006. Relationships of subalpine forest fires in the Colorado Front Range with interannual and multidecadal-scale climatic variation. *Journal of Biogeography* 33, 833-842.

Sibold, J. S., Veblen, T. T. and Gonzalez, M. E. 2006. Spatial and temporal variation in historic fire regimes in subalpine forests across the Colorado Front Range in Rocky Mountain National Park, Colorado, USA. *Journal of Biogeography* 33, 631-647.

Sibold, J. S., Veblen, T. T., Chipko, K., Lawson, L., Mathis, E., and Scott, J. 2007. Influences of secondary disturbances on lodgepole pine stand development in Rocky Mountain National Park. *Ecological Applications* 17, 1638-1655.

Stewart, I. T., Cayan, D. R. and Dettinger, M. D. 2005. Changes toward earlier streamflow timing across western North America. *Journal of Climate* 18, 1136-1155.

Stokes, M. A. and Smiley, T. L. 1968: *An introduction to tree-ring dating*. University of Arizona Press.

Stuiver, M. and Reimer, P.J. 1993. Extended ^{14}C database and revised CALIB 3.0 ^{14}C age calibration program. *Radiocarbon* 35, 215-230.

Thackray, G. D. 2008. Varied climatic and topographic influences on Late Pleistocene mountain glaciation in the western United States. *Journal of Quaternary Science* 23, 671-681.

Tande, G. F. 1979. Fire history and vegetation pattern of coniferous forests in Jasper National Park, Alberta. *Canadian Journal of Botany* 57, 1912-1931.

Trumbore, S. E. 2000: Radiocarbon geochronology. In Noller, J. S., Sowers, J. M. and Lettis, W. R., editors, *Quaternary Geochronology: methods and applications, AGU reference shelf 4,* American Geophysical Union, 41-58.

Turner, M. G. and Romme, W. H. 1994. Landscape dynamics in crown fire ecosystems. *Landscape Ecology* 9, 59-77.

Vail, B. J. 1998. Human ecological perspectives on Norse settlement in the North Atlantic. *Scandinavian Studies* 70, 293-312.

Westerling, A. L., Hidalgo, H. G., Cayan, D. R., and Swetnam, T. W. 2006. Warming and earlier spring increase western U. S. forest wildfire activity. *Science* 313, 940-943.

Wright, H. A. and Bailey, A. W. 1982: *Fire Ecology*. John Wiley and Sons.

Yamaguchi, D. K. 1991. A simple method for cross-dating increment cores from living trees. *Canadian Journal of Forest Research* 21, 414-416.

APPENDIX A: DENDROCHRONOLOGY

Dating Fire Scars

I dated fire scars from Douglas-fir using the list method (Yamaguchi 1991), in which a list is compiled of years when most trees showed narrow or wide rings. Jeremy Whitman (Meridian Academy) constructed a Douglas-fir chronology in program Cofecha (Holmes 1983; Grissino-Mayer 2001) to verify the dating of the wood and the fire dates. The Cofecha Douglas-fir chronology spans 406 years (1602 to 2007) and includes 31 series (series intercorrelation 0.51; average mean sensitivity 0.2; 55 segments with possible problems).

I dated fire scars from lodgepole pine using the list method (Yamaguchi 1991) and constructed a lodgepole chronology on program Cofecha (Holmes 1983; Grissino-Mayer 2001) to verify the dating of the wood and the fire dates. The Cofecha lodgepole chronology consists of 21 cross-dated series covering 257 years (1750 to 2006). Average mean sensitivity was 0.2, indicating the rings were relatively complacent; many cores rejected from the chronology had mean sensitivities lower than 0.2. Sixteen segments were flagged as having possible problems.

Lodgepole Cores

When lodgepole pine were cored, the pith was not obtained in most cases. Estimated seedling dates (ESDs) were calculated using the following formula: A/B = the number of rings over the last 10 mm of core divided by 10 mm; D/2 = the radius of the circle that fits the last visible ring; r = (A/B)(D/2) = the number of rings to be added to the unadjusted date to estimate the pith date or seedling date (Kipfmueller and Baker 1998). When “r” was greater than 20, the core was excluded from analysis (e.g., Sibold *et al.* 2006).

Trees were cored at a height of 25 cm. Tande (1979) estimated that lodgepole seedlings that germinate after a stand-replacing fire take four years (plus or minus 2 years) to reach 25 cm in height. Accordingly, 4 years were subtracted from the ESD to obtain the estimated germination date (EGD). A small number of trees were too rotten to be cored at the base, so they were cored at breast height. Three breast-height saplings that appeared to have germinated in sunny locations were sectioned to estimate the number of years (~15) required for a seedling to reach breast height. The breast height correction was not applied if the resulting EGD was older than the oldest EGD of the trees that were cored at 25 cm; it was assumed that such trees had grown exceptionally fast, and the 25 cm correction was applied instead.

Figure 50 shows locations of the 15 lodgepole plots that were sampled for this study. Table 5 provides latitudes/longitudes and elevations of the plots.

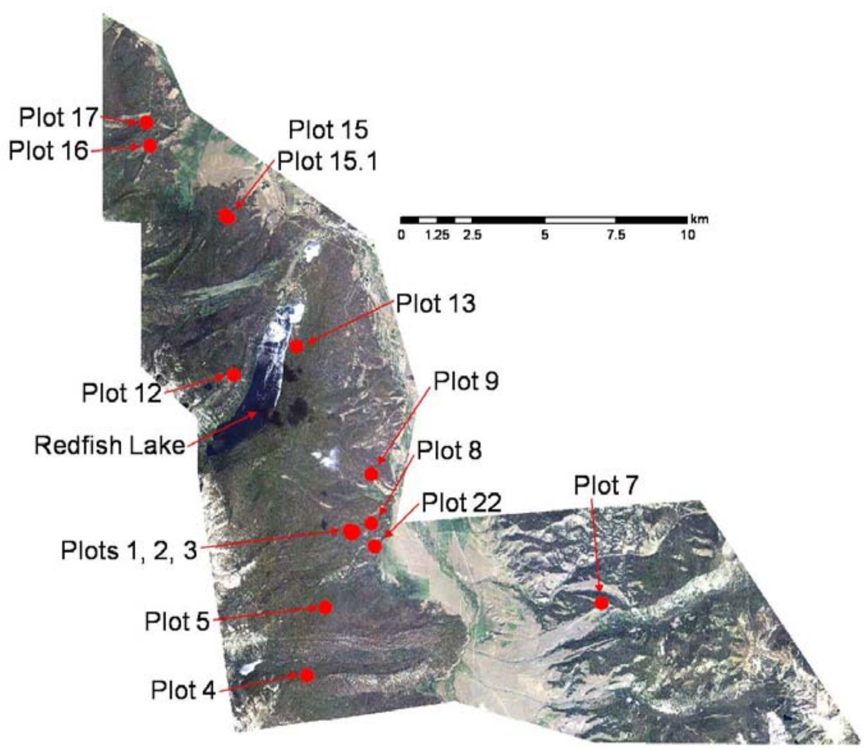

Figure 50. Fifteen lodgepole plots were sampled in the Sawtooth Valley.

Table 5. Locations and elevations of the 15 lodgepole plots.

Plot	Lat/Lon	Elevation (m)	Plot	Lat/Lon	Elevation (m)
1	44^o 04’ 10”	2171	12	44^o 07’ 14”	2253
	114^o 53’ 17”			114^o 56’ 36”	
2	44^o 04’ 07”	2171	13	44^o 07’ 48”	2026
	114^o 53’ 20”			114^o 54’ 56”	
3	44^o 04’ 11”	2172	15	44^o 10’ 23”	2107
	114^o 53’ 24”			114^o 56’ 53”	
4	44^o 01’ 18”	2376	15.1	44^o 10’ 19”	2109
	114^o 54’ 30”			114^o 56’ 48”	
5	44^o 02’ 39’	2295	16	44^o 11’ 43”	2094
	114^o 54’ 03”			114^o 58’ 58”	
7	44^o 02’ 47”	2391	17	44^o 12’ 10”	2039
	114^o 46’ 32”			114^o 59’ 04”	
8	44^o 04’ 19”	2068	22	44^o 03’ 52”	2048
	114^o 52’ 49”			114^o 52’ 43”	
9	44^o 05’ 18”	2133			
	114^o 52’ 52”				

APPENDIX B: CHARCOAL

Potential Inaccuracies from Inbuilt Age

Heartwood, bark, and down snags are not in equilibrium with the atmosphere (e.g., Gavin 2001). If this dead wood burns in a fire, radiocarbon dates from the charcoal could be centuries older than the fire. Such charcoal is said to possess in-built age. Ideally, burned needles and seeds, which would have been in equilibrium with the atmosphere during the fire, should be dated (Pierce *et al.* 2004). No burned seeds were identified among the Sawtooth charcoal, and rare pieces of burned needles were too small for dating. Inaccuracies from in-built age were minimized by dating charcoal samples with discernable ring curvature. Observations in areas burned by the 2005 Valley Road Fire indicate that the fire was carried by small branches in the crowns and that the tree trunks and larger branches remained largely unburned. Ring curvature, therefore, likely indicates a twig or small branch that was at least in near-equilibrium with the atmosphere. If the pith of a down snag burned, the charcoal could show ring curvature, but my assumption is that the ratio of charcoal from burned twigs and small branches over charcoal from the piths of down snags is high. A wildcard could be small branches or twigs lying dead on the forest floor, but I assume these would have decomposed after ~100 years. Eight of 16 samples were classified as twigs or small branches. Two sites yielded no single piece large enough to be dated, so composites were made from smaller pieces. Ring curvature in six samples could not be verified; these samples were chosen based on relatively large size, which facilitated processing.

Reporting of Radiocarbon Ages

Radiocarbon ages (Table 4) are reported in calendar years before 1950 (years BP). Calibrated dates are reported in calendar years BP (if older than 1950 cal yr BP) or in years AD (if younger than 1950 cal yr BP). A calibrated radiocarbon date does not date the sample to a single year, but gives a date range (or date ranges, if the radiocarbon age intersects more than one point on the calibration curve) with a probability of fire assigned to each year. A 1-sigma date range includes 1 standard deviation under the probability curve; a 2-sigma date range includes 2 standard deviations. Two-sigma ranges are reported in this study. A number between 0 and 1 in parentheses following the date range indicates the proportion of the area under the 2-sigma range of the probability curve that falls between those dates. If the radiocarbon age intersected the calibration curve at one point, the proportion in parentheses will be “1”; if the intersection occurred at more than one point, the proportion will be a decimal.

Charcoal Sites: Supplementary Information

Locations, site descriptions, sample codes, and notes (including stratigraphies) for the 16 charcoal samples are reported in Table 6.

Table 6. Supplementary information on charcoal samples from the Sawtooth Valley.

Location	Site Description	Sample	Notes	Latitude	Longitude	Elev (m)
Fisher Creek	Alluvial Fan	IFC08	Hyperconcentrated flow w/ charcoal deposited on a burned surface	44° 03' 44"	114° 46' 8"	2232
		IFC10b	Hyperconcentrated flow w/ charcoal			
Fourth July Creek	Floodplain	SC04	Silty matrix	44° 02' 27"	114° 45' 25"	2278
		SC05	Silty matrix, interbedded with deposits of fine sand			
		SC06b	Sandy-silt matrix, formed a dark layer obvious to the eye			
		SC07b	Silty matrix, formed a dark layer obvious to the eye			
Decker Lake	Soil In Situ	Plot 3	Stratigraphy (cm): -2 to 0 = organic, 0 to 3 = loess, 3 to 33 = medium to coarse sand with cobbles	44° 04' 11"	114° 53' 24"	2172
Hellroaring Creek	Soil In Situ	Plot 4	Kame terrace near top of moraine	44° 01' 18"	114° 54' 30"	2376
Huckleberry Creek	Soil In Situ	Plot 5	Stratigraphy (cm): -2 to 0 = organic, 0 to 5 = loess, 5 to 17 = silt w/ sand, granules, 17 to bottom = till	44° 02' 39"	114° 54' 03"	2295
East Redfish	Soil In Situ	Plot 13	Stratigraphy (cm): -1 to 0 = organic, 0 to 5 = loess, 5 to bottom = bioturbated till	44° 07' 48"	114° 54' 56"	2026
Iron Creek	Soil In Situ	Plot 17	Stratigraphy (cm): -8 to 0 = organic, 0 to 24 = silt/fine sand, 24 to bottom = till; micro-depositional site on hillslope	44° 12' 10"	114° 59' 04"	2039
4th July moraine	Soil Depositional	SC12	Stratigraphy (cm): -3 to 0 = organic, 0 to bottom = silt, sand, angular granules/pebbles, max b-axis ~3cm	44° 02' 47"	114° 46' 32"	2391
Lower Decker	Soil Depositional	SC16	Stratigraphy (cm): -2 to 0 = organic, 0 to bottom = silt, sand, angular granules/pebbles	44° 04' 19"	114° 52' 49"	2068
	Soil Depositional	SC14				
Near Plot 15.1	Soil Depositional	SC15.1	Stratigraphy (cm): -4 to 0 = organic, 0 to 2 = loess, 2 to 12 = silt, sand, granules, 12 to bottom = till	44° 10' 29"	114° 56' 21"	1999
Goat Creek	Soil Depositional	SC09	Stratigraphy (cm): -2 to 0 = organic, 0 to bottom = silt w/ angular clasts, max b-axis ~3 cm	44° 11' 43"	114° 58' 58"	2094